مجلة المختار للعلوم

AL-Mukhtar Journal of Sciences

Volume: 36 Issue:1 2021

ISSN:26-17-2178 (Print) ISSN:26-17-2186 (Online)
دار الكتب الوطنية - رقم الإيداع القانوني 280-2013

مجلة المختار للعلوم

جامعة عمر المختار

البيضاء، ليبيا

مجلة علمية محكّمة، المجلد السادس والثلاثون، العدد الأول، 2021

تصدر عن جامعة عمر المختار، البيضاء، ليبيا.

مجلة المختار للعلوم

رقم الايداع في المكتبة الوطنية 2013/280/بنغازي

جامعة عمر المختار – البيضاء – ليبيا

مجلة محّكمة تصدر عن جامعة عمر المختار، البيضاء، ليبيا

مجلة علمية محكّمة، المجلد السادس والثلاثون، العدد الأول، 2021

بريد إلكتروني: omu.j.sci@omu.edu.ly

ص.ب. 919 البيضاء – ليبيا، فاكس: 7053 463 69 218+

أعضاء هيئة التحرير

مجلة المختار للعلوم 36:(1)، 2021

Al-Mukhtar Journal of Sciences 36: (1), 2021

Al-Mukhtar Journal of Sciences 36 (1): 01-11, 2021

Effects of Different Levels of Urea as Nitrogen Source on Chemical Composition of Marine Microalgae *Nannochloropsis oculata*

Ali Mahmoud Abougrara
Department of Marine Resources, Faculty of Natural Resources and Environmental Sciences, Omar Al-Mukhtar University, Libya.

Received: 10 June 2019/ Accepted: 30 January 2021
Doi: https://doi.org/10.54172/mjsc.v36i1.5

Abstract: Microalgae breeding media must be cost-effective, enable high growth, meet exact requirements and be readily available. The effect of different levels of urea [25, 50, 75, and 100%] in the growth medium on the biochemical constituents (protein, carbohydrates, lipids, fatty acids, and amino acids) of the *Nannochloropsis oculata,* was assessed compared to the F/2 Guillard standard medium. The obtained results revealed that the chemical constituents of *N. oculata* were influenced by the different levels of urea. The highest total protein was obtained by A4 medium (100% urea) (26.44%) and A3 medium (75% urea) (25.84%). The maximum percentage of essential amino acids (EAA) (51.54%) was obtained by using the A4 medium (100% urea) as compared to the control (100% F/2). The highest total lipid content was achieved by using the A1 medium (25% urea) producing (17.33 %) and A4 medium (100% urea) (16.98%). Accordingly, the highest total saturated fatty acids percentage (TSFA) of *N. oculata* was recorded by the A3 medium. In conclusion, the addition of urea is an excellent policy to increase chemical composition and lipid accumulation. The present study recommended taming results for aquaculture feeding through using the proposed A1 medium as a lipid promoter or A4 medium as a protein promoter.

Keywords: Amino Acids, Fatty Acids, *Nannochloropsis oculata*, Proximate Composition

INTRODUCTION

Algae are a diverse group of eukaryotic organisms with important roles in marine, freshwater, and even terrestrial ecosystems. For instance, 30–50% of the planetary net photosynthetic productivity (the difference between autotrophic gross photosynthesis and respiration) is of marine origin and dependent on phytoplankton biomass (Boyce et al., 2010; Field et al., 1998). Unicellular microalgae are capable of harnessing sunlight and CO_2 to produce energy-rich chemical compounds, such as lipids and carbohydrates, which can be converted into fuels (Hu et al., 2008; Rodolfi et al., 2009; Wijffels & Barbosa, 2010). Marine phytoplankton is often categorized into groups based on taxonomic traits, its abundance role in biogeochemical fluxes, and/or primary production. While diatoms are considered the principal group contributing to primary production and carbon export in coastal areas, dinoflagellates are important contributors to biomass in stratified or silica-limited areas, and microalgae are the dominant group in the marine continental shelf and oceanic waters (da Silva et al., 2009). Microalgae strains are fast-growing microorganisms with very high growth rates under optimal culture conditions. It is rapidly growing, along with great chemical diversity, it opens up applications in many fields, such as aquaculture, biotechnology, and food science (Spolaore et al., 2006; Templeton & Laurens, 2015).

Applications involving microalgae are expected to increase and diversify as a result of the ongoing search for more productive systems to supply the community with food, feed

***Corresponding Author:** Ali Mahmoud Abougrara amhofm1963@gmail.com, Department of Marine Resources, Faculty of Natural Resources and Environmental Sciences, Omar Al-Mukhtar University, Libya

stock, and high-value biochemical products (Lee Chang et al., 2013; Zeng et al., 2011) Particularly in foodstuffs, microalgae are beneficial in improving the nutritional content of traditional foods, and thus, have a positive effect on human health due to their proper chemical composition.On the other hand, biological issues include the domestication of promising strains (Lim et al., 2012) and successful uses of mechanisms stimulating microalgae to grow and produce target substances (Kaye et al., 2015).

All possible applications of microalgae are directly associated with high growth and a favourable chemical profile of the species (Borges-Campos et al., 2010). Fluctuations in the chemical profile of microalgae in cultures are a key issue in their study and applications (Lourenco et al., 2002). The chemical content of microalgae can vary with culture age and with changes in culture conditions (Carvalho et al., 2009). *Nannochloropsis* is considered the main algal species cultured in marine hatcheries and plays an important role in aquaculture development (Bondioli et al., 2012). The effect of variation of culture parameters on many microalgae species has been studied in order to better understand their physiology, as well as to answer specific and relevant questions for mass culture (Grobbelaar, 2014). In the industrial production scale in marine hatcheries, it is very important to optimize a suitable nutrient culture media for culturing this species (Ashour & Kamel, 2017). The microalgae nutrient media should be easy to prepare, economical, achieve high growth, and satisfy all the microalgae quality and quantity. Although the F/2 Guillard medium is considered the most commonly used medium in the culturing of *Nannochloropsis* in marine hatcheries, it has some disadvantages, such as being difficult to prepare and set up for outdoor mass culture and being expensive (Ashour & Kamel, 2017). The objective of this study is to determine the effect of adding a percentage of CH_4N_2O on the chemical composition, fatty acid, and amino acid of *Nannochloropsis oculata.*

MATERIALS AND METHODS

Microalgal strains and culture condition: The *Nannochloropsis oculata* strain was from an algae unit of the marine hatchery at the kilo 21 Alexandria - Egypt.

The experiment was conducted in the marine hatchery of the National Institute of Floating Seas and Fisheries Alexandria (NIOF), Egypt. *N. oculata* were kept and cultured under controlled conditions of temperature (22± 2C˚), salinity (35 ± 2 ppt), and illumination (750-3000 Lux /24 h.) using F/2 Guillard standard medium (Guillard & Ryther, 1962), with continuous aeration.

Experiment design: The experiment was conducted in plastic bottles of 1.5 liters filled with 1 liter of sterile saline water (35 ± 2 ppt). Comparing to F/2 standard media as a control treatment (CO), four treatments (A1, A2, A3, and A4) were conducted with different levels of urea as a replacement of nitrogen source, as presented in Table 1. To prepare a stock solution of urea (CH_4N_2O), 4 g was dissolved in 250 ml of distilled water and used in proportions as shown in Table(1) with 24 hours lighting for eight days and then harvested using NaOH.

Table (1): Present of media F/2 and urea.

	CO	A1	A2	A3	A4
F/2	100	0.75	0.50	0.25	0
urea	0	0.25	0.50	0.75	100

Biochemical Analysis

Dry matter: Approximately 2 g of sample was added into a pre-weighed porcelain crucible and oven-dried at 60°C for 24 h. It was then cooled in a desiccator and then weighed to a constant weight. The moisture content and dry matter (DM) content was calculated as follows:
DM (%) = 100 – Moisture (%)

Crude ash: After moisture measurement, the crucible was incinerated at 500°C for 2 h. Once cooled in a desiccator, the crucible was re-weighed.

ISSN: online 2617-2186 print 2617-2178

Crud proteins: Extraction and determination of total protein were conducted according to the methods of (Hatree, 1972; Rausch, 1981), respectively.

Crude fiber: Crude fiber was determined according to the method (Chemists & Horwitz, 1995).

Crude carbohydrates: Extraction and determination of total carbohydrates were conducted according to (Dubois et al., 1956; Myklestad & Haug, 1972), respectively.

Total lipid fatty acids profile: Total lipid and fatty acids were extracted as described by (Bligh & Dyer, 1959; Folch et al., 1957). Preparation of fatty acids methyl ester from total lipids was performed according to the procedure of (Radwan, 1978).

All analyses for the identification of fatty acid fractions were performed on GS-MS model HP (Hewlett Packard) 7890 GC equipped with a flame ionization detector. GC Conditions: Device Model: HP (Hewlett Packard) 6890GC, Column: HP-INNOWax (Polyethylene glycol), 60m, 0.25mm ID, 0.2µm film thickness. Detector: FID (Flame Ionization Detector). Detector temperature: 250°C. Injector temperature: 220°C, injection volume 3µl, split ratio 50:1.

Amino acids determination: Amino acids of *N. oculata* were analyzed by hydrolysis in 6N HCL for 22hrs at 110°C; after hydrolysis, the acid was evaporated in a vacuum oven. The residue of the algal sample was dissolved in 1 ml of sample dilution (diluting buffer) (0.2M, pH 2.2) to complete the sample dissolving. An automatic amino acid analyzer was used for amino acid determination (Dionex ICS3000) (Block, 1948).

Statistical analysis: Data were presented (n=3) as mean± standard deviation (SD). Statistical analysis was performed using analysis of the one-way (ANOVA), followed by Duncan's test was used to test for statistically significant differences between all treatments at $p < 0.05$
SPSS (2007).

RESULTS

The effect of different experimented media on the biochemical composition of *N.oculata* was presented in Table2. The total protein, lipid, and fiber content were significantly ($p<0.05$) higher in all treatments comparing to control, while the carbohydrates were significantly higher in control. In addition, the highest protein and lipid were in treatment A4 (26.44%) and A2 (17.330%) respectively, while the lowest fiber (6.18%) and carbohydrate (19.74%) were in treatment A1 and A4 respectively.

Table (2): The effect of different levels of urea on the chemical composition of marine microalgae *Nannocloropsis oceanica*

	Dry matter	Protein	Lipid	Carbohydrate	Fiber	Ash
CO	10.27 ± 0.01^{d}	22.28 ± 0.01^{e}	14.03 ± 0.01^{e}	26.44 ± 0.01^{a}	6.18 ± 0.01^{e}	20.74 ± 0.01^{b}
A1	10.68 ± 0.01^{b}	24.12 ± 0.00^{d}	17.33 ± 0.01^{a}	22.29 ± 0.01^{b}	6.35 ± 0.01^{c}	19.18 ± 0.01^{e}
A2	10.92 ± 0.01^{a}	25.50 ± 0.01^{c}	16.46 ± 0.01^{c}	21.17 ± 0.01^{c}	6.37 ± 0.01^{b}	19.52 ± 0.01^{d}
A3	10.22 ± 0.00^{e}	25.84 ± 0.01^{b}	15.46 ± 0.01^{d}	20.49 ± 0.01^{d}	6.65 ± 0.01^{a}	21.29 ± 0.01^{a}
A4	10.34 ± 0.01^{c}	26.44 ± 0.01^{a}	16.98 ± 0.01^{b}	19.74 ± 0.01^{e}	6.20 ± 0.01^{d}	20.24 ± 0.01^{c}

Mean different between CO, A1, A2, A3, A4, significant at P<0.05.

Fatty acid profile: The highest total fatty acid profile (TFA, µg/100g/DW) of *N. oculata* was obtained by CO (252.38), followed by A4 (248.26), and A3 (247.83), as presented in Table 3.The highest total saturated fatty acids (TSFA) was obtained by A2 (33.18%), followed by A3 (33.12%), A4 (32.69%), and CO (32.37%), while the lowest TSFA were obtained by A1 (32.24%). The highest Palmitic acid C16:0 percent was obtained in CO (22.13%) followed by A2 (21.89%), A1 A3 (21.78%), and A4 (21.36%). Myristic acid C14:0 percentages were high in A3 (4.19%), A2A4 (4.17%), CO (3.64%) and A1 (3.29%).

ISSN: online 2617-2186 print 2617-2178

Stearic acid C18:0 percentages of CO, A1, A2, A3, and A4 were 3.29 %, 3.70 %, 3.68 %, 3.59 % and 3.72 %, respectively, as shown in Table 3. On the other hand, the lowest unsaturated fatty acids (UFA) were obtained by CO (51.34%), presenting monounsaturated fatty acids (MUFA) of 24.87%, and polyunsaturated fatty acids (PUFA) of 26.47%. The highest UFA was obtained by A1 (55.39%), and consisted of MUFA of 30.25% and PUFA of 25.09.

In addition, CO obtained the highest HUFA (∑U-3 and ∑U-6), (26.47%), whereas the highest MUFA was obtained by A1 (30.25%), followed by A3 (29.17%), A4 (28.28%), A2 (27.81%), and CO (24.87%), respectively. The lowest n-3 (HUFA) was achieved by A1 (10.96%), and the highest was obtained by CO (13.71%), followed by A3 (11.40%), A4 (11.32%) and A1 (11.13%). Table 3 showed that the highest Σ U-3/ Σ U-6 ratio was recorded at CO (1.07), followed by A4 (0.88), A2 (0.85), A3 (0.83), and the lowest ratio was obtained by A1 (0.79). As well as the highest Docosahexaenoic acid (DHA) was achieved by (8.17%), A3 (7.64%), A4 (7.58%), and A1 (7.39%), while the lowest was achieved by A2 (7.21%), as shown in Table 3.

Table (3): Fatty acids profiles (% total fatty acid) TFA (µg/100g/DW) of selected *N.oculata*.

Fatty acid	CO	A1	A2	A3	A4
TFA (µg/100g/DW	252.38	245.78	244.78	247.83	248.26
C14:0 (Myristic acid)	3.61±0.04^{c}	3.28±0.01^{d}	4.16±0.01^{b}	4.18±0.01^{a}	4.16±0.01^{bb}
C15:0 (Pentadecylic acid)	0.57±0.01^{d}	0.64±0.02^{b}	0.64±0.01^{bb}	0.68±0.01^{a}	0.63±0.01^{c}
C16:0 (Palmitic acid)	22.12±0.01^{a}	21.77±0.01^{c}	21.88±0.01^{b}	21.77±0.02^{cc}	21.35±0.01^{d}
C17:0 (Margaric acid)	0.23±0.01^{d}	0.43±0.01^{b}	0.38±0.01^{c}	0.45±0.01^{a}	0.38±0.01^{cc}
C18:0 (Stearic acid)	3.28±0.02^{e}	3.60±0.01^{c}	3.68±0.01^{b}	3.58±0.01^{d}	3.71±0.02^{a}
C21:0 (Heneicosanoic acid)	0.92±0.01^{a}	0.85±0.01^{d}	0.91±0.02^{b}	0.86±0.01^{c}	0.83±0.01^{e}
C24:0 (Lignoceric acid)	1.56±0.01^{a}	1.51±0.02^{c}	1.47±0.01^{d}	1.53±0.02^{b}	1.56±0.01^{aa}
∑Saturated (SFA)	32.29	32.08	33.12	33.05	32.62
C14:1 (Myristoleic acid)	0.13±0.01^{c}	0.14±0.01^{b}	0.16±0.02^{a}	0.12±0.01^{d}	0.12±0.01^{dd}
C15:1 (cis-10-pentadecenoic acid)	0.06±0.01^{c}	0.07±0.01^{b}	0.09±0.01^{a}	0.06±0.01^{cc}	0.06±0.01^{cd}
C16:1 (Palitoleic acid)	4.77±0.02^{e}	5.16±0.01^{b}	5.09±0.01^{d}	5.14±0.01^{c}	5.18±0.01^{a}
C17:1(cis-10-Heptadecenoic acid)	0.40±0.01^{e}	0.42±0.01^{d}	0.46±0.01^{a}	0.43±0.01^{c}	0.45±0.01^{b}
C20:1 (Paullinic acid)	2.92±0.01^{a}	1.47±0.02^{c}	1.52±0.01^{b}	1.41±0.02^{e}	1.44±0.01^{d}
C18:1n9 (Oleic acid)	15.86±0.01^{e}	22.54±0.01^{a}	20.04±0.01^{d}	21.53±0.01^{c}	20.55±0.01^{b}
C22:1 (Erucic acid methyl)	0.68±0.01^{a}	0.40±0.01^{c}	0.38±0.01	0.42±0.01^{b}	0.40±0.01^{cc}
∑Monosaturated (MUFA)	24.82	30.20	27.74	29.11	28.20
C18:2n6 (Linoleic acid)	11.68±0.01^{e}	13.40±0.01^{b}	12.35±0.01^{c}	13.51±0.02^{a}	12.26±0.01^{d}
C18:3n6 (y-Linoleic acid)	0.15±0.01^{c}	0.22±0.01^{a}	0.20±0.01^{b}	0.22±0.01^{aa}	0.20±0.01^{bb}
C18:3n3 (α- Linoleic acid)	1.42±0.01^{a}	0.86±0.01^{d}	0.90±0.01^{c}	0.83±0.02^{e}	0.91±0.02^{b}
C20:2n6 (Eicosadienoic acid)	0.90±0.01^{a}	0.37±0.01^{b}	0.32±0.01^{e}	0.36±0.01^{c}	0.34±0.02^{d}
C20:5n-3 (Ecosapentaenoic acid)	4.12±0.01^{a}	2.86±0.01^{c}	2.83±0.01^{d}	2.91±0.02^{b}	2.81±0.02^{e}
C22:6n-3 (Docosahexaenoic acid)	8.16±0.01^{a}	7.38±0.01^{d}	7.20±0.01^{e}	7.63±0.01^{b}	7.57±0.01^{c}
∑Polyunsaturated (PUFA)	26.45	25.09	23.80	25.46	24.09
∑Usaturated	51.27	55.29	51.54	54.57	52.29
Sat./Monosat.	1.30	1.06	1.19	1.14	1.16
Sat./Polsat.	1.22	1.28	1.39	1.30	1.35
Sat./Unsat.	0.63	0.58	0.64	0.61	1.35
∑U-3	13.70	11.10	10.93	11.37	11.29
∑U-6	12.76	13.99	12.87	14.09	12.80
∑U-3/∑U-6	1.07	0.79	0.85	0.81	0.88
EPA/DHA	0.51	0.39	0.39	0.38	0.37
DHA/EPA	1.98	2.58	2.54	2.62	2.69

ISSN: online 2617-2186 print 2617-2178

Amino acids analysis: Amino acid profiles of different experimented media were presented in Table 4. The present study revealed that there is no change in the amino acid profile between the different media. In contrast, there is a clear variation in the content of each individual amino acid between the different treatments. The results showed that *N. oculata* recorded the highest percentage of essential amino acids EAA (51.54%) by A4 medium (100% urea), while the lowest value was achieved by CO medium (100% F/2). The results showed that the highest four EAA in the A1 medium were arginine (5.67%), leucine (7.92%), phenylalanine (5.64%), and threonine (5.30%), as presented in Table 4. The most abundant four NEAA in the CO medium were glutamine (11.89%), aspartate (9.70%), proline (7.90%), and alanine (6.60%), as presented in Table 4.

Table (4): Amino acids profiles (%) in *N.oculata* of different level urea and F/2 media.

Amino acid	CO	A1	A2	A3	A4
Essential amino acids (EAA)					
Arginine	5.09±0.01^{e}	5.63±0.01^{d}	5.21±0.02^{c}	5.30±0.01^{b}	5.67±0.01^{a}
Histidine (HIS)	1.69±0.01^{e}	2.27±0.01^{d}	2.73±0.02^{c}	2.88±0.02^{b}	2.92±0.01^{a}
Isoleucine (ILE)	5.09±0.01^{c}	4.49±0.01^{e}	4.66±0.01^{d}	4.42±0.01^{b}	5.05±0.02^{a}
Leucine (LEU)	8.19±0.01^{a}	6.51±0.02^{e}	6.66±0.02^{d}	6.64±0.01^{b}	7.92±0.02^{c}
Lysine (LYS)	4.09±0.01^{e}	4.70±0.01^{d}	5.12±0.01^{c}	4.35±0.02^{b}	4.51±0.02^{a}
Methionine (MET)	2.49±0.01^{e}	3.44±0.02^{d}	3.83±0.02^{c}	4.80±0.01^{b}	4.92±0.01^{a}
Phenylalanine (PHE)	5.69±0.01^{a}	5.47±0.01^{e}	4.62±0.01^{d}	5.36±0.02^{c}	5.46±0.01^{b}
Threonine (THR)	4.59±0.01^{c}	4.06±0.01^{e}	4.43±0.01^{d}	5.26±0.02^{b}	5.30±0.01^{a}
Tryptophan (TRP)	2.49±0.01^{e}	3.40±0.01^{d}	4.25±0.01^{c}	4.32±0.01^{b}	4.43±0.01^{a}
Valine (VAL)	5.09±0.01^{a}	4.69±0.01^{e}	5.18±0.01^{d}	5.25±0.01^{c}	5.36±0.02^{b}
Total EAA	44.50	44.66	46.69	48.06	51.54
Alanine (ALA)	6.60±0.02^{a}	5.76±0.02^{b}	5.39±0.02^{d}	5.36±0.02^{e}	5.41±0.02^{c}
Aspartate (ASP)	9.70±0.01^{a}	9.61±0.01^{b}	9.43±0.01^{c}	7.57±0.01^{d}	6.63±0.01^{e}
Cystine (C-C)	3.64±0.01^{e}	4.41±0.01^{d}	5.01±0.01^{c}	5.62±0.01^{a}	5.52±0.01^{b}
Glutamate (GLU)	11.89±0.02^{c}	11.63±0.02^{d}	12.27±0.02^{b}	12.54±0.02^{a}	10.71±0.02^{e}
Glycine (GLY)	5.27±0.01^{c}	5.31±0.01^{b}	5.42±0.01^{a}	4.72±0.01^{d}	4.75±0.01^{e}
Proline (PRO)	7.90±0.01^{a}	7.57±0.01^{b}	7.34±0.01^{c}	6.58±0.01^{e}	7.13±0.01^{d}
Serine (SER)	5.20±0.01^{b}	5.63±0.01^{a}	4.29±0.01^{d}	4.68±0.01^{c}	4.24±0.01^{e}
Tyrosine (TYR)	5.30±0.01^{b}	5.42±0.01^{a}	4.16±0.01^{d}	4.93±0.01^{c}	4.07±0.01^{e}
Total NEAA	55.5	55.34	53.31	51.94	48.46
EAA/NEAA	0.80	0.81	0.88	0.93	1.07
NEAA/EAA	1.25	1.24	1.14	1.08	0.94

DISCUSSION

The production cost of microalgae utilized as live food in marine hatcheries is nearly 30% of the total cost of the fish larva production (Borowitzka, 1997). However, if stable and economical microalgae production can be developed, the production cost of marine fish larvae will decrease. The present study showed that additions of urea to replace F/2 medium, to reduce the cost production of marine fish larvae production enhance the medium culture of *N. oculata* (the most important species used in marine hatcheries). Using *N. oculata* grown on urea achieved biochemical composition (such as lipid, protein, fiber, and carbohydrates), and the amino acids from the fatty acids are close to those cultured on F/2 Guillard medium.

Although F/2 Guillard medium has been widely used in the cultivation of microalgae for more than fifty years, nowadays, due to different applications of microalgae in biotechnology fields, F/2 Guillard medium has some disadvantages, such as its price and materials used for installation. Additions of urea in all replacement levels could increase protein while carbohydrate contents were decreased in *N. oc-*

ISSN: online 2617-2186 print 2617-2178

ulata. Simultaneously to the increase of protein quantity, carbohydrate amount tended to decrease in the microalgal species studied (Otero & Fábregas, 1997). High microalgae protein content can be explained by the intake of nitrogen internally from urea media.

The results of this study indicated that some urea formulas obtained significant ($P < 0.05$) biochemical composition higher than F/2, to optimize the production of *N. oculata* for aquaculture purposes in marine hatcheries. A possible explanation for the protein content in microalgae is that it results from nitrogen consumption, which is assumed to have arisen due to the abundant absorption of nitrates. Protein in all ratios was close to the result (Lourenço et al., 1998; Millán-Oropeza et al., 2015; Paes et al., 2016).

The accumulation of high concentrations of carbohydrates may contribute to enlarge cells. (Dean et al., 2010; Lourenço & Vieira, 2004; Millán-Oropeza et al., 2015; Paes et al., 2016; Traller & Hildebrand, 2013).

As for lipid concentrations, these results are similar to those found by (Li et al., 2008; Machado & Lourenço, 2008; Millán-Oropeza et al., 2015; Paes et al., 2016). Fiber was higher than CO and was, therefore, higher than what was found by (Kalpa W et.al., 2015).

Fatty acids: Several pieces of research concluded the presence of UFAs in algae lipids; they have been considered as wellsprings of PUFAs for the aquaculture industry, as stated by (Patil et al., 2005).

Oleic acid was recorded in *N.oculata*, and these results are also consistent with those of his findings (Ötleş & Pire, 2001). Furthermore, (Gerasimenko et al., 2010) stated that algal lipids could be a source of polyunsaturated fatty acids (PUFAs) of ω-3 and ω-6 series. In this current study, PUFAs ω-6 have been detected with nearly high concentrations in *N.oculata*. These results were higher than the results of (Cavonius et al., 2015; Malakootian et al., 2015; Olofsson et al., 2014), who revealed that the PUFAs contents in *N.oculata* were low, which is due to the type of media used.

Typical amino acid analysis of experimented microalgae is shown in Table 4. It indicated the presence of essential amino acids in the profile of screened microalgae. Essential amino acids cannot be made by the body, as a result, they must come from food. From the nine essential amino acids, seven are found in the profile of algae: Histidine, Leucine, Methionine, Phenylalanine, Threonine, Tryptophan, and Valine.

The high protein content of various microalgae species is one of the main reasons to consider them as an unconventional source of protein (Soletto et al., 2005) which is well-illustrated by the great interest in microalgae as a single-cell protein (SCP) during the 1950s. In addition, the amino acid pattern of almost all algae compares favorably with that of other food proteins. Since the cells are capable of synthesizing all amino acids, they can provide the ones essential to humans and animals (Guil-Guerrero et al., 2004). As other bioactive compounds are synthesized by microalgae, amino acids, especially the free amino acids, vary greatly between species as well as with growth conditions and growth phase (MA, 1988). The amino acid profile of the experiment showed a good pattern including essential amino acids which cannot be produced by the human body. These are needed to be absorb by external sources. The results were higher than what was reached by (Safi et al., 2013) for the same algae with a different type and ratio of nitrogen source, and also with the results of (Safi et al., 2014).

CONCLUSION

The study showed that the percentage of protein was higher in A4, fat percentage was higher in A1, fiber was higher in A1, and carbohydrates were higher in A3.

In summary, using urea as a source of nitrogen at different rates gives high protein and fat rati-

ISSN: online 2617-2186 print 2617-2178

os as well as the essential amino acids and fatty acids content of the microalgae.

REFERENCES

Ashour, M., & Kamel, A. (2017). Enhance growth and biochemical composition of Nannochloropsis oceanica cultured under nutrient limitation using commercial agricultural fertilizers. *J. Mar. Sci. Res. Dev, 7*, 233 .

Bligh, E. G., & Dyer, W. J. (1959). A rapid method of total lipid extraction and purification. *Canadian journal of biochemistry and physiology, 37*(8), 911-917 .

Block, R. J. (1948). Quantitative estimation of amino acids on paper chromatograms. *Science (Washington), 108*, 608-609 .

Bondioli, P ،.Della Bella, L., Rivolta, G., Zittelli, G. C., Bassi, N., Rodolfi, L., Casini, D., Prussi, M., Chiaramonti, D., & Tredici, M. R. (2012). Oil production by the marine microalgae Nannochloropsis sp. F&M-M24 and Tetraselmis suecica F&M-M33. *Bioresource technology, 114*, 567-572 .

Borges-Campos, V., Barbarino, E., & Lourenço, S. d. O. (2010). Crescimento e composição química de dez espécies de microalgas marinhas em cultivos estanques. *Ciência Rural, 40*(2), 309-317 .

Borowitzka, M. A. (1997). Microalgae for aquaculture: opportunities and constraints. *Journal of applied phycology, 9*(5), 393-401 .

Boyce, D. G., Lewis, M. R., & Worm, B. (2010). Global phytoplankton decline over the past century. *Nature, 466*(7306), 591-596 .

Carvalho, A. P., Monteiro, C. M & ،.Malcata, F. X. (2009). Simultaneous effect of irradiance and temperature on biochemical composition of the microalga Pavlova lutheri. *Journal of applied phycology, 21*(5), 543-552 .

Cavonius, L. R., Albers, E., & Undeland, I. (2015). pH-shift processing of Nannochloropsis oculata microalgal biomass to obtain a protein-enriched food or feed ingredient. *Algal research, 11*, 95-102 .

Chemists, A. o. O. A., & Horwitz, W. (1995). *Official methods of analysis* (Vol. 222). Association of Official Analytical Chemists Washington, DC .

da Silva, A. F., Lourenço, S. O., & Chaloub, R. M. (2009). Effects of nitrogen starvation on the photosynthetic physiology of a tropical marine microalga Rhodomonas sp. (Cryptophyceae). *Aquatic botany, 91*(4), 291-297 .

Dean, A. P ،.Sigee, D. C., Estrada, B., & Pittman, J. K. (2010). Using FTIR spectroscopy for rapid determination of lipid accumulation in response to nitrogen limitation in freshwater microalgae. *Bioresource technology, 101*(12), 4499-4507 .

Dubois, M., Gilles, K. A ،.Hamilton, J. K., Rebers, P. t., & Smith, F. (1956). Colorimetric method for determination of sugars and related substances. *Analytical chemistry, 28*(3), 350-356 .

Field, C. B., Behrenfeld, M. J., Randerson, J. T., & Falkowski, P. (1998). Primary production of the biosphere: integrating terrestrial and oceanic components. *Science, 281*(5374), 237-240 .

ISSN: online 2617-2186 print 2617-2178

Folch, J., Lees, M., & Stanley, G. S. (1957). A simple method for the isolation and purification of total lipides from animal tissues. *Journal of biological chemistry, 226*(1), 497-509 .

Gerasimenko, N., Busarova, N., & Moiseenko, O. (2010). Seasonal changes in the content of lipids, fatty acids, and pigments in brown alga Costaria costata. *Russian journal of plant physiology, 57*(2), 205-211 .

Grobbelaar, N. (2014). *Rising powers in international development: the state of the debate in South Africa* .

Guil-Guerrero, J., Navarro-Juárez, R., López-Martınez, J., Campra-Madrid, P., & Rebolloso-Fuentes, M. (2004). Functional properties of the biomass of three microalgal species. *Journal of food engineering, 65*(4), 511-517 .

Guillard, R. R., & Ryther, J. H. (1962). Studies of marine planktonic diatoms: I. Cyclotella nana Hustedt, and Detonula confervacea (Cleve) Gran. *Canadian journal of microbiology, 8*(2 .239-229 ،(

Hatree, E. (1972). Determination of protein: a modification of the Lowry method that gives a linear photometric response. *Anal Biochem., 48*, 422-427 .

Hu, Q., Sommerfeld, M., Jarvis, E., Ghirardi, M., Posewitz, M., Seibert, M., & Darzins, A .(2008) .Microalgal triacylglycerols as feedstocks for biofuel production: perspectives and advances. *The plant journal, 54*(4), 621-639 .

Kalpa W. S., Ju-Young Ko, Md. Mahfuzur R. Shah, Ji-Hyeok Lee, Min-Cheol K., Kwon O-Nam, Joon-Neda S., Ali M.L, N. Alnajar, Mehrouz D., Shadman S., Mohammad H. and Ali C. .(2015). Biochemical and Physiological Characterization of Tree Microalgae spp. as Candidates for Food Supplement. Journal of Applied Biotechnology Reports, Volume 3, Issue 1, Winter ; 377-381.

Kaye, Y., Grundman, O., Leu, S., Zarka, A., Zorin, B., Didi-Cohen, S., Khozin-Goldberg, I., & Boussiba, S. (2015). Metabolic engineering toward enhanced LC-PUFA biosynthesis in Nannochloropsis oceanica: Overexpression of endogenous Δ12 desaturase driven by stress-inducible promoter leads to enhanced deposition of polyunsaturated fatty acids in TAG. *Algal research, 11*, 38 .398-7

Lee Chang, K. J., Nichols, P. D., & Blackburn, S. I. (2013). More than biofuels ‐ Potential uses of microalgae as sources of high ‐ value lipids. *Lipid Technology, 25*(9), 199-203 .

Li, Y., Horsman, M., Wang, B., Wu, N., & Lan, C. Q. (2008). Effects of nitrogen sources on cell growth and lipid accumulation of green alga Neochloris oleoabundans. *Applied microbiology and biotechnology, 81*(4), 629-636 .

Lim, D. K., Garg, S., Timmins, M., Zhang, E. S., Thomas-Hall, S. R., Schuhmann, H., Li, Y., & Schenk ،P. M. (2012). Isolation and evaluation of oil-producing microalgae from subtropical coastal and brackish waters. *PLoS ONE, 7*(7), e40751 .

Lourenco, S. O., Barbarino, E., Mancini-Filho, J., Schinke, K. P., & Aidar, E. (2002). Effects of different nitrogen sources on the growth and biochemical profile of 10 marine microalgae in batch culture: an evaluation for aquaculture. *Phycologia, 41*(2), 158-168 .

ISSN: online 2617-2186 print 2617-2178

Lourenço, S. O., Barbarino, E., Marquez, U. M. L., & Aidar, E. (1998). Distribution of intracellular nitrogen in marine microalgae: basis for the calculation of specific nitrogen ‐ to ‐ protein conversion factors. *Journal of Phycology, 34*(5), 798-811 .

Lourenço, S. O., & Vieira, A. A. (2004). Culture collections of microalgae in Brazil: progress and constraints. *Nova Hedwigia*, 149-173 .

MA, B. (1988). Vitamins and fine chemicals from Microalgae: Borowitzka, MA and Borowitzka, LJ, Cambridge University Press

Machado, R., & Lourenço, S. (2008). Propriedades nutricionais de microalgas usadas como alimento de moluscos bivalves: uma revisão. Museu Nacional. *Série Livros, 30*, 281-304 .

Malakootian, M., Hatami, B., Dowlatshahi, S., & Rajabizadeh, A. (2015). Optimization of culture media for lipid production by Nannochloropsis oculata for Biodiesel production. *Environmental Health Engineering and Management Journal, 2*(3), 141-147 .

Millán-Oropeza, A., Torres-Bustillos, L. G., & Fernández-Linares, L. (2015). Simultaneous effect of nitrate (NO3-) concentration, carbon dioxide (CO2) supply and nitrogen limitation on biomass, lipids, carbohydrates and proteins accumulation in Nannochloropsis oculata. *Biofuel Research Journal, 2*(1), 215-221 .

Myklestad, S., & Haug, A. (1972). Production of carbohydrates by the marine diatom Chaetoceros affinis var. willei (Gran) Hustedt. I. Effect of the concentration of nutrients in the culture medium. *Journal of Experimental Marine Biology and Ecology, 9*(2), 125-136 .

Olofsson, M., Lamela, T., Nilsson, E., Bergé, J.-P., Del Pino, V., Uronen, P., & Legrand, C. (2014). Combined effects of nitrogen concentration and seasonal changes on the production of lipids in Nannochloropsis oculata. *Marine drugs, 12*(4), 1891-1910 .

Otero, A., & Fábregas, J. (1997). Changes in the nutrient composition of Tetraselmis suecica cultured semicontinuously with different nutrient concentrations and renewal rates. *Aquaculture, 159*(1-2), 111-123 .

Ötleş, S., & Pire, R. (2001). Fatty acid composition of Chlorella and Spirulina microalgae species. *Journal of AOAC international, 84*(6), 1708-1714 .

Paes, C. R., Faria, G. R., Tinoco, N. A., Castro, D. J ،.Barbarino, E., & Lourenço, S. O. (2016). Growth, nutrient uptake and chemical composition of Chlorella sp. and Nannochloropsis oculata under nitrogen starvation. *Latin American Journal of Aquatic Research, 44*(2), 275-292 .

Patil, V., Reitan, K. I., Knutsen, G., Mortensen, L. M., Källqvist, T., Olsen, E., Vogt, G., & Gislerød, H. R. (2005). Microalgae as source of polyunsaturated fatty acids for aquaculture. *Plant Biol, 6*(6), 57-65 .

Radwan, S. (1978). Coupling of two-dimensional thin-layer chromatography with gas chromatography for the quantitative analysis of lipid classes and their constituent fatty acids. *Journal of Chromatographic Science, 16*(11), 538-542 .

ISSN: online 2617-2186 print 2617-2178

Rausch, T. (1981). The estimation of micro-algal protein content and its meaning to the evaluation of algal biomass I. Comparison of methods for extracting protein. *Hydrobiologia, 78*(3), 237-251 .

Rodolfi, L., Chini Zittelli, G., Bassi, N., Padovani, G., Biondi, N., Bonini, G., & Tredici, M. R. (2009). Microalgae for oil: Strain selection, induction of lipid synthesis and outdoor mass cultivation in a low ‐ cost photobioreactor. *Biotechnology and bioengineering, 102*(1), 100-112 .

Safi, C., Charton, M., Pignolet, O., Silvestre, F., Vaca-Garcia, C., & Pontalier, P.-Y. (2013). Influence of microalgae cell wall characteristics on protein extractability and determination of nitrogen-to-protein conversion factors. *Journal of applied phycology, 25*(2), 523-529 .

Safi, C., Charton, M., Ursu, A. V., Laroche, C., Zebib, B., Pontalier, P.-Y., & Vaca-Garcia ،C. (2014). Release of hydro-soluble microalgal proteins using mechanical and chemical treatments. *Algal research, 3*, 55-60 .

Soletto, D., Binaghi, L., Lodi, A., Carvalho, J., & Converti, A. (2005). Batch and fed-batch cultivations of Spirulina platensis using ammonium sulphate and urea as nitrogen sources. *Aquaculture, 243*(1-4), 217-224 .

Spolaore, P., Joannis-Cassan, C., Duran, E., & Isambert, A. (2006). Commercial applications of microalgae. *Journal of bioscience and bioengineering, 101*(2), 87-96 .

Templeton, D. W., & Laurens, L. M. (2015). Nitrogen-to-protein conversion factors revisited for applications of microalgal biomass conversion to food, feed and fuel. *Algal research, 11*, 359-367 .

Traller, J. C., & Hildebrand, M. (2013). High throughput imaging to the diatom Cyclotella cryptica demonstrates substantial cell-to-cell variability in the rate and extent of triacylglycerol accumulation. *Algal research, 2*(3), 244-252 .

Wijffels, R. H., & Barbosa, M. J. (2010). An outlook on microalgal biofuels. *Science, 329*(5993), 796-799 .

Zeng, X., Danquah, M. K., Chen, X. D., & Lu, Y. (2011). Microalgae bioengineering: from CO2 fixation to biofuel production. *Renewable and Sustainable Energy Reviews, 15*(6), 3252-3260.

ISSN: online 2617-2186 print 2617-2178

تأثير مستويات مختلفة من اليوريا كونها مصدرا للنيتروجين على التركيب الكيميائي للطحالب البحرية المجهرية نانوكلوروبس أوكولاتا

على محمود أبوغرارة

قسم الموارد البحرية، كلية الموارد الطبيعية وعلوم البيئة، جامعة عمر المختار، البيضاء، ليبيا

تاريخ الاستلام: 10 يونيو 2019 / تاريخ القبول: 30 يناير 2021

Doi:https://doi.org/10.54172/mjsc.v36i1.5

المستخلص: يجب أن تكون وسائط تربية الطحالب الدقيقة فعالة من حيث التكلفة، وتتيح نموًا عاليًا، وتفي بالمتطلبات الدقيقة، وتكون متاحة بسهولة. تم تقييم تأثير المستويات المختلفة من اليوريا [25 ، 50 ، 75 و 100٪] في وسط النمو على المكونات الكيميائية الحيوية (البروتين، والكربوهيدرات، والدهون، والأحماض الدهنية، والأحماض الأمينية) في نانو كلوروبس أوكولاتا مقارنةً بـ F / 2 جيلارد كوسط قياسي. أوضحت النتائج المتحصل عليها أن المكونات الكيميائية للطحلب قد تأثرت بالمستويات المختلفة لليوريا المستخدمة. تم الحصول على أعلى نسبة بروتين باستخدام بيئة الزرع A4 (100٪ يوريا) (26.44٪) و A3 وسط (75٪ يوريا) (25.84٪)، وأعلى نسبة من الأحماض الأمينية الأساسية (EAA) (51.54٪) باستخدام بيئة الزرع A4 (100٪ يوريا) بالمقارنة مع الوسط القياسي (100٪ F / 2). تم تحقيق أعلى محتوى إجمالي للدهون باستخدام بيئة الزرع A1 (25٪ يوريا) ينتج (17.33٪) وبيئة الزرع A4 (100٪ يوريا) (16.98٪). وفقًا لذلك، تم تسجيل أعلى نسبة إجمالية للأحماض الدهنية المشبعة (TSFA) للطحلب بواسطة بيئة الزرع A3. خلصت الدراسة الى ان اضافة اليوريا هي ساسة ممتازة لزيادة المكونات الكيميائية وتجمع الدهون. أوصت الدراسة الحالية بإمكانية استخدام بيئة الزرع A4 المقترح كونها محفزا للدهون، أو بيئة الزرع A1 كونها محفزا للبروتين.

الكلمات المفتاحية: الأحماض الأمينية، الأحماض الدهنية، الطحالب البحرية المجهرية، التركيب الكيميائي.

*على محمود أبوغرارة amhofm1963@gmail.com قسم الموارد البحرية ، كلية الموارد الطبيعية وعلوم البيئة ، جامعة عمر المختار ، البيضاء ، ليبيا

Al-Mukhtar Journal of Sciences 36 (1): 12-23, 2021

Measurements of Radioactivity Concentrations in Granites and Sedimentary-Rocks and their Leaching Components in Egyptian Deserts

Salha D. Y. Alsaadi, Jemila Mussa Ali, Areej Hazawi and Asma Mohammed AL-abrdi.
Physics Department, Faculty of Science, Omar Al-Mukhtar University, Libya.

Received: 09 January 2020/ Accepted: 30 January 2021
Doi: https://doi.org/10.54172/mjsc.v36i1.6

Abstract: Concentrations of radionuclides in sediments and granite samples were determined by γ-ray spectrometer using High Pure Germanium Detector; HPGe, with a specially designed shield. Six different rock samples were collected from different sites: four samples of sediments from Um Bogma southwest Sinai, and two granite samples from Gabal Gattar, the northern part of the Eastern Desert of Egypt, where all samples were subject to investigation. Their samples were selected because the activity before being dissociated in sulfuric acid was less than after dissociation. The samples were dissolved in sulfuric acid with the same parameters of solid to liquid ratio; S/L, acid concentration, and leaching time. After the leaching process, the pregnant solution was separated from the residual, and the latter was dried. The two units, named the pregnant solutions and residuals, were also measured radiometrically using the HPGe detector to determine the activity concentrations (Bq/kg) of the different radionuclides of the six samples. The results showed that the relation between the sum of activities of both pregnant solutions and residuals with the originals have different categories. In the sediment samples; the activity of solution+ residual was 72.37% from the original of siltstone, the activity of solution + residual was 90.02% from the original claystone sample, the activity of solution + residual was 92.6% from the original of shale, the activity of solution + residual was 74.07% from the original claystone. In the granite samples, the activity of solution + residual was 130.39% from the original of the first granite sample and 142.3% from the original of the second granite sample. This phenomenon varied in magnitude due to the different radionuclides in each sample. These variations depend mainly on the nature of the grain surfaces in the different rock types and their Pb content. As for leachability analysis, leaching experiments have been performed using sulfuric acid. The leaching efficiency (%) of uranium is estimated by the measurements of the HPGe detector. The result showed almost constant values for leachability. The non-frequent appearance of attenuation of gamma activities during leaching processes indicates that the acid solutions may have led to clean the grain surfaces and thus permit gamma activities of the inner grains to be measured. The treatment of the samples before measurements may have been needed.

Keywords: Natural Radioactivity; HPGe Detector; Sediment; Granite; Leaching

INTRODUCTION

In the leaching process, oxidation potential, temperature, and pH of the solution are important parameters, and are often manipulated to optimize the dissolution of the desired metal component into the aqueous phase (Merritt, 1971). The radium-226 (^{226}Ra) is the main radionuclide in the tailings after leaching process for uranium extraction and is highly active with its solid decay products. The main danger is not during the radioactive releases in the leaching processes only but remains for many years after the end of operations (Metzler, 2004). Sulfuric acid (H_2SO_4) as an acidic reagent is widely used for urani-

***Corresponding Author:** Salha D. Y. Alsaadi *salha.dawood@omu.edu.ly* , Physics Department, Faculty of Science, Omar Al-Mukhtar University, Libya.

um leaching because of its availability and low cost. In addition, nitric and hydrochloric acids are not only effective in uranium dissolution but also produce undesirable impurities in the leach liquor ore. Nitric acid appears to be attractive as an oxidizing agent, being suitable for later recovery processes by solvent extraction. In addition, the acid may also be generated autogenously by treating ore that has appreciable sulfides content with air or oxygens under pressure before leaching (Mahdy et al., 1996).

The physical and chemical processes used to extract uranium from ore, such as crushing and acid treatment, produce large amounts of mill tailings. In France today, approximately 50 million tons of uranium mill tailings (UMT) are stored on the surface in specific areas. They contain 99% of the radium present in the original ore and have much higher porosity and permeability than that of the rock from which they were derived. The average activity of 226Ra for French UMTs lies between 4000 and 60,000 Bq/kg. (Ferry. et al., 2002) studied the behavior of most of the different radionuclides in the uranium-238 (238U) series and thorium-232 (232Th) series during acidic leaching. They concluded that the nuclides preceding 226Ra in the 238U decay series are easily released in the pregnant solution, compared with the 226Ra itself and its solid daughters: lead (214Pb) and bismuth (214Bi) (El Aassy, et al., 2012).

Aim of the work: First to study the transfer of different radionuclides from a solid material (ore) to the liquid phase (leachate). Then to measure the activity concentrations and activity ratios of radionuclides in original, leachate, and residual using an HPGe detector.

MATERIALS AND METHODS

Samples Description and Preparation: Four samples of sediments were collected from Um Bogma, southwest Sinai, Egypt (Fig.1), and two Granite samples were collected from Gabal Gattar in the northern parts of the Eastern Desert (Asma, 2018) in fig(2). The collected samples were crushed and then quartered and packed in 250 ml bottles. The bottles were completely sealed for one month to allow radioactive equilibrium to be reached. This step is necessary to ensure that radon gas is confined within the volume and that the daughters will also remain in the sample. Four samples (Table 1) of different varieties were collected from the sedimentary rock in Um Bogma, southwest Sinai, Egypt.

Table (1): Description of the collected of sedimentary samples

Samples	Description
2S	Shale from the middle member of the Um Bogma Formation yellowish-brown, soft, fissile ferruginous with 2m thickness 6900 cps.
3S	Siltstone from the middle member of the Um Bogma Formation and overlying the previous sample, violet with brown patches, and ferruginous 0.2 m, 4200 cps.
7S	Claystone from the middle member of the Um Bogma Formation (MUF), reddish to yellowish-brown, soft to medium hard, highly ferruginous, 3500 cps.
17S	Gibbsite – bearing Shale, from the middle member of the Um Bogma Formation, yellow to brown with black patches and concretions of carbonaceous organic matter, 0.5 m, 4000 cps.

Fig. (1): Geologic map of the Um Bogma area (El Aassy et al.,1986; Omar., 2016).

ISSN: online 2617-2186 print 2617-2178

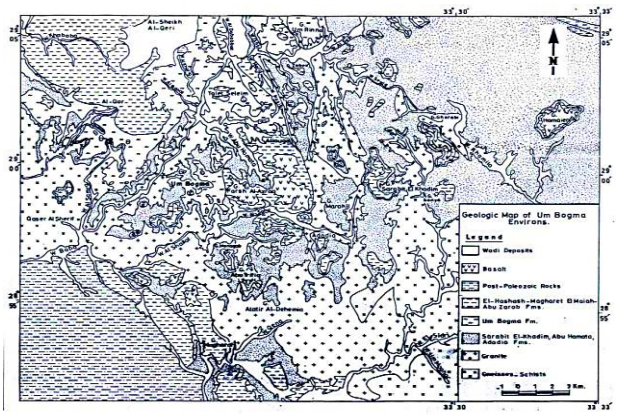

Fig. (2): Location map of G. Gattar (2). (Shalaby, et al., 2001).

Leaching experiments: The leaching process was carried out by using Sulfuric acid (H2SO4), acid leaching on 150 g sample weight under the conditions; solid/liquid ratio 1:3, acid concentration 30%, stirring time of one hour, and at room temperature. Filtration was carried out to separate leachate from residual that was then dried. The leachate was packed well in 250 ml Marinelli beakers. Also, the residual was left for one month to be measured by an HPGe-detector.

The vertically mounted HPGe detector was coupled with a multichannel analyzer card which is pre-installed on a PC. The radiation measuring system is also composed of the usual electronic components; a preamplifier, an amplifier, and power supply units. The detector has a resolution (FWHM) of 1.85 keV for the 1332.5 keV γ-ray line of cobalt (60Co). The γ-ray spectrometer energy calibration was performed using 60Co, 226Ra, and americium (241Am) point sources. The detector was surrounded by a special heavy lead shield of 10 cm thickness with an inside diameter of 28 cm and height of 40.5 cm. The absolute detection efficiency of the HPGe detector was determined by using three well-known reference materials obtained from the International Atomic Energy Agency for U, Th, and K (potassium) activity measurements: RGU-1, RGTh-1, and RGK-1 (IAEA., 1987; Anjos et al., 2005). The sample containers were placed on top of the detector for counting. The same geometry and size were used for both the samples and the reference materials (Turhan et al., 2008). The Uranium standard (RGU-1) is U-ore diluted with silica with 4940 Bq/kg of 238U, 228 Bq/kg of uranium-235 (235U), a negligible amount of 40K (less than 0.63 Bq/kg), and some traces of 232Th (less than 4 Bq/kg). The thorium standard (RGTh-1) is Th-ore diluted with silica having 3250 Bq/kg of 232 Th, but containing some 238U (78 Bq/kg) and 40K (6.3 Bq/kg).

The potassium calibration standard (RGK-1) is produced from high purity (99.8%) potassium sulfate with 14000 Bq/kg of potassium with uranium and thorium contents lower than 0.001 and 0.01 ppm (parts per million), respectively (Anjos et al., 2005).

The γ-ray transitions used to measure the concentration of the assigned nuclides in the series are as follows: 238U was determined from the gamma rays emitted by its daughter products (Sutherland and de Jong., 1990), 234Th and 234mPa activities determined from the 63.3 and 1001 keV photo peaks, respectively, 214Bi (609.3, 1120.3, 1238.1, 1377.7, and 1764.5 keV), 214Pb (295.1 and 352.0 keV). The specific activity of 226Ra was measured using the 186.1 keV from its own gamma-ray (after the subtraction of the 185.7 keV of 235U). The specific activity of 232Th was measured using the 338.4, 911.2, and 968.9 keV from 228Ac, and 583 keV from 208Tl and 40K was measured using 1460.8 keV for potassium.

In order to determine the background contribution due to naturally occurring radionuclides in the environment around the detector, an empty polyethylene beaker of the same 250 cm3 volume was counted with the same geometrical conditions as the sample. The measurement time for both activity and background set at 70,000 seconds. The background spectra were used to correct the net

ISSN: online 2617-2186 print 2617-2178

gamma-ray peak areas for the studied isotopes.

X-Ray Fluorescence (XRF) Spectrometry: XRF is used to determine the chemical analysis of major and trace elements in the samples. Detection limits for major and trace elements are typically of the order of a percent and part per million (ppm). Six samples were chosen for processing this application within the Scale of the laboratory:Four sediment samples from Um Bogma (siltstone (3S), claystone (17S), shale (2S), and (7S) claystone), and two samples of granite from Gabal Gattar. The collected technological sample had intermixed with organic-rich earthy soil materials and were crushed to a size of 200 mesh. Proper quartering of the technological sample was performed after its grinding to less than 200 mesh size to obtain a representative sample which was subjected to a complete chemical analysis of both major and trace elements content which were analyzed at the laboratories of the National Research Center (NRC), Cairo, Egypt, by the XRF technique, using Philips Unique II unit fitted with an automatic sample changer PW 1510 (30position),connected to a computer system using X-40 controlling program for spectrometry. The detection limit of the measured elements by the XRF technique was estimated to be 5ppm.

RESULTS AND DISCUSSION

The results of gamma-detector of radionuclides in original samples (Bq/kg), leachates (Bq/l), and residuals (Bq/kg) are presented in table (2, 3, 4, 5, 6, and 7) and fig (3). From this table, it is noticed that there is a difference between the sum of activities of residuals and leachates with the activity of the original sample. This difference in gamma activity is sometimes positive (+ve); the sum is greater than the original, and in other times is negative (-ve); the sum is lower than the original. This difference varied mostly with the variation of the lithological type and /or geochemical composition.

Table (2): Gamma radioactivities for different radionuclides in pregnant solution and residual (in percentages) of shale sample No. (2S)

	Sediment sample (2S)		
Radionuclide	Original [Orig.] (Bq/Kg)	Residual [Resid.] (Bq/Kg)	Solution [Sol.] (Bq/l)
^{238}U series			
234^{Th}	6159.5±31.6	7754.0±60.3	1996.8±11.2
234mPa	6483.8±152.1	5735.7±283.8	1682.6±46.1
Average	6321.7±91.9	6744.8±172.1	1839.7±28.6
234U	6127.6±674.2	6917.2±184.7	1327.4±124.5
230^{Th}	4746.4±182	1042.6±736.7	591.4±42.9
226Ra subseries			
226Ra	4841.9±14.93	7711.9±34.0	25.9±0.8
214Pb	4279.4±9.8	5536.3±18.23	17.8±0.8
214Bi	4107.1±25.4	4945±45.3	29.2±2.4
Average	4409.4±16.7	6064.4±32.5	24.3±1.3
235U	328.8±7.8	288.8±13.1	95.8±2.0
^{232}Th series			
228Ac	55.9±3.7	91.9±8.4	6.2±0.9
208Tl	60.7±2.3	64.93±4.9	6.7±0.6
Average	58.3±3	78.4±6.7	6.5±0.7
40K	342.8±13.3	619.4±28.1	143.0±4.8

ISSN: online 2617-2186 print 2617-2178

Table (3): Gamma radioactivities for different radionuclides in pregnant solution and residual (in percentages) of Siltstone sample No. (3S)

Sediment sample (3S)			
Radionuclide	Original [Orig.] (Bq/Kg)	Residual [Resid.] (Bq/Kg)	Solution [Sol.] (Bq/l)
^{238}Useries			
234Th	2610.67±22.5	2094.3±102.4	759.1±4.4
234mPa	2032.9±107.3	1817.7±527.6	568.1±21.6
Average	2321.7±64.9	1656.0±315	663.6±13.0
234U	3946.5±91.9	1346.2±401	513.1±97.5
230Th	2230.0±158.8	2972.2±218.4	92.3±7.6
^{226}Ra subseries			
226Ra	2385.8±12.2	2645.4±31.1	15.5±0.6
^{214}Pb	2099.3±7.2	2008.2±10.8	8.6±0.5
214Bi	2001.7±18.6	1807.0±31.6	2.7±0.3
Average	2162.2±12.6	2153.5±24.5	8.9±0.5
235U	114.8±5.1	94.6±9.4	28.5±1.4
^{232}Th series			
228Ac	67.8±3.5	116.1±7.8	1.4±0.01
208Tl	68.5±2.1	81.6±4.5	5.1±0.4
Average	68.2±2.7	98.9±6.1	3.2±0.2
40K	562.4±13.5	906.3±28.5	92.1±3.4

Table (4): Gamma radioactivities for different radionuclides in pregnant solution and residual (in percentages) of claystone sample No. (7S)

Sediment sample (7S)			
Radionuclide	Original [Orig.] (Bq/Kg)	Residual [Resid.] (Bq/Kg)	Solution [Sol.] (Bq/l)
^{238}U series			
234^{Th}	2941.5±22.9	3097.4±61.8	865.9±5.9
234mPa	3318.5±124.9	3345.2±28.3	518.3±25.8
Average	3130.0±73.8	3221.3±45.1	692.1±15.8
234U	3333.2±79.7	1124.3±91.1	390.9±84.3
230^{Th}	2264.7±161	1565.7±118.1	133.5±10.7
^{226}Ra subseries			
226Ra	2448.7±11.3	3230.8±32.1	62.9±1.8
214Pb	2081.9±6.94	2164.2±15.8	19.1±0.7
214Bi	1983.2±17.8	1898.1±37.2	20.6±0.8
Average	2171.2±12.0	2431.0±28.6	34.3±1.1
235U	155.8±5.3	70.9±8.2	34.5±1.8
^{232}Th series			
228Ac	59.2±3.2	54.1±6.8	8.5±1.0
208Tl	59.1±2.1	45.1±4.7	7.5±0.6
Average	59.1±2.6	49.6±5.8	8.0±0.8
40K	352.5±11.3	609.4±31.2	106.6±4.1

ISSN: online 2617-2186 print 2617-2178

Table (5): Gamma radioactivities for different radionuclides in pregnant solution and residual (in percentages) of Gibbsite sample No. (17S)

Sediment sample (17S)			
Radionuclide	Original [Orig.] (Bq/Kg)	Residual [Resid.] (Bq/Kg)	Solution [Sol.] (Bq/l)
^{238}Useries			
234Th	3724.3±30.2	3862.7±47.7	1212.3±9.5
234mPa	4482.5±150.5	2907.8±274.7	1304.7±44.6
Average	4103.0±22.5	3385.3±161.1	1258.5±27.1
234U	4198.9±86.3	3276.0±121.2	760.6±107.3
230Th	3722.8±213.9	1631.1±119.9	250.6±19.22
^{226}Ra subseries			
226Ra	4102.9±14.3	6048.5±30.6	20.2±0.8
214Pb	3322.8±8.8	3860.7±16.1	36.2±1.1
214Bi	3232.6±22.9	3299.0±38.9	40.9±3.0
Average	3552.7±15.3	4402.7±28.5	32.4±1.6
235U	190.0±6.9	161.9±13.7	54.7±2.3
^{232}Th series			
228Ac	73.9±4.4	18.5±5.3	7.3±1.2
208Tl	57.5±2.3	29.0±4.3	5.2±0.6
Average	65.7±3.4	23.7±4.8	6.3±0.9
40K	523.9±14.4	759.1±30.7	106.5±5.1

Table (6): Gamma radioactivities for different radionuclides in pregnant solution and residual (in percentages) of granite sample No. (2G).

Granite sample (2G)			
Radionuclide	Original [Orig.] (Bq/Kg)	Residual [Resid.] (Bq/Kg)	Solution [Sol.] (Bq/l)
^{238}Useries			
234Th	2589.5±21.8	1176.6±40.1	872.8±6.5
234mPa	2363.5±111.1	2043.2±23.8	727.2±30.1
Average	2476.5±66.4	1609.9±31.9	800.0±8.3
234U	2397.1±54.8	8155.3±208.2	1336.3±105.5
230Th	2269.8±109.2	3870.3±85.9	483.7±35.2
^{226}Ra subseries			
226Ra	2258.9±9.0	4293.0±31.5	2.5±0.2
214Pb	1925.9±5.8	3936.7±17.2	17.9±0.7
214Bi	1901.6±15.1	3651.3±43.4	17.9±0.4
Average	2028.8±9.9	3960.3±30.7	12.7±0.4
235U	115.1±5.5	54.5±6.3	33.0±1.5
^{232}Th series			
228Ac	88.7±3.8	132.3±11.5	3.9±0.3
208Tl	74.5±2.1	56.7±7.0	12.7±0.6
Average	81.6±2.9	94.5±9.3	8.3±0.5
40K	1195±14.6	2096.4±37.3	100.6±3.6

ISSN: online 2617-2186 print 2617-2178

Table (7): Gamma radioactivities for different radionuclides in pregnant solution and residual (in percentages) of granite sample No. (5G)

	Granite sample (5G)		
Radionuclide	Original [Orig.] (Bq/Kg)	Residual [Resid.] (Bq/Kg)	Solution [Sol.] (Bq/l)
^{238}Useries			
234Th	2705.3±19.4	1076.7±37.4	950.5±11.4
234mPa	2660.0±118.5	1049.6±31.9	992.9±49.4
Average	2682.6±68.9	1063.1±34.6	971.7±30.4
234U	2958.0±64.8	7016.0±196.1	1330.1±150.2
230Th	2549.7±180.5	3906.2±17.3	772.1±56.1
^{226}Ra subseries			
226Ra	2316.7±9.7	4100.6±31.9	23.5±0.9
214Pb	2020.1±6.3	3868.7±15.1	34.4±1.3
214Bi	2016.2±16.5	3474.9±46.6	47.2±3.6
Average	2117.6±10.8	3814.7±31.2	35.1±1.9
235U	123.7±4.8	56.2±5.8	42.4±2.5
^{232}Th series			
228Ac	95.1±4.1	112.2±7.8	13.4±1.5
208Tl	83.1±2.2	56.4±4.3	25.3±1.1
Average	89.1±3.2	84.3±6.1	19.3±1.3
40K	1264±15.8	2092.5±37.5	189.4±6.3

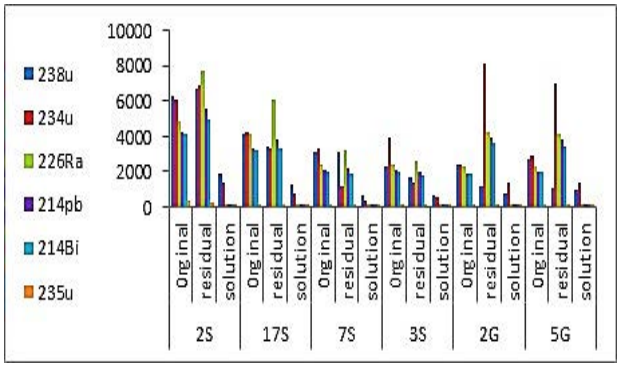

Fig. (3): Activity concentration of 238U, 234U, 226Ra, 214Bi and 235U in the original samples (Bq/kg), leachate (solution) (Bq/l) and residual (Bq/kg)

The measurements of leachability (leaching efficiency %): The chemical behavior of each radionuclides clearly varies in the same sample. The measurements of leaching efficiency % by using the HPGe detector showed that leachability is the highest (55.7%) for ^{234}U in sample (2G) table (8), while the ^{238}U is 36.2% in (5G) and ^{235}U is 34.3% in (5G).

The variation of leachability was also according to the type of sample, the increased release of ^{234}U and the variability of ^{234}U/^{238}U was observed before by several authors who mentioned that the release of excess ^{234}U could arise from preferential release from damaged lattice sites (Bourdon et al., 2009). It is worth noticing that the values of leachabilities for ^{235}U and ^{238}U are about the same for most samples, and they are almost identical for samples (2S and 7S).

^{234}U and ^{238}U have similar chemical behavior. However, in Table (8) it is noticed that the leachability % for ^{234}U is more than ^{238}U for samples (7S, 3S, 5G, 2G). So these samples have physical transfer alongside the chemical transfer of ^{234}U. The physical transfer is due to α-recoil and the natural ^{238}U decay.

ISSN: online 2617-2186 print 2617-2178

Table (8): The leachability of the chosen samples measured by HPGe.

	Radionuclide Concentration	Original	Residual	Solution	Leachability	sum	%
	^{238}U(ppm)	509.8±7.4	543.9±13.8	148.4±2.3	29.1	692.3	135.8
2S	^{234}U(ppb)	26.5±2.6	29.9±0.1	5.7±0.5	21.6	35.6	134.5
	^{235}U(ppm)	4.1±0.7	3.6±1.1	1.2±0.2	29.1	4.8	116.7
	^{238}U(ppm)	252.4±5.9	259.7±3.6	55.8±1.3	22.1	305.6	121.1
7S	^{234}U(ppb)	14.4±0.3	4.8±0.4	1.7±0.4	11.7	6.5	45.4
	^{235}U(ppm)	1.95±0.4	0.8±0.4	0.4±0.1	22.2	1.3	67.3
	^{238}U(ppm)	187.2±1.8	133.5±12.9	53.5±2.2	28.6	187.1	100
3S	^{234}U(ppb)	17.1±0.4	5.8±0.5	2.2±0.5	13.0	8.1	47.7
	^{235}U(ppm)	1.4±0.6	1.2±1.1	0.4±0	24.9	1.5	107.6
	^{238}U(ppm)	330.8±5.2	273.0±25.4	101.5±1.0	30.6	374.5	113.2
17S	^{234}U(ppb)	18.2±0.4	14.2±1.7	3.3±0.3	18.1	17.5	96.1
	^{235}U(ppm)	2.4±0.4	2.0±0.8	0.7±0.1	28.8	2.7	113.9
	^{238}U(ppm)	190.6±5.3	94.8±2.5	64.5±0.7	33.85	159.4	83.6
2G	^{234}U(ppb)	10.4±0.2	35.3±0.9	5.7±0.5	55.74	41.1	396.1
	^{235}U(ppm)	1.4±0.4	0.3±0.5	0.4±0.1	28.66	0.8	52.4
	^{238}U(ppm)	216.3±5.6	86.88±2.8	78.4±2.4	36.22	165.3	76.4
5G	^{234}U(ppb)	12.80±0.3	30.37±0.8	5.7±0.6	44.96	36.12	282.2
	^{235}U(ppm)	1.54±0.0	0.35±0.4	0.5±31	34.32	0.88	57.1

ppm = part per million ppb= part per billion

Table (9): Major elements in sediment and granite samples

Major	3S %	17S %	2S %	7S %	2G %	5G %
SiO_2	39.57	28.608	21.451	20.998	70.755	70.45
Al_2O_3	26.38	16.31	14.297	12.66	13.041	13.092
TiO_2	0.199	0.927	0.529	0.454	0.115	0.107
Fe_2O_3	4.063	23.195	41.024	35.696	3.536	3.654
MnO	0.014	2.168	0.069	0.099	0.055	0.055
CaO	1.963	0.246	0.247	0.612	1.458	1.504
MgO	0.772	0.763	0.459	0.537	0.293	0.334
Na_2O	4.999	3.587	1.575	7.434	5.344	5.475
K_2O	0.132	2.004	0.859	0.765	5.094	4.973
P_2O_5	0.132	0.069	0.062	0.06	0.032	0.034
SO_3	2.22	0.427	0.389	0.129	0.094	0.083

ISSN: online 2617-2186 print 2617-2178

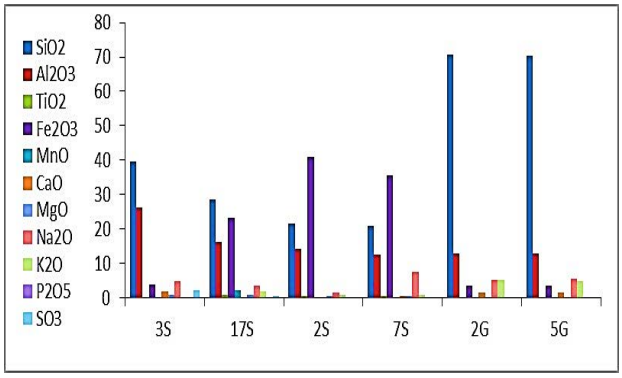

Fig. (4): The concentration of major elements in the selected sample

From Table (9), it is obvious that the sample of siltstone (3S) has a high level of loss on ignition. Silica, alumina, and iron oxide contents are 39.57, 26.38, and 4.06% respectively.
The claystone sample (17S) has a high level of loss on ignition. Silica, alumina, and high iron oxide contents are 28.60, 16.31, and 23.19% respectively. The shale sample (2S) has a high content of loss on ignition. Silica, alumina, and iron oxide contents are 21.45, 14.29, and 41.02% respectively. The claystone sample (7S) has a high loss on ignition, attaining silica, alumina, and high iron oxide contents of 20.998, 12.66, and 35.69% respectively.

The chemical analysis of the two granite ore samples (2G, 5G) shows they are mainly composed of SiO2 and Al2O3 as 70.7% and 13% respectively for 2G, and 70.35% and 13.09% respectively for sample 5G. Meanwhile, a total ignition loss of about 1% was obtained at 1000 °C for the two samples 2G and5G.

Table (10) presents the trace element analysis in the samples. The more interesting detail in these results is that the sedimentary samples contain a high concentration of Cl, Cu, Zn, Ni, Pb, U, Co, Cr, and some REEs which affect the characterization of these samples and their behavior during the radioactivity measurements process as will be seen later.

Table (10): Trace elements in sediment and granite samples.

Trace	3S (ppm)	17S (ppm)	2S (ppm)	7S (ppm)	2G (ppm)	5G (ppm)
Ni	416.0	1742.7	1138.2	7300.5	0	0
Cu	127.6	718.2	0	287.2	63.8	0
Zn	2192.1	25760.2	21777.3	16573.9	176.6	168.6
Rb	91.4	164.5	0	0	329.0	319.9
Sr	591.5	371.8	321.1	202.8	0	42.2
Y	78.7	393.5	259.7	165.2	0	0
Zr	651.2	984.2	466.2	310.8	266.4	259
Nb	55.9	0	0	0	167.7	146.7
Ba	143.2	349.0	0	0	0	0
Ce	230.3	3684.9	0	0	0	0
Pb	798.1	1688.9	1865.2	204.1	111.3	102.1
CL	2887	22510	11570	33240	0	630
U	250	1020	1050	300	280	280
V	0	5488	5488	0	0	0
Co	0	2130.0	0	550.2	0	0
Rh	0	110	0	0	0	0
Mo	0	0	226.4	159.8	0	0
Nd	0	0	0	154.2	0	0
As	0	0	0	332.0	0	0
Cr	465.1	0	362.5	259.9	143.6	157.3

ISSN: online 2617-2186 print 2617-2178

From Tables (2 and 5), the lithological type played its role as in sample 7S in which the sum of gamma activity is lower by 20% than the activity of the original sample. The geochemical composition is very clear in samples 2S, 3S, and 17S. In these samples, the lead (Pb) content is 1865.3 ppm, 798 ppm, and 1689 ppm respectively, as shown in Table (10). The sum of γ- activity in leachate and residual is higher than the original sample. The sum is higher by 26.3% than the original in the sample 2S, while it is higher by 11.6% in the sample 17S respectively. The relation between the gamma attenuation and (Pb) concentration is very clear in Fig (5), in which the gamma attenuation increases with the increase of the Pb concentration in the measured sample.

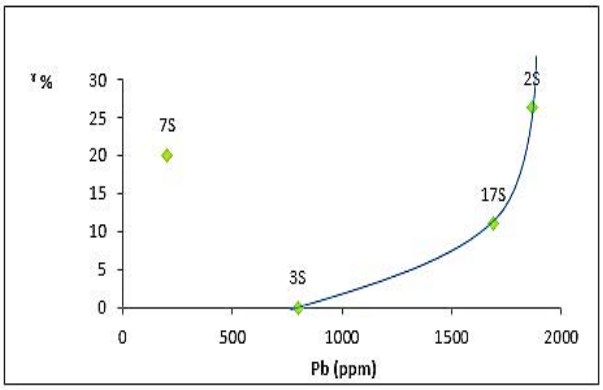

Fig. (5): Correlation between γ – attenuation and Pb concentration on sediment samples.

CONCLUSION

The results showed that the sum of activities of both pregnant solutions and residuals in four samples is higher than that of the originals. Two samples (siltstone sample 3S) and (granite 5G) showed lower summation than the original. This phenomenon is varied in magnitude within the different radionuclides. The type of samples plays its role in these variations. The none-frequent appearance of the gamma attenuation activities is inevitable during the leaching process. In other logical cases, no attenuation or other causes for altering the measured activities are observed. In the leaching process, using acid solutions may have led to clean the grain surface and permitted gamma activities of the inner grains to be measured, which means that the treatment of samples before measurements may have been needed.

REFERENCES

Anjos, R., Veiga, R., Soares, T., Santos, A., Aguiar, J., Frascá, M., Brage, J., Uzêda, D., Mangia, L., & Facure, A. (2005). Natural radionuclide distribution in Brazilian commercial granites. *Radiation measurements, 39*(3), 245-253.

Asma M Abdulrahman, (2018). *Assessment of natural radioactivity levels and radiation hazards of radionuclides released from granite and different sedimentary rock types*, Thesis for the Ph.D. To Physics Department Faculty of women for Art, Science and Education, Ain Shams University.

Bourdon, B., Bureau, S., Andersen, M. B., Pili, E., & Hubert, A. (2009). Weathering rates from top to bottom in a carbonate environment. *Chemical Geology, 258*(3-4), 275-287.

El Aassy, I., Botros, N., Abdel Razik, A., Sherif, H., Al Moafy, A., Atia, K., El Terb, R., & Ashami, A. (1986). Report on the prospection and proving of some radioactive occurrences in West Central Sinai. *Egypt. Inter. Report, NMA, Cairo, 12p*.

El Aassy, I. E., Nada, A. A., El Galy, M. M., El Feky, M. G., Abd El Maksoud, T. M., Talaat, S. M., & Ibrahim, E. M. (2012). Behavior and environmental impacts of radionuclides during the hydrometallurgy of calcareous and argillaceous rocks, southwestern Sinai, Egypt. *Applied radiation and isotopes, 70*(6), 1024-1033.

ISSN: online 2617-2186 print 2617-2178

Ferry, C., Richon, P., Beneito, A., & Robé, M.-C. (2002). Evaluation of the effect of a cover layer on radon exhalation from uranium mill tailings: transient radon flux analysis. *Journal of environmental radioactivity, 63*(1), 49-64.

IAEA, P. (1987). *certification of IAEA gamma spectrometry reference materials RGU-1, RGTh-1 and RGK-1*.

Mahdy, M., & El-Hazek, M. (1998). Leaching characteristics of Wadi Belih uraniferous Hammamat sediments, eastern desert, Egypt.

Merritt, R. C. (1971). Extractive metallurgy of uranium.

Metzler, D.R., 2004. Uranium Mining: Environmental Impact. *Encyclopedia of Energy*, 6: 299-315.

Omer, A. (2016). *Geo-environmental and radioactivity assessment of East Abu Zenima area, Southwestern Sinai, Egypt, using remote sensing and GIS* Ph. D Thesis, Suez Canal Univ., Fac. of Sci., Geol. Dept., Ismailia, Egypt.

Shalaby, M., & Moharem, A. (2001). Geochemistry and radioelement distribution in the fresh and altered hammamat sedimentary rocks along Wadi Baligh, North Eastern Desert, Egypt. *Sedimentology of Egypt: journal of the Sedimentological Society of Egypt, 9*, 145.

Sutherland, R., & De Jong, E. (1990). Statistical analysis of gamma-emitting radionuclide concentrations for three fields in southern Saskatchewan, Canada. *Health physics, 58*(4), 417-428.

Turhan, Ş., & Gündüz, L. (2008). Determination of specific activity of 226Ra, 232Th and 40K for assessment of radiation hazards from Turkish pumice samples. *Journal of environmental radioactivity, 99*(2), 332-342.

ISSN: online 2617-2186 print 2617-2178

قياسات تركيزات النشاط الإشعاعي في الصخور الرسوبية والجرانيت ومكونات الترشيح الخاصة بها في الصحاري المصرية

صالحه ذاوود يوسف الساعدي، جميلة موسى علي، أريج إبراهيم هزاوي وأسماء محمد العبردي

قسم الفيزياء، كلية العلوم، جامعة عمر المختار، مدينة البيضاء، ليبيا.

تاريخ الاستلام: 09 يناير 2020 / تاريخ القبول: 30 يناير 2021

Doi:https://doi.org/10.54172/mjsc.v36i1.6

المستخلص: أجريت عملية قياس تركيزات النويدات المشعة في عينات الرسوبيات والجرانيت بواسطة مطياف الأشعة باستخدام كاشف الجرمانيوم عالي النقاوة مدرع مصمم خصيصًا لهذه القياسات. تم جمع ستة عينات صخرية مختلفة من مواقع مختلفة؛ أربع عينات من الصخور الرسوبية جمعت من أم بوقما في جنوب غرب سيناء، وعينتين من الجرانيت من جبل قطار بالصحراء الشرقية في مصر. تم اختيار عيناتها لان النشاط قبل الذوبان في حمض الكبريتيك اقل من النشاط بعد الذوبان. أذيبت العينات الستة من الصخور المختلفة في حمض الكبريتيك مع مراعاة الظروف نفسها، من حيث نسبة العينة الصلبة إلى المذيب (S / L)، تركيز الحمض المذيب، وزمن الإذابة، ثم تمت عملية ترشيحها. بعد عملية الترشيح، فصل المحلول عن المتبقي وتم تجفيف الأخير، وأجريت عملية قياس النشاط الإشعاعي لهما باستخدام كاشف الجرمانيوم عالي النقاوة لتحديد تركيزات النشاط (بيكريل/كجم) للنويدات المشعة المختلفة للعينات الست. أظهرت النتائج أن العلاقة بين مجموع أنشطة كل من المحاليل والمتبقيات والأصل لها فئات مختلفة. في العينة الأولى لعينات الرواسب، كان نشاط المحلول والمتبقي 72.37 ٪ من الأصل للطمي المتحجر، ونشاط المحلول والمتبقي 90.02 ٪ من عينة الحجر الطيني، ونشاط المحلول والمتبقي 92.6 ٪ من الأصل للحجر الصخري (الزيتي)، ونشاط المحلول والمتبقي 74.07 ٪ من الأصل للعينة الطينية. أما في عينات الجرانيت، كان نشاط المحلول والمتبقي 130.39 ٪ من العينة الأصلية الأولى من الجرانيت و142.3 ٪ من العينة الأصلية الثانية من الجرانيت. تختلف هذه الظاهرة في المقادير بسبب النويدات المشعة المختلفة في كل عينة. تعتمد هذه الاختلافات بشكل أساسي على طبيعة أسطح الحبيبات في أنواع الصخور المختلفة ومحتواها من الرصاص. أما بالنسبة لتحليل القابلية للترشيح، فقد تم إجراء تجارب الترشيح باستخدام حامض الكبريتيك. وتقدير كفاءة ترشيح اليورانيوم (٪) من خلال قياسات جهاز الكشف HPGe. أظهرت النتيجة قيمًا ثابتة تقريبًا لقابلية الترشيح. يشير الظهور غير المتكرر للتوهين لأنشطة جاما أثناء عمليات الترشيح إلى أن المحاليل الحمضية قد تؤدي إلى تنظيف أسطح الحبوب، وبالتالي تسمح بقياس أنشطة جاما للحبوب الداخلية. قد تكون هناك حاجة إلى معالجة العينات قبل القياسات.

الكلمات المفتاحية: لنشاط الإشعاعي الطبيعي، كاشف HPGe، الرسوبيات، الجرانيت، الترشيح.

*1 صالحة ذاوود الساعدي salha.dawood@omu.edu.ly ، قسم الفيزياء ، كلية العلوم ، جامعة عمر المختار ، مدينة البيضاء ، ليبيا.

Al-Mukhtar Journal of Sciences 36 (1): 24-33, 2021

Size Structure of *Cupressus sempervirens* L. and *Pistacia lentiscus* L. Populations in Wadi Alkuf, East of Libya

Mabroka A. G. Abdalrhim
Department of Botany, Faculty of Arts and Science - Al marj, Benghazi University, Libya

Received: 15 November 2020/ Accepted: 30 January 2021
Doi: https://doi.org/10.54172/mjsc.v36i1.7

Abstract: Wadi Alkuf is one of the richest of all the phytogeographical regions of Al-Jabal Al-Akhder. The present work aims to study the size structure of *Cupressus sempervirens* L. and *Pistacia lentiscus* L. populations in relation to their physiographic and soil conditions in Wadi Alkuf, northeast of Libya. Eighteen terraces (25 m × 25 m) were selected at Wadi Alkuf of Al-Jabal Al-Akhder at three different levels (six downstream, midstream, and upstream). The number of individuals of each species was counted while the height (H) and mean crown diameter (D) were measured. The size index of each individual was calculated and then used to classify the population into 7 size classes: 1 m to 7 m. The height, mean diameter, height to diameter ratio, size index, and volume per individual in each size class were determined. Generally, the height to diameter ratio was more than unity for *C. sempervirens* L., this means that the diameter of these species tend to expand vertically rather than horizontally, while the height to diameter ratio was less than unity for *P. lentiscus* L, this means that the diameter of these species tends to expand horizontally rather than vertically. The total size structure of *C. sempervirens* L. in the study area is characterized by the preponderance of the young individuals comparing with the old ones, while that of *P. lentiscus* L. showed a reverse pattern (i.e., preponderance of mature individual compared with the young ones). Five forms of size distributions along the different elevations were recognized: more or less inverse J-shaped distribution, positively skewed distribution, bell-shaped distribution, more or less J-shaped distribution, and more or less stationary size distribution biased to large size. The study's results show that density histograms of size distributions are good indicators of future trends in population numbers for the studied species. The field observations were consistent with the results of the investigation of soil properties. The soil downstream has the highest values of pH, EC, HCO^{-3}, SO_4^{-2}, Cl^- and Na^+, while that of the upstream has the lowest values except for K^+.

Keywords: Population Dynamic; Size Distribution; *Cupressus sempervirens* L.; *Pistacia lentiscus* L.; Wadi Alkuf, Libya.

INTRODUCTION

The human impacts and their effects on plant vegetation and biodiversity became a field of major interest in the last few years. Many human activities occurred in the AL-Jabal AL-Akhdar area as a result of an increase in the development activities and growth of the population (Kamal Shaltout et al., 2014).

Although this region is one of the important areas of wildlife in Libya, it suffers from extreme biodiversity destruction and degradation. It is imperative now, more than ever, to begin extensive environmental studies and conservation programs, including not only soil and biodiversity conservation but also beauty conservation and attention to local inhabitants because they play an important role in the ecological systems throughout the whole area (El-Barasi & Saaed, 2013). The main natural reasons affecting these degradation processes are often climate and aridity, which lead to a reduction in the plant cover

***Corresponding Author:** Mabroka A. G. Abdalrhim *mabrokagbril@yahoo.com*, Department of Botany, Faculty of Arts and Science - Al marj, Benghazi University, Benghazi, Libya.

and soil depth. Besides these, the human-induced reasons leading to this process are fires, felling, and overgrazing (Kosmas, Kirkby, & Geeson, 1999); Desertlinks, 2001).

There is no doubt that these activities adversely affected not only size structure but also species diversity in the area under study. The structure of plant populations can be described in terms of the age, size, and forms of the individuals that compose it (J. Harper & White, 1974). Since the fecundity and survival of plants are often much more closely related to size than to age (Caswell, 1986; J. L. Harper, 1977; KH Shaltout & Ayyad, 1988; Watkinson & White, 1986; Weiner, 1986), it is better to classify the life history of plants by size rather than age which is the most widely used classification for unitary organisms (Caswell, 1986; Kirkpatrick, 1984; Werner & Caswell, 1977)

The present study aimed at analyzing the population structure of *Cupressus sempervirens* and *Pistacia lentiscus* populations in Wadi Alkuf. *Cupressus sempervirens*, the Mediterranean cypress, is a species of cypress native to the eastern Mediterranean region, in northeast Libya, southern Albania, southern coastal Croatia (Dalmatia), southern Greece, southern Turkey, Cyprus, northern Egypt, western Syria, Lebanon, Israel, Malta, Italy, western Jordan, and also a disjunct population in Iran. *Cupressus sempervirens* is a tall tree (usually 15 - 20 m high but can reach 30 - 40 m) with a well-developed trunk (up to 3 m in circumference). It grows quickly until the age of 20 and can live to be 500. Its leaves are evergreen, dark green, acicular (in young stages), or very small, scale-like, and overlapping in four ranks. The female cones are globular (2 - 4 cm.), shiny, with 6-12 woody, peltate, unequal scales, opposed crosswise on a short axis (Zohary, 1973). The seeds are jagged, shiny brown, and narrowly winged. Flowering takes place in spring; the cones mature the following spring. The Cupressus genus includes, for the sake of convenience, an aggregate called *Cupressus sempervirens* aggr, formed by a group of three species that are often confused and usually very close to each other (Greuter, Burdet, & Long, 1984); Farjon, 2013).

Pistacia lentiscus is a shrub or dioecious tree, with separate male and female plants, an evergreen from 1 to 5 m high, with a strong smell of resin, growing in dry and rocky areas in Mediterranean Europe. It resists heavy frosts and grows on all types of soils, and can grow well in limestone areas and even in salty or saline environments, making it more abundant near the sea. It is also found in woodlands, Dehesas (almost deforested pasture areas), oak and Kermes oak woods, Garrigue, Maquis, hills, gorges, canyons, and rocky hillsides of the entire Mediterranean area. It is a very typical species that grows in Mediterranean mixed communities of myrtle, Kermes oak, Mediterranean dwarf palm, buckthorn, sarsaparilla, etc., and serves as protection and food for birds and other fauna in this ecosystem. It is a very hardy pioneer species dispersed by birds. When older, it develops large trunks and numerous thicker and longer branches. Within appropriate areas, when allowed to grow freely and age, it often becomes a tree of up to 7 m. However, logging, grazing, and fires often prevent its development (Mohannad G & Duncan M, 2011; Zohary, 1952).

The present work aims to study the size structure of *Cupressus sempervirens* L. and *Pistacia lentiscus* L. populations in relation to their physiographic and soil conditions in Wadi Alkuf, northeast of Libya.

MATERIALS AND METHODS

Wadi Alkuf is located at 32° 41' N latitude and 21° 38' E longitude, at an altitude of 360 m in Al Jabal Al Akhder of Libya (Figure. 1). The valley is about 22 km long, starting from Benghazi-Albayda road towards the north and ends in the Mediterranean Sea. The soil

ISSN: online 2617-2186 print 2617-2178

varies from clay to clay loam at different locations. It is rich in calcium carbonate (25%) with pH 8 and nitrogen. Organic matter content were about 0.33 and 7%. The average annual rainfall in the valley is 450.5 mm, most of which is received during the months from December to February. The temperature shows significant fluctuations in summer and winter. The minimum temperature drops to 12° on cold frosty nights of January, and the maximum rises up to 27° in June. Relative humidity ranges from 50-55 (May and June) to 65-70% (November to January) Source: Meteorological data of Shahat station (Figure.2).

Figure: (1). Location map indicating the study area. (Source: Google Earth, 2016).

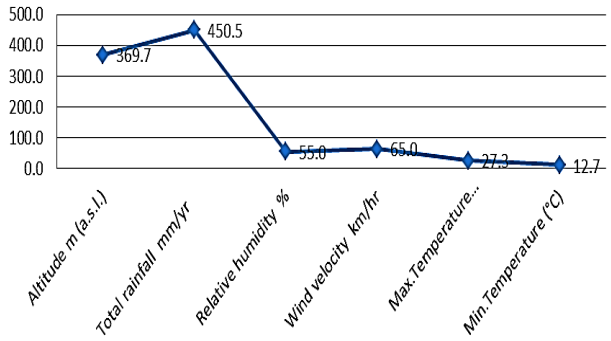

Figure: (2). Metrological data recorded at Shahat from January 2018 to January 2019.

A total of 18 sample plots were selected along the Wadi Alkuf under study (upstream, midstream, and downstream parts, including the different wadi tributaries) in the period from January 2018 to January 2019. Vegetation was sampled using a transect/quadrant method. A stratified sampling technique was utilized. The stand size was 25 × 25 m (approximate the minimal area of the plant communities). In each stand, the following data were recorded: 1- a list of species, 2- first and second dominant species, and 3- a visual estimate of the percentage total cover and the cover of each species according to the Braun-Blanquet dominance abundance scale. Voucher specimens of all plant species were collected. Species identification followed (Ali & Jafri, 1976; Jafri, 1977, 1993; Tackholm & Boulos, 1974), and the Latin names were following (Boulos, 1972, 1977; Boulos, 1979; Boulos, 1995; Boulos, 2005, 2009; Loutfy & Boulos, 1979).

The population structure of these species was evaluated in terms of size distribution. For achieving this, the height and mean crown diameter of each individual in the whole locations were measured (based on 2-4 diameter measurements / ind.) and its volume was calculated as a cylinder. The size index of each individual was calculated as the mean of its height and diameter [(H+D)/2]. The size estimates were then used to classify the population into nine size classes. The size classes (m / ind.) are (1=0< 1, 2=1.1-2, 3=2.1–3, 4=3.1–4, 5=4.1–5, 6=5.1–6 and 7= 6.1–7). The soil was analyzed following (Richards, 1954; Ryan, Garabet, Harmsen, & Rashid, 1996). The data were statistically treated using ANOVA and the simple linear correlation coefficient (SPSS, 1999).

RESULTS

The relationships between the individual heights and diameters of *Cupressus* and *Pistacia* species are simple linear with r values of 0.335 for *Cupressus sempervirens* and 0.279 for *Pistacia lentiscus* (Figure 5). Generally, the height to diameter ratio was more than unity for *Cupressus sempervirens*. This means that the diameter of these species tends to expand vertically rather than hori-

ISSN: online 2617-2186 print 2617-2178

zontally, while the height to diameter ratio was less than unity for *Pistacia lentiscus*. This means that the diameter of these species tends to expand horizontally rather than vertically.

Cupressus sempervirens

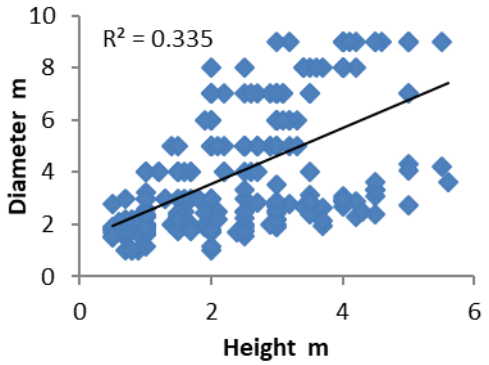

Figure: (3). The relationships between the individual heights and diameters of *Cupressus sempervirens.*

Pistacia lentiscus

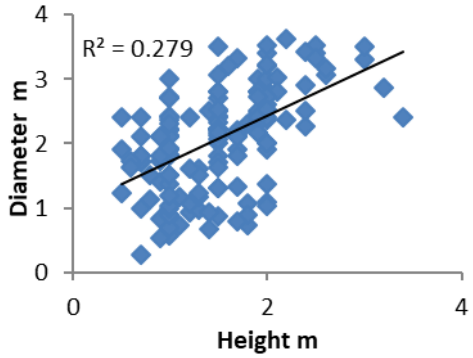

Figure: (4). The relationships between the individual heights and diameters of *Pistacia lentiscus* species.

Regarding the variation in relation to habitat type, both the height and diameter of *Cupressus sempervirens* (8.4 and 4.1 m) and *Pistacia lentiscus* (4 and 5.23 m) have the highest values downstream, respectively, and the lowest values upstream were for *Cupressus sempervirens* species (3.6 and 2.7m respectively). *Pistacia lentiscus* shows the lowest value for height and diameter in midstream (2 and 4.5m, respectively) (Table .1).

Table: (1) Mean (±) standard deviation of some demographic variables: (H: Height, D: Diameter, r simple linear correlation coefficient between height and diameter and size index.

Species	site	H (m)	D (m)	H/D	r	Size index (m)
Cupressus sempervirens L. var. horizontalis (Mill.) Gord.	Downstream	8.4 ± 3.130	4.1 ± 0.962	2.4 ± 0.645	0.964	6.75 ± 0.966
	Midstream	5.1 ± 0.629	3.1 ± 0.751	1.6 ± 0.387	0.696	4.6 ± 0.784
	Upstream	3.6 ± 0.401	2.7 ± 0.392	1.3 ± 0.111	0.534	2.5 ± 0.588
Pistacia lentiscus L.	Downstream	4 ± 0.719	5.23 ± 0.582	0.8 ± 0.253	0.551	4.5 ± 0.774
	Midstream	2 ± 8.21	4.5 ± 6.69	0.75 ± 0.301	0.263	3.15 ± 5.51
	Upstream	3± 0.326	3.5 ± 0.787	0.4 ± 0. 292	0.243	3.25 ± 0.703

The diagrams illustrating the size distribution of *Cupressus and Pistacia* populations in the three different levels could be classified into (Figure 5).

1) More or less stationary size distribution for *Cupressus sempervirens* populations in the downstream and J-shape for *Pistacia lentiscus* populations in the downstream level.

2) Inverse J shape for *Cupressus sempervirens* populations upstream and Bell shape for *Cupressus sempervirens* populations in the midstream level.

3) More or less stationary size distribution for *Pistacia lentiscus* populations downstream and Bell shape for *Pistacia lentiscus* populations in the midstream level.

4) Positively skewed distribution towards the small individuals (i.e saplings) of *Cupressus sempervirens* populations in the downstream level.

ISSN: online 2617-2186 print 2617-2178

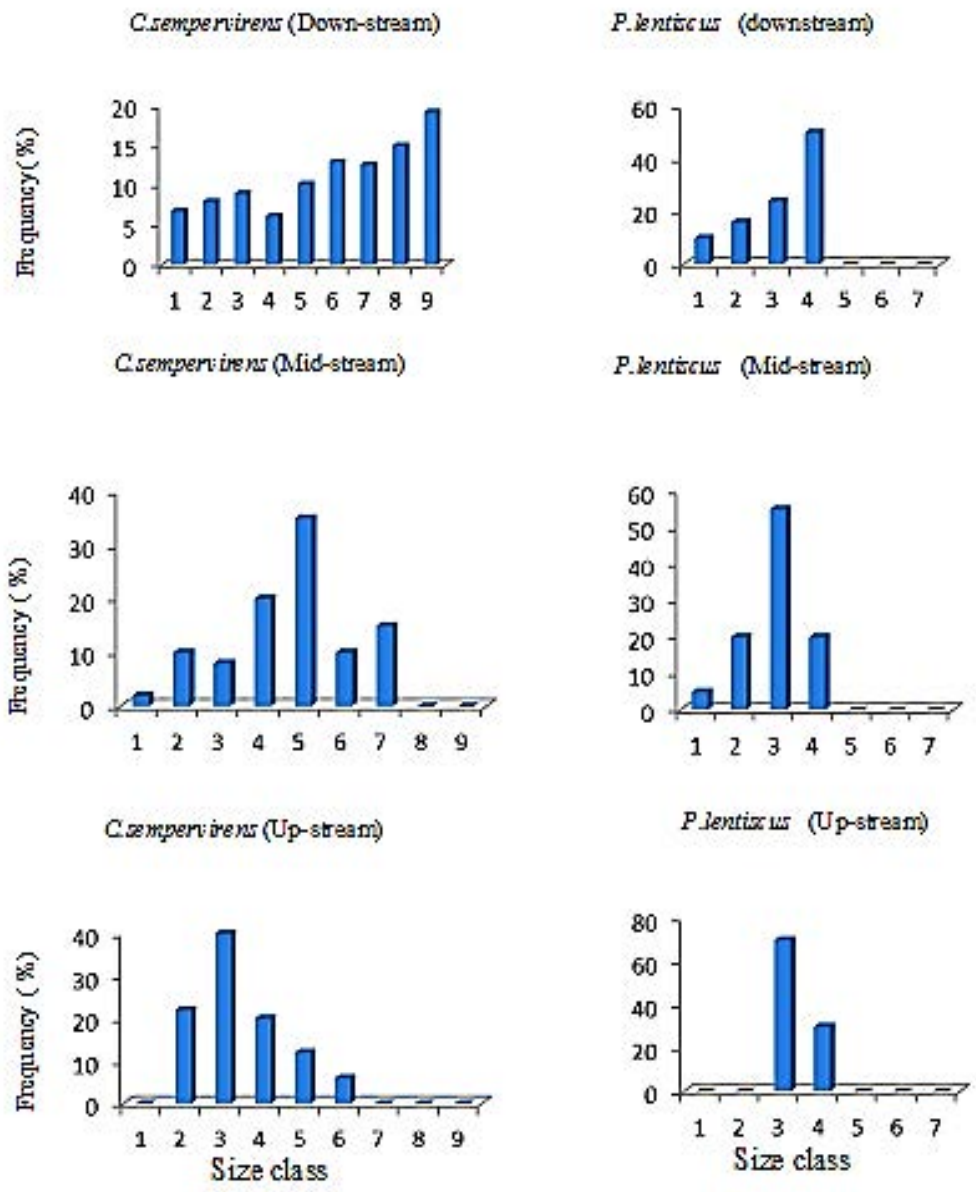

Figure: (5) Size frequency distribution of *Cupressus sempervirens and Pistacia lentiscus* populations from three levels. The mean volume within each size class is also indicated. The ranges of size classes are: 1>1 , 2=1.1-2, 3=2.1-3 ,4=3.1-4 ,5=4.1-5, 6=5.1-6, 7=6.1-7

The soil of the downstream level has the highest values of pH, EC, $HCO^{-3,}$ SO_4^{-2}, Cl^-, and Na^+ (8.20, 0.337, 3.81, 3.26, 1.9, and 1.55, respectively) while that of the upstream has the lowest values except for K^+. Calcium and magnesium have the highest values in the soil of midstream (0.28 and 0.26 respectively), while the lowest values were for Na^+ and K^+ (0.67 and 0.12, respectively). Soil of the upstream level has the lowest values of pH, EC, $HCO^{-3,}$ SO_4^{-2}, Cl^-, Ca^{+2}, Mg^{+2}, and Na^+ (7.89, 0.226, 2.54, 1.88, 1, 0.12, 0.13, and 1.12, respectively). (Table 2).

ISSN: online 2617-2186 print 2617-2178

Table: (2) Means ± standard errors of some soil variables in each of the three habitats recognized in the study area.

Sites				Downstream	Midstream	Upstream
Physical analysis	Sand (%)			10.33 ± 0.02	11.38 ± 0.017	12.34 ± 0.002
	Silt (%)			41.28 ± 0.02	30.88 ± 0.03	31.02 ± 0.01
	Clay (%)			42.31 ± 0.03	42.72 ± 0.01	48.54 ± 0. 01
	Soil texture			Clay-Silt	Clay	Clay
Chemical analysis	pH			8.20 ± 0.01	8.16± 0.03	7.89± 0.01
	E.C ds/m			0.337 ± 0.01	0.263 ± 0.01	0.226± 0.02
	HCO^{-3}			3.81 ± 0.01	3.33 ± 0.03	2.54 ± 0.01
	SO_4^{-2}	Anions	m.eq./L	3.26± 0.2	2.11± 0.01	1.88± 0.1
	CI^-			1.9± 0.01	1.30 ± 0.1	1± 0. 1
	Ca^{+2}			0.25 ± 0.1	0.28 ± 0.1	0.12 ± 0.1
	Mg^{+2}	Cations		0.16 ± 0.001	0.26 ± 0.01	0.13 ± 0.01
	Na^+			1.55 ± 0.02	1.33 ± 0.04	1.12 ± 0.01
	K^+			0.18 ± 0.1	0.12 ± 0.1	0.28 ± 0.01

DISCUSSION

The height/diameter ratio gives an idea about the growth habit of the plant. In the present study, the height to diameter ratio was more than unity for *Cupressus sempervirens,* which means that the diameter of these species tends to expand vertically rather than horizontally. While the height to diameter ratio was less than unity for *Pistacia lentiscus*, this means that the diameter of these species tends to expand horizontally rather than vertically. On average, its height and hence individuals of these species tend to expand horizontally rather than vertically.

This may be a strategy of the desert shrubs in order to provide safe sites for their self-regeneration, as the horizontal expansion usually provides shade, which leads to a decrease in the severe heating effect and an increase in the soil moisture (KH Shaltout & Mady, 1993). On the other hand, the height to diameter ratio in some species was exceeding unity, such as *Cupressus sempervirens*, which means that their individuals tend to expand vertically rather than horizontally. This may be attributed to the high density or consequently high intra-specific competition of these plants (Galal, 2011).

The distribution of plant species along elevation gradients is governed by a series of interacting biological, environmental, and historical factors (Colwell & Lees, 2000). Our results show that density histograms of size distributions are good indicators of future trends in population number for the studied species, especially for *C. sempervirens* L. Furthermore, (Gray, 1975) reported that the positively skewed distribution is indicative of a self-perpetuating species, with markedly more frequency of the smaller (younger) size classes. A similar conclusion was made by (KH Shaltout & Ayyad, 1988).

In the present study, there was more or less stationary size distribution for *Pistacia lentiscus* populations in the downstream level and Bell shape for the *Pistacia lentiscus* populations midstream. This distribution characterizes a declining population; because the population has a large proportion of larger individuals than smaller ones (i.e., limited regeneration capacity). This may indicate that the recruitment of these species is rare, which may be related to hyper-aridity and low fertility (Kamal Shaltout et al., 2014; K. H. Shaltout et al., 2015).

The study endeavors to establish factors related to local management; that may have caused the declines that we can observe. It is

ISSN: online 2617-2186 print 2617-2178

recognized that there are undoubtedly many reasons for such degradation in the natural vegetation. These include the nature of the soils, the extreme weather, alongside human land use. Assumptions are often made in terms of landscape change, desertification, and climate change, but the role of local inhabitants and their impacts may outweigh other influences. This may be due to the soil in Wadi El-Kouf. The nature of the soil surface characteristics is one of the most important factors influencing the floristic richness of the landforms along with the climatic variations.

CONCLUSION

In conclusion, the total size structure of *C. sempervirens* L. in the study area is characterized by the preponderance of the young individuals compared with the old ones. While that of *P. lentiscus* L. showed a reverse pattern (i.e., the preponderance of mature individuals compared with the young ones).

REFERENCES

Ali, S., & Jafri, S. (1976). Flora of Libya. 1-24. *Department of Botany, El-Faateh University, Tripoli*.

Boulos, L. (1972). Our present knowledge on the Flora and vegetation of Libya bibliography. *Webbia, 26*(2), 365-400.

Boulos, L. (1977). *A Check-list of the Libyan Flora*.

Boulos, L. (1979). A Check-List Of The Libyan Flora. Iii. Compositae.(By C. Jeffrey).

Boulos, L. (1995). Flora of Egypt. Checklist.

Boulos, L. (2005). Flora of Egypt. Volume 4. Monocotyledons: Al Hadara Publishing, Cairo. 617pp.

Boulos, L. (2009). Flora of Egypt checklist, revised annotated edition. *Al-Hadara Publishing, Cairo*, 198-201.

Caswell, H. (1986). Life cycle models for plants. *Lectures on mathematics in the life sciences, 18*, 171-233.

Colwell, R. K., & Lees, D. C. (2000). The mid-domain effect: geometric constraints on the geography of species richness. *Trends in ecology & evolution, 15*(2), 70-76.

Desertlinks, (2001). Combating desertification in Mediterranean Europe: linking science with stakeholders (2001-2005, EU funding), International and interdisciplinary research project funded by the European Commission under Framework Programme 5.

El-Barasi, Y. M. M., & Saaed, M. W. B. (2013). Threats to plant diversity in the north eastern part of Libya (El-Jabal El-Akahdar and Marmarica Plateau). *Journal of Environmental Science and Engineering. A, 2*(1A), 41.

Farjon, A. (2013). *Cupressus sempervirens* - Version 2014.2. The International Union for Conservation of Nature (IUCN) Red List of Threatened Species.

Galal, T. M. (2011). Size structure and dynamics of some woody perennials along elevation gradient in Wadi Gimal, Red Sea coast of Egypt. *Flora-Morphology, Distribution, Functional Ecology of Plants, 206*(7), 638-645.

Gray, B. (1975). Size-composition and regeneration of Araucaria stands in New Guinea. *The Journal of Ecology*, 273-289.

Greuter, W., Burdet, H. M., & Long, G. (1984). *Med-checklist*: Secretariat Med-

ISSN: online 2617-2186 print 2617-2178

Checklist, Botanischer Garten & Botanisches Museum Berlin-Dahlem.

Harper, J., & White, J. (1974). The demography of plants. *Annual review of ecology and systematics, 5*(1), 419-463.

Harper, J. L. (1977). Population biology of plants. *Population biology of plants.*

Jafri, S. (1977). Cistaceae in SMH Jafri & El. Gadi (eds.) Flora of Libya no. 48: Tripoli.

Jafri, S. (1993). Cistaceae in SMH Jafri & El. Gadi (eds.) Flora of Libya no. 48: Tripoli.

Kirkpatrick, M. (1984). Demographic models based on size, not age, for organisms with indeterminate growth. *Ecology, 65*(6), 1874-1884.

Kosmas, C., Kirkby, M. J., & Geeson, N. (1999). *The Medalus Project: Mediterranean desertification and land use: Manual on key indicators of desertification and mapping environmentally sensitive areas to desertification*: Directorate-General Science, Research and Development.

Loutfy, B., & Boulos, L. (1979). A Check-List Of The Libyan Flora. Ii: Salicaceae To Neuradaceae.

Mohannad G, A.-S., & Duncan M, P. (2011). Taxonomic revision of the genus Pistacia L.(Anacardiaceae). *American Journal of Plant Sciences, 2012*.

Richards, L. A. (1954). *Diagnosis and improvement of saline and alkali soils* (Vol. 78): LWW.

Ryan, J., Garabet, S., Harmsen, K., & Rashid, A. (1996). A soil and plant analysis manual adapted for the West Asia and North Africa region. *ICARDA, Aleppo, Syria, 140*.

Shaltout, K., & Ayyad, M. (1988). Structure and standing crop of Egyptian Thymelaea hirsuta populations. *Vegetatio, 74*(2), 137-142.

Shaltout, K., Fawzy, M., Galal, T., Awad, M., El‐Barasi, Y., & Saeed, B. (2014). Impact of waste water discharge on the plant communities and size structure of Wadi El‐Shees, Al‐Jabal Al‐Akhdar, Libya. *Feddes Repertorium, 125*(1‐2), 1-13.

Shaltout, K., & Mady, M. (1993). Current situation of the raudha's woody plant populations in the Central Saudi Arabia With 3 Figures and 3 Tables. *Feddes Repertorium, 104*(7‐8), 503-509.

Shaltout, K. H., Fawzy, M., Ahmed, D. A., Awad, M. h. A., El‐Barasi, Y. M., & Al‐hasi, S. M. (2015). Impact of waste water discharge on the plant diversity and community structure of Al‐Marj Plain, Libya. *Feddes Repertorium, 126*(1‐2), 6-15.

SPSS Inc. (1999). SPSS 10.0 for Windows: Statistics. SPSS Inc., Chicago, IL.

Tackholm, V., & Boulos, L. (1974). Students' flora of Egypt.

Watkinson, A. R., & White, J. (1986). Some life-history consequences of modular construction in plants. *Philosophical Transactions of the Royal Society of London. B, Biological Sciences, 313*(1159), 31-51.

Weiner, J. (1986). How competition for light and nutrients affects size variability in Ipomoea tricolor populations. *Ecology, 67*(5), 1425-1427.

ISSN: online 2617-2186 print 2617-2178

Werner, P. A., & Caswell, H. (1977). Population growth rates and age versus stage‐distribution models for teasel (Dipsacus sylvestris Huds.). *Ecology, 58*(5), 1103-1111.

Zohary, M. (1952). A monographical study of the genus Pistacia. *Palestine Journal of Botany (Jerusalem Series), 5*(4), 187-228.

Zohary, M. (1973). *Geobotanical foundations of the Middle East*: Fischer.

ISSN: online 2617-2186 print 2617-2178

التوزيع الحجمي لمجموعات السرو *Cupressus sempervirens L.* و البطوم *Pistacia lentiscus L.* في وادي الكوف شرق ليبيا

مبروكة عبدالله جبريل عبدالرحيم

قسم علم النبات، كلية الآداب والعلوم، المرج، جامعة بنغازي – ليبيا

تاريخ الاستلام: 15 نوفمبر 2020/ تاريخ القبول: 30 يناير 2021

Doi:https://doi.org/10.54172/mjsc.v36i1.7

المستخلص : وادي الكوف من أغنى المناطق الجغرافية النباتية في الجبل الأخضر. يهدف البحث الحالي إلى دراسة التركيب الحجمي لأفراد السرو *Cupressus sempervirens L.* والبطوم *Pistacia lentiscus L.* فيما يتعلق بظروف التربة في وادي الكوف شمال شرق ليبيا. تم اختيار ثمانية عشر مدرجًا (25 م × 25 م) في وادي الكوف بالجبل الأخضر على ثلاثة مستويات مختلفة (ستة في أعلى الجبل، ستة في المنتصف، وستة أسفل المجري). تم تقييم التركيبة السكانية لكل نوع وتم قياس الارتفاع (H) و متوسط قطر تاج الشجرة (D) لعدد من الأفراد لكل الأنواع. و حساب مؤشر الحجم لكل فرد باستخدام التصنيف السكاني إلى 7 فئات: 1 م إلى 7 م. تم تحديد الارتفاع ، متوسط القطر ، نسبة الارتفاع إلى القطر، مؤشر الحجم، والحجم لكل فرد في كل فئة حجم. بشكل عام كانت نسبة الارتفاع إلى القطر أكثر في السرو *C. sempervirens L.* وهذا يعني أن قطر هذه الأنواع يميل إلى التوسع عموديا بدلا من أفقيا، في حين كانت نسبة الارتفاع للقطر أقل في البطوم *P. lentiscus L.* ، وهذا يعني أن قطر هذه الأنواع يميل إلى التوسع أفقيا بدلا من عموديا. يتسم هيكل الحجم الكلي للسرو *C. sempervirens L.* في منطقة الدراسة بغلبة صغار السن مقارنة مع الكبار ، بينما أظهر البطوم *P. lentiscus L.* نمطًا عكسيًا (أي كثرة الفرد الناضج مقارنة بالصغار). تم التعرف على خمسة أشكال لتوزيعات الحجم على طول الارتفاعات المختلفة: توزيع عكسي على شكل حرف (J) إلى حد ما ، توزيع منحرف إيجابي ، توزيع على شكل جرس ، توزيع على شكل(J) أكثر أو أقل، وتوزيع حجم ثابت إلى حد ما منحاز إلى الحجم الكبير. أظهرت نتائج الدراسة أن الرسوم البيانية للكثافة لتوزيعات الحجم هي مؤشرات جيدة للاتجاهات المستقبلية في عدد السكان للأنواع المدروسة. كانت الملاحظات الميدانية متوافقة مع نتائج التحقيق في خصائص التربة. تحتوي تربة أسفل المجري على أعلى قيم الأس الهيدروجيني و EC و HCO^{-3} و SO_4^{-2} و Cl^- و Na^+ ، بينما تحتوي تربة أعلي الجبل على أدنى قيم باستثناء K^+ .

الكلمات المفتاحية : ديناميكا سكانية، التوزيع الحجمي، السرو، البطوم، وادي الكوف، ليبيا.

*[1] مبروكة عبدالله جبريل عبدالرحيم mabrokagbril@yahoo.com، قسم علم النبات . كلية الآداب و العلوم المرج . جامعة بنغازي – ليبيا.

Al-Mukhtar Journal of Sciences 36 (1): 34-41, 2021

Topical Cyclosporine A 0.05% for the Treatment of Dry Eye Disease

Naeima M. Elzlitni , Samar A. Bukhatwa * and Sabah S. Eldressi

Ophthalmology Department, Faculty of medicine, University of Benghazi, Bengahzi, Libya.

Received: 04 January 2021/ Accepted: 31 January 2021
Doi: https://doi.org/10.54172/mjsc.v36i1.8

Abstract: Dry eye disease (DED) is a common clinical condition that challenges ophthalmologists. Topical Cyclosporine A is an anti-inflammatory therapy being approved by the Food and Drug Administration (FDA) for the therapy for DED. This study aimed to evaluate the efficacy and patient tolerability of topical Cyclosporine A 0.05% for the treatment of DED. A total of 87 patients diagnosed with DED were included in this study. Dry eye symptoms (foreign body sensation, burning, and pain) were scored. As a baseline measurement, the tear break-up time test (TBUT) and the Schirmer's test were performed for all the patients. Cyclosporine A 0.05% was given topically twice daily to all the patients for four months. They were followed up every month for a period of four months. The clinical signs (Schirmer's test, the TBUT), and the symptoms scores, were recorded for each visit. The mean age of the patients was 57.25±9.70 years (Range 32 - 80 years); 25 males (28.7%) and 62 females (71.3%). Out of them, 23 (26.4%) cases had Sjögren's syndrome, and 12 (13.7%) cases had previous LASIK (laser in-situ keratomileusis). The symptoms score of the cases improved from (4.95±1.73) pretreatment to (0.40±.70) four months after treatment (P <0.001). The Schirmer's test results improved from (4.10 ±1.089) pretreatment to (10.80±2.40) four months post-treatment (P <0.0001), and the TBUT test results improved from (5.54±1.77 s) pretreatment to (12.95±3.12 s) four months post-treatment (P <0.0001). Only seven patients (8%) developed ocular side effects in the form of redness, pain, and systemic side effects in the form of headache. In conclusion, Cyclosporine A 0.05% eye drops is an effective treatment for DED, improving both signs and symptoms of DED with few ocular side effects.

Keywords: Cyclosporine A, Dry Eye Disease (DED), Anti-inflammatory

INTRODUCTION

Dry eye disease (DED) is a common clinical condition challenging ophthalmologists and affecting 14% to 33% of the population (Brewitt & Sistani, 2001; Pei-Yu et al., 2003; Schaumberg et al., 2003; Schein et al., 1997). The 2007 International Dry Eye Workshop (DEWS) updated the definition of dry eye disease to incorporate inflammation as an association with DED (Definition, 2007). The definition of dry eye disease was revised by (Craig et al., 2017) as follows:

"Dry eye is a multifactorial disease of the ocular surface characterized by a loss of homeostasis of the tear film, and accompanied by ocular symptoms, in which tear film instability and hyperosmolarity, ocular surface inflammation and damage, and neurosensory abnormalities play etiological roles." (P. 278)

DED was classified pathophysiologically into two overlapping groups; evaporative dry eye and aqueous deficient dry eye (Lemp et al., 2012). In DED, the tears variations initiate positive feedback of ocular surface inflammatory response, damaging the surface in which T-cell lymphocytes play a role (Definition, 2007; Javadi & Feizi, 2011). To interrupt the inflammatory cascade in the

***Corresponding Author:** Samar A. Bukhatwa, samar.bukhatwa@uob.edu.ly, Ophthalmology Department, Faculty of Medicine, University of Benghazi, Benghazi, Libya.

management of DED, the usual trend of using tear replacement therapy, punctal occlusion, and environmental control is now changing toward anti-inflammatory therapy like corticosteroids, tetracyclines, and cyclosporine (Javadi & Feizi, 2011; Kymionis et al., 2008). Cyclosporine is an anti-T-cell immunosuppressive drug used systematically to prevent rejection after organ transplantation (Barbarino et al., 2013). It has been reported that the anti-inflammatory effect of Cyclosporine improves Schirmer's test results, increases the goblet cell number, with therapeutic benefits being achieved in about a month (Behrens et al., 2006; Phogat et al., 2019). Cyclosporine could be a better alternative to corticosteroids because of lacking steroid-related ocular side effects such as glaucoma and cataract (Phogat et al., 2019; Strong et al., 2005). Cyclosporine A (Restasis®) is approved by the Food and Drug Administration (FDA) for the therapy of DED (De Paiva et al., 2019).

This study aimed to assess the efficacy and patient tolerability of topical cyclosporine A 0.05% for the treatment of moderate to severe dry eye disease (DED).

MATERIALS AND METHODS

A prospective study was conducted at the Ophthalmology outpatient department in Benghazi/ Libya during a one-year period from January to December 2019; patients with dry eye disease of both genders were included. Written informed consent was obtained from the patients before their enrolment in the current study, which adhered to the tenets of the Declaration of Helsinki for research in human subjects.

Inclusion criteria: Patients aged ≥ 21 years presented to the outpatient department complaining of dry eye-related symptoms; burning, pain, or foreign body sensation were evaluated, including patients having DED associated with Sjögren's syndrome or previous LASIK (laser in-situ keratomileusis), and those with a tear film break-up time ≤10 s, and Schirmer tear test with anesthesia ≤5 mm in 5 minutes were included. Schirmer's test was done under topical anesthetic eye drops, by inserting the Schirmer strip into the lower conjunctival sac at the junction of the middle and outer third of the lower eyelid without touching the cornea, then informing the patient to keep the eyes gently closed. After 5 minutes, the strip was removed and the amount of wetting from the fold was measured (Li et al., 2012). For the tear break-up time test (TBUT); fluorescein strips were introduced into the conjunctival sac with minimal stimulation, the patient was asked to blink several times, then the tear film over the cornea was examined with a cobalt-blue filter. The time between the last blink and the appearance of a random dry spot was recorded in seconds as the tear film breakup time (Isreb et al., 2003). Grading the severity of the symptoms of burning, pain and a foreign body sensation was done for each symptom as follows: 0 (none), 1 for mild (occasional symptoms), 2 for moderate (frequent symptoms), and 3 for severe (constant symptoms), consequently, the total ocular symptoms were given a score from 0 to 9. The complete evaluation was based on both eyes' examination. All patients were instructed to stop all topical eye drops for two weeks. Cyclosporine 0.05% (Restasis) eye drops were prescribed as monotherapy twice daily for four months, and the patients were instructed to keep in contact any time they feel any problem. The patients were followed up after the first, second, third, and fourth months. They were examined and scored for ocular symptoms, amount of wetting on Schirmer paper, and for the TBUT at each visit. Additionally, they were examined for any ocular side effects of the drug.

Exclusion criteria: Patients who were not willing to give consent, or unable to buy the drug due to its cost were excluded. In addition to patients with ocular surgery/ trauma within the previous six months, patients with active lid margin inflammation, blepharitis,

ISSN: online 2617-2186 print 2617-2178

Meibomian gland disease, or ocular allergy, and any structural abnormalities on external eye examination e.g., entropion, trichiasis, lid scarring and many more, any systemic or topical medication other than artificial tears. Pregnant or lactating mothers and patients with a history of hypersensitivity to cyclosporine were also excluded.

Statistical analysis: Data were presented as frequencies and mean ±SD. Statistical analyses were performed using SPSS (Statistical Package for the Social Sciences) version 23.0. The data were analyzed statistically for the treated eye or the mean data for both eyes (if the patient was given treatment for both eyes). A nonparametric paired-samples test (Wilcoxon signed-ranks) was used to statistically analyze the changes in the results of Schirmer's test, TBUT tests, and the symptoms' score after treatment with Cyclosporine A 0.05 %. *P*-values of 0.05 or less were considered statistically significant.

RESULTS

A total of 87 patients diagnosed with dry-eye syndrome were included in this study with a mean age of 57.25±9.70 (Range 32 - 80 years). There were 62 female cases (71.3%) and 25 males (28.7%). (tab.1)

Table: (1). Showing demographic data of the patients included in the current study.

Age group (years)	No. of Females (%)	No. of Males (%)
30-40	4 (4.6%)	0 (0%)
41-50	17 (19.5%)	3 (3.4%)
51-60	19 (21.8%)	9 (10.3%)
61-70	17 (19.5%)	9 10.3%)
71-80	5 (5.7%)	4 (4.6%)
Total	62 (71.3%)	25 (28.7%)

Out of the 87 patients, 52 (59.8%) patients only had dry eye with no other associations. 23 (26.4%) patients had DED associated with Sjögren's syndrome, and 12 (13.7%) patients had previous LASIK.

There was a statistically significant difference ($Z = -8.122$, $p < 0.0001$) between Schirmer's test results pretreatment compared to Schirmer's test results four months after the initiation of the therapy.

Similarly, the TBUT test showed a statistically significant difference ($Z = -8.110$, $p < 0.0001$) of pretreatment results compared to the results 4 months after the initiation of the therapy.

The symptoms' score showed a significant improvement ($Z = -8.134$, $p < 0.0001$) 4 months after the initiation of the therapy compared to the pretreatment score. The improvement in Schirmer's test, TBUT test, and symptoms' score results over four months of treatment are shown in table 2.

Only seven patients (8%) had ocular side effects in the form of redness, pain, and systemic side effect in the form of headache. Two of them discontinued the study.

DISCUSSION

The symptoms of DED affect the patient's daily activities, so patients should be treated appropriately. The advancement in the understanding of the pathophysiology of DED and the inflammatory role in the reduction of tear film production led to the emergence of new therapeutic drugs (Definition, 2007; Stern et al., 1998).

Cyclosporine A is an immunomodulatory drug having anti-inflammatory properties (Barbarino et al., 2013; Matsuda & Koyasu, 2000). It improves tear production as measured by the Schirmer's test, decreases elevated tear osmolarity (Sullivan et al., 2012), decreases the numbers of activated lymphocytes within the conjunctiva (Kunert et al., 2000), in addition to an increase in goblet cell density in the conjunctiva of subjects with DED (Pflugfelder et al., 2008).

The benefits of topical Cyclosporine A eye

ISSN: online 2617-2186 print 2617-2178

drops on DED are noticed both; subjectively by the improvement of symptoms and objectively as measured by Fluorescein staining tests, TBUT, and Schirmer's tests (Tuan et al., 2020).

Table :(2). Showing pre-treatment and post-treatment (one, two, three and four months), Schirmer's, TBUT, and symptoms' score with respective *P* -values.

Test parameter Mean ±SD	Pre-treatment	One-month	Two-months	Three-months	Four-months	*P*-value
Schirmer's test (mm)	4.10 ±1.08	7.01±2.28	8.43±2.65	9.71±2.57	10.80±2.40	< 0.0001
TBUT (s)	5.54±1.77	6.76± 2.23	8.99±2.54	11.22±2.84	12.95±3.12	< 0.0001
Symptoms score	4.95±1.73	2.49±1.75	1.74±1.12	.83±.89	0.40±.70	< 0.0001

P-values based on Wilcoxon signed-ranks test.
TBUT (s) = Tear break up time test (seconds); SD = standard deviation

In the present study, the Schirmer's test results improved from (4.10 ±1.089) pretreatment to (10.80±2.40) four months after the initiation of Cyclosporine A treatment (P<0.0001). The TBUT test results improved from (5.54±1.77s) pretreatment to (12.95±3.12s) four months post-treatment (P<0.0001). These results are comparable to the results of a study conducted by AL-Nashar (2015) on 35 eyes of 20 patients of DED, in which the Schirmer's test results improved significantly (P = 0.001) from (1.15 ± 0.58) pretreatment to (5.86 ± 0.29 mm) 3months after treatment and the TBUT increased from (5.57 ± 1.36 s) before treatment to (9.9 ± 0.92 s) after 3 months of treatment (P = 0.001).

Another study was done by (Othman et al., 2018), who evaluated 32 cases of DED and yielded significant improvement in all the evaluated indices including TBUT and Schirmer's test (P<0.0001), which were also similar to the present study.

Similarly, the significant improvement in the objective clinical signs in the present study was associated with a parallel improvement in the symptoms' score of the patients, which changed from (4.95±1.73) pretreatment to (0.40±.70) four months after treatment (P<0.001). This is similar to a study done by Byun et al. on a large number of patients;

(362 patients) with DED who were studied prospectively and treated with Cyclosporine A 0.05% for three months, they showed a significant reduction in all ocular symptoms scores from baseline values (Byun et al., 2011).

There is no detectable systemic absorption associated with the topical application of Cyclosporine A due to its low concentration and low solubility in water, resulting in less penetration into the bloodstream and no systemic side effects (Baudouin et al., 2017; Leonardi et al., 2016; Yavuz et al., 2012). However, few ocular side effects are reported. In the current study, only seven patients (8%) had ocular side effects, which are similar to the previous reports by (Al-Nashar, 2015; Phogat et al., 2019), but less than what was reported by other studies (Mah et al., 2012; Prabhasawat et al., 2013).

The present study shows the capability of Cyclosporine A in improving the signs and symptoms of DED with different etiology, supporting the hypothesis of the role of inflammation in the process of DED irrespective of the cause (Byun et al., 2011; Definition, 2007).

One of this study's difficulties was that Cyclosporine A topical eye drops were not always available in pharmacies, in addition to its high cost, making its prescription to the patients occasionally limited.

ISSN: online 2617-2186 print 2617-2178

CONCLUSION

Cyclosporine A eye drops improve both subjective symptoms and objective clinical parameters of DED. They are effective in the treatment of DED regardless of the etiology, with few ocular side effects.

REFERENCES

Al-Nashar, H. Y. (2015). Efficacy of topical cyclosporine 0.05% eye drops in the treatment of dry eyes. *Journal of the Egyptian Ophthalmological Society, 108*(4), 233.

Barbarino, J. M., Staatz, C. E., Venkataramanan, R., Klein, T. E., & Altman, R. B. (2013). PharmGKB summary: cyclosporine and tacrolimus pathways. *Pharmacogenetics and genomics, 23*(10), 563.

Baudouin, C., Figueiredo, F. C., Messmer, E. M., Ismail, D., Amrane, M., Garrigue, J.-S., Bonini, S., & Leonardi, A. (2017). A randomized study of the efficacy and safety of 0.1% cyclosporine A cationic emulsion in treatment of moderate to severe dry eye. *European journal of ophthalmology, 27*(5), 520-530.

Behrens, A., Doyle, J. J., Stern, L., Chuck, R. S., McDonnell, P. J., Azar, D. T., Dua, H. S., Hom, M., Karpecki, P. M., & Laibson, P. R. (2006). Dysfunctional tear syndrome: a Delphi approach to treatment recommendations. *Cornea, 25*(8), 900-907.

Brewitt, H., & Sistani, F. (2001). Dry eye disease: the scale of the problem. *Survey of ophthalmology, 45*, S199-S202.

Byun, Y.-S., Rho, C. R., Cho, K., Choi, J. A., Na, K. S., & Joo, C.-K. (2011). Cyclosporine 0.05% ophthalmic emulsion for dry eye in Korea: a prospective, multicenter, open-label, surveillance study. *Korean journal of ophthalmology: KJO, 25*(6), 369.

Craig, J. P., Nichols, K. K., Akpek, E. K., Barbara Caffery, O., Dua, H. S., Joo, C.-K., Liu, Z., Nelson, J. D., Nichols, J. J., & Tsubota, K. (2017). TFOS DEWS II-Relazione su Definizione e Classificazione. *Ocular Surface, 30*, 276-283.

De Paiva, C. S., Pflugfelder, S. C., Ng, S. M., & Akpek, E. K. (2019). Topical cyclosporine A therapy for dry eye syndrome. *Cochrane Database of Systematic Reviews*(9).

Definition, D. (2007). The definition and classification of dry eye disease: report of the Definition and Classification Subcommittee of the International Dry Eye Workshop. *Ocul Surf, 5*, 75-92.

Isreb, M., Greiner, J., Korb, D., Glonek, T., Mody, S., Finnemore, V., & Reddy, C. (2003). Correlation of lipid layer thickness measurements with fluorescein tear film break-up time and Schirmer's test. *Eye, 17*(1), 79-83.

Javadi, M.-A., & Feizi, S. (2011). Dry eye syndrome. *Journal of ophthalmic & vision research, 6*(3), 192.

Kunert, K. S., Tisdale, A. S., Stern, M. E., Smith, J., & Gipson, I. K. (2000). Analysis of topical cyclosporine treatment of patients with dry eye syndrome: effect on conjunctival lymphocytes. *Archives of ophthalmology, 118*(11), 1489-1496.

Kymionis, G. D., Bouzoukis, D. I., Diakonis, V. F., & Siganos, C. (2008). Treatment of chronic dry eye: focus on

ISSN: online 2617-2186 print 2617-2178

cyclosporine. *Clinical Ophthalmology (Auckland, NZ), 2*(4), 829.

Lemp, M. A., Crews, L. A., Bron, A. J., Foulks, G. N., & Sullivan, B. D. (2012). Distribution of aqueous-deficient and evaporative dry eye in a clinic-based patient cohort: a retrospective study. *Cornea, 31*(5), 472-478.

Leonardi, A., Van Setten, G., Amrane, M., Ismail, D., Garrigue, J.-S., Figueiredo, F. C., & Baudouin, C. (2016). Efficacy and safety of 0.1% cyclosporine A cationic emulsion in the treatment of severe dry eye disease: a multicenter randomized trial. *European journal of ophthalmology, 26*(4), 287-296.

Li, N., Deng, X.-G., & He, M.-F. (2012). Comparison of the Schirmer I test with and without topical anesthesia for diagnosing dry eye. *International journal of ophthalmology, 5*(4), 478.

Mah, F., Milner, M., Yiu, S., Donnenfeld, E., Conway, T. M., & Hollander, D. A. (2012). PERSIST: Physician's Evaluation of Restasis® Satisfaction in Second Trial of topical cyclosporine ophthalmic emulsion 0.05% for dry eye: a retrospective review. *Clinical Ophthalmology (Auckland, NZ), 6*, 1971.

Matsuda, S., & Koyasu, S. (2000). Mechanisms of action of cyclosporine. *Immunopharmacology, 47*(2-3), 119-125.

Othman, T. M., Mousa, A., Gikandi, P. W., AbdelMabod, M., & Abdelrahman, A. M. (2018). Efficacy and safety of using topical cyclosporine A for treatment of moderate to severe dry eye disease. *Saudi Journal of Ophthalmology, 32*(3), 217-221.

Pei-Yu, L., Su-Ying, T., Ching-Yu, C., Jorn-Hon, L., Pesus, C., & Wen-Ming, H. (2003). Prevalence of dry eye among an elderly Chinese population in Taiwan. *Ophthalmology, 110*(6), 1096-1101.

Pflugfelder, S. C., De Paiva, C. S., Villarreal, A. L., & Stern, M. E. (2008). Effects of sequential artificial tear and cyclosporine emulsion therapy on conjunctival goblet cell density and transforming growth factor-β2 production. *Cornea, 27*(1), 64-69.

Phogat, J., Verma, R., Rathi, M., Sachdeva, S., & Pandey, L. (2019). Efficacy of cyclosporine 0.05% in patients with dry eye syndrome. *International Journal of Community Medicine and Public Health, 6*(8), 3339.

Prabhasawat, P., Tesavibul, N., Karnchanachetanee, C., & Kasemson, S. (2013). Efficacy of cyclosporine 0.05% eye drops in Stevens Johnson syndrome with chronic dry eye. *Journal of ocular pharmacology and therapeutics, 29*(3), 372-377.

Schaumberg, D. A., Sullivan, D. A., Buring, J. E., & Dana, M. R. (2003). Prevalence of dry eye syndrome among US women. *American journal of ophthalmology, 136*(2), 318-326.

Schein, O. D., MUÑO, B., Tielsch, J. M., Bandeen-Roche, K., & West, S. (1997). Prevalence of dry eye among the elderly. *American journal of ophthalmology, 124*(6), 723-728.

Stern, M. E., Beuerman, R. W., Fox, R. I., Gao, J., Mircheff, A. K., & Pflugfelder, S. C. (1998). The pathology of dry eye: the interaction between the ocular surface and lacrimal glands. *Cornea, 17*(6), 584-589.

ISSN: online 2617-2186 print 2617-2178

Strong, B., Farley, W., Stern, M. E., & Pflugfelder, S. C. (2005). Topical cyclosporine inhibits conjunctival epithelial apoptosis in experimental murine keratoconjunctivitis sicca. *Cornea, 24*(1), 80-85.

Sullivan, B. D., Crews, L. A., Sönmez, B., Maria, F., Comert, E., Charoenrook, V., de Araujo, A. L., Pepose, J. S., Berg, M. S., & Kosheleff, V. P. (2012). Clinical utility of objective tests for dry eye disease: variability over time and implications for clinical trials and disease management. *Cornea, 31*(9), 1000-1008.

Tuan, H.-I., Chi, S.-C., & Kang, Y.-N. (2020). An updated systematic review with meta-analysis of randomized trials on topical cyclosporin A for dry-eye disease. *Drug design, development and therapy, 14*, 265.

Yavuz, B., Bozdağ Pehlivan, S., & Ünlü, N. (2012). An overview on dry eye treatment: approaches for cyclosporin a delivery. *The Scientific World Journal, 2012*.

ISSN: online 2617-2186 print 2617-2178

سيكلوسبورين أ الموضعي 0.05٪ لعلاج أمراض العين الجافة (DED)

نعيمة مختار الزليتني، سمر عبد الكريم بوخطوة* وصباح سعد الدرسي

قسم العيون، كلية الطب البشري، جامعة بنغازي، بنغازي، ليبيا

تاريخ الاستلام: 04 يناير 2021/ تاريخ القبول: 31 يناير 2021

Doi:https://doi.org/10.54172/mjsc.v36i1.8

المستخلص: مرض العين الجافة (DED) هو حالة سريرية شائعة تتحدى أطباء العيون. السيكلوسبورين أ الموضعي هو علاج مضاد للالتهابات تمت الموافقة عليه من قبل إدارة الغذاء والدواء (FDA) لعلاج DED. هدفت هذه الدراسة إلى تقييم فعالية وتحمل المريض للسيكلوسبورين أ الموضعي 0.05٪ لعلاج DED. تم تضمين مجموعة من 87 مريضًا تم تشخيصهم بمرض DED في هذه الدراسة، و تسجيل أعراض جفاف العين (الإحساس بجسم غريب، والحرق، والألم) كمقياس خط اساس، تم إجراء اختبار وقت تفكك الدموع (TBUT)، واختبار شيرمر للمرضى جميعهم. تم إعطاء السيكلوسبورين أ 0.05 ٪ للمرضى جميعهم موضعياً مرتين يومياً لمدة 4 أشهر، ومتابعتهم شهريا لمدة أربعة أشهر. في كل زيارة يتم قياس العلامات السريرية [اختبار شيرمر و (TBUT)]، و تسجيل درجات الأعراض. كان متوسط عمر المرضى 57.25 ± 9.70 سنة (المدى 32–80 سنة)؛ 25 ذكرا (28.7٪) و62 أنثى (71.3٪). كان هناك عدد 23 (26.4٪) من الحالات مصابة بمتلازمة سجوجرن Sjögren's و12 (13.7٪) حالة لديها سابقة ليزك (تصحيح القرنية بالليزر في الموقع). تحسنت درجة أعراض الحالات من (4.95 ± 1.73) قبل المعالجة إلى (0.40 ± 7.) بعد 4 أشهر من العلاج (P <0.001)، و تحسنت نتائج اختبار شيرمر من (4.10 ± 1.089) إلى (10.80 ± 2.40) بعد 4 أشهر من العلاج (P <0.0001)، وتحسنت نتائج اختبار TBUT من (5.54 ± 1.77 ثانية) قبل المعالجة إلى (12.95 ± 3.12 ثانية) 4 أشهر بعد العلاج (P <0.0001). أصيب 7 مرضى فقط (8٪) بآثار جانبية على العين على شكل احمرار وألم، وتأثيرات جانبية جهازية على هيئة صداع. تستخلص الدراسة أن قطرات العين سيكلوسبورين أ الموضعي 0.05٪ فعالة لعلاج DED، فهي تحسن كل من الأعراض، والعلامات السريرية الموضوعية لـ DED، مع القليل من الآثار الجانبية.

الكلمات المفتاحية: السيكلوسبورين أ، مرض جفاف العين، مضاد الالتهابات.

*سمر بوخطوة samar.bukhatwa@uob.edu.ly قسم العيون كلية الطب البشري، جامعة بنغازي، بنغازي، ليبيا

Al-Mukhtar Journal of Sciences 36 (1): 42-56, 2021

α-Reflexive Rings with Involution

Muna E. Abdulhafed[1*] and Aafaf E. Abduelhafid[2]

[1] *Department of Mathematics, Faculty of Science, Azzaytuna University, Tarhunah, Libya.*

[2] *Department of Mathematics - Faculty of Education, Azzaytuna University, Tarhunah, Libya.*

Received: 13 January 2021/ Accepted: 31 January 2021
Doi: https://doi.org/10.54172/mjsc.v36i1.22

Abstract: This paper studies the concept of the α-quasi-*-IFP (resp., α -*-reflexive) *-rings, as a generalization of the quasi-*-IFP (resp., *-reflexive) *-rings and every quasi-*-IFP (resp., *-reflexive) *-ring is α -quasi-*-IFP (resp., α-*-reflexive). This paper also discusses the sufficient condition for the quasi-*-IFP (resp., *-reflexive) *-ring in order to be α-quasi-*-IFP (resp., α-*- reflexive). Finally, this study investigates the α-quasi-*-IFP (resp., α-*-reflexivity) by using some types of the polynomial rings.

Keywords: **-reduced; *-rigid; α-*-rigid; α-*-IFP; α-quasi-*-IFP; α-*-reversible; α-*-reflexive *-rings.*

INTRODUCTION

Throughout this paper, R denotes an associative *-ring with unity and α denotes a nonzero nonidentity endomorphism of a given *-ring, unless specified otherwise. IFP stands for "insertion-of-factors property", R is semicommutative or has IFP if the right annihilator $r(a) = \{x \in R | ax = 0\}$ of every element $a \in R$ is a two-sided ideal. A *-ring R is said to have IFP when all $ab \in R, ab = 0$ which implies that $aRb = 0$ by (Kim & Lee, 2003). In both studies (Başer & Kwak, 2010) and (Başer et al., 2008) discussed an endomorphism α of a ring R, the endomorphism α is called semicommutative if $ab = 0$ implies $aR\alpha(b) = 0$ for $a \in R$. Also, a ring R is called α- semicommutative, if there exists a semicommutative endomorphism α of R.

Another study (Zhao & Zhu, 2012) shows that, an endomorphism α of a ring R is called reflexive whenever $aRb = 0$ for $a, b \in R$, $bR\alpha(a) = 0$. A ring R is called α-reflexive if there exists a reflexive endomorphism α of R.
A *-ring R is said to have *-IFP if all $a, b \in R, ab = 0$ implies $aRb^* = 0$. For more details see (Aburawash & Saad, 2014). By (Aburawash & Saad, 2019) R has quasi-*-IFP if all $a, b \in R, ab = ab^* = 0$ implies $aRb = 0$, a *-ring R is called *-reversible (resp., *-reflexive) if for all $a, b \in R, ab = ab^* = 0$ (resp., $aRb = aRb^* = 0$) implies $ba = 0$ (resp., $bRa = 0$).

According to (Abdulhafed, 2019), a *-ring R is said to be *-rigid if for $a, b \in R, ab^2 = abb^* = 0$ implies $ab = 0$, an α be a *-endomorphism of R. α is called a *-rigid *-endomorphism if $a\alpha(a) = a\alpha(a^*) = 0$ implies $a = 0$ for all $a \in R$. A *-ring R is called α-*-rigid if there exists a *-rigid *-endomorphism α of R and a *-endomorphism α of a *-ring R is called *-reversible if whenever $ab = ab^* = 0$, then $\alpha(b)\alpha(a) = 0$, for $a, b \in R$ (also, $\alpha(b^*)\alpha(a) = 0$). A *-ring R is called α-*-reversible if there exists a *-endomorphism α on R. A *-rigid *-rings are equivalent to *-reduced *-rings.

In view of the studies mentioned above, this paper introduces the class of α-quasi-*-IFP (resp., α-*-reflexive) *-rings, which is the *-

***Corresponding Author:** Muna E. Abdulhafed *muna.am2016@gmail.com*, Department of Mathematics, Faculty of Science, Azzaytuna University, Tarhuna-Libya

version (and also a generalization) of the quasi-*-IFP (resp., *-reflexive) *-rings.

Moreover, some properties and results of these classes of *-rings are investigated. The class of α-*-reflexive *-rings is introduced as a generalization of *-reflexive and *-reduced *-rings, since, by definition, *-reflexive *-rings are α-*-reflexive *-rings and α-*-reversible is α-*-reflexive.

Also, other relative results are given. Here, finally, we conclude the results of the paper by explaining the diagram and the relations among the corresponding classes.

α-*-IFP rings

In this section, α-*-IFP *-rings are introduced as a generalization of *-IFP *-rings.

Definition 1. A *-endomorphism α of a *-ring R is called **-IFP* if whenever $ab = 0$, then $\alpha(arb^*) = 0$ for all $a, b, r \in R$. A *-ring R is called *α-*-IFP* if there exists a *-endomorphism α on R.

It is clear that a ring R is *-IFP if R is I_R-*-IFP, where I_R is the identity *-endomorphism of R. It is easy to see that every *-subring S with $\alpha(S) \subseteq S$ of an α-*-IFP *-ring is also α -*-IFP.

Obviously, in general, the reverse implication in the above definition does not hold by the following example which also shows that there exists *-endomorphism α of α -*-IFP *-ring R such that R is not α -IFP.

Example 1. Assume both $\mathbb{F}$ to be a field, the *-ring $R = \mathbb{F} \oplus \mathbb{F}$ with exchange involution $(a, b)^* = (a^*, b^*)$ and *-endomorphism $\alpha: R \to R$ is given by $\alpha\big((a, b)\big) = (b, a)$ for all $a, b \in \mathbb{F}$. Since Since A=(1,0), B=(0,1),A = (1,0), B = (0,1)R clearly α-*-IFP, but it does not have α-IFP.

Proposition 1. Let R be α- *-IFP *-ring and α is *-monomorphism on R, then R *-IFP.

α-quasi-*-IFP rings

In this part of the paper the focus is on the α-quasi-*-IFP *-rings and how to introduce a generalization for quasi-*-IFP *-rings.

Definition 2. A *-endomorphism α of a *-ring R is called *quasi-*-IFP,* when $ab = 0 = ab^*$, then $\alpha(arb) = 0$, for all $a, b, r \in R$ (consequently $\alpha(arb^*) = 0$). A *-ring R is called *α-quasi-*-IFP* if there exists a *-endomorphism α on R.

It is clear that it is needed to exclude the identity *-endomorphism I_R, because the *-ring R is I_R-quasi-*-IFP if and only if R is quasi-*-IFP. In general, α-quasi-*IFP *-ring R is quasi-*-IFP if α is a *-monomorphism on R.

Proposition 2. *Let* R *be* α*-quasi-*-IFP *-ring and* α *is *-monomorphism on* R*, then* R *quasi-*-IFP.*

Proposition 3. *Let* R *be* α *is *-monomorphism a *-ring. If* R *is* α*-quasi-*-IFP and it has *-IFP, then* R *is IFP.*

Proof. It is obvious, since $ab = 0$, implies $aRb^* = 0$, by the *-IFP property and R α -quasi-*-IFP, we have $\alpha(arb) = 0$, for all $a, b, r \in R$. Hence, $aRb = 0$ since α is *-monomorphism. Thus R is IFP.

It is clear that, a ring R is quasi-*-IFP if $R$is I_R-quasi-*-IFP, where I_R is the identity *-endomorphism of R. It is easy to note that every *-subring S with $\alpha(S) \subseteq S$ of an α-quasi-*-IFP *-ring is also α-quasi-*-IFP.

Notice that, in general, the reverse implication in the above definition does not hold by the following example, which shows also that, there exists *-endomorphism α of α-quasi-*-IFP *-ring R such that R is not α-IFP.

ISSN: online 2617-2186 print 2617-2178

Example 2. The *-ring $R = \mathbb{Z}_2 \oplus \mathbb{Z}_2$, with the changeless involution * defined as $(a,b)^* = (a^*, b^*)$ and *-automorphism $\alpha: R \to R$ given by $\alpha((a,b)) = (b,a)$ is not α-IFP but, it is IFP, since the nonzero element $A(0,1), B = (1,0)$ satisfies that $AB = AB^* = 0$, while $\alpha(A)RB \neq 0$ and also $AR\alpha(B) \neq 0$, $ARB = 0$. Moreover, R is α-quasi-*-IFP.

Proposition 4. *Let* R *be an* α-**-reversible *-ring, then* R *is* α-*quasi-*-IFP.*

The converse to **Proposition 4** is not true according on the following example:

Example 3. The *-ring $R = \begin{pmatrix} \mathbb{F} & \mathbb{F} \\ 0 & \mathbb{F} \end{pmatrix}$ over a field $\mathbb{F}$, with the adjoint involution * is α-quasi-*-IFP. Moreover, R with the *-endomorphism $\alpha: R \to R$ defined by $\alpha\left(\begin{pmatrix} a & b \\ 0 & c \end{pmatrix}\right) = \begin{pmatrix} a & -b \\ 0 & c \end{pmatrix}$, is not α-*-reversible by (Abdulhafed, 2019). The following example declares that, $T_4(R)$ is not an $\tilde{\alpha}$-quasi-*-IFP *-ring, even if R is an α-rigid *-ring. Since *-endomorphism α of a *-ring R is also extended to the *-endomorphism $\tilde{\alpha}$ of $T_4(R)$ defined by $\tilde{\alpha}\left((a_{ij})\right) = (\alpha(a_{ij}))$.

Example 4. Consider R be a commutative α-rigid *-ring. Then, the *-ring $T_4(R)$ is not $\tilde{\alpha}$-quasi-*-IFP, since the matrices

$$A = \begin{pmatrix} 0 & 1 & -1 & 0 \\ 0 & 0 & 0 & 0 \\ 0 & 0 & 0 & 0 \\ 0 & 0 & 0 & 0 \end{pmatrix},$$

$$B = \begin{pmatrix} 0 & 0 & 0 & 0 \\ 0 & 0 & 0 & 1 \\ 0 & 0 & 0 & 1 \\ 0 & 0 & 0 & 0 \end{pmatrix} \in T_4(R),$$

satisfy $AB = AB^* = 0$ while, $\tilde{\alpha}(A)\tilde{\alpha}(C)\tilde{\alpha}(B) \neq 0$, while, $\tilde{\alpha}(A)\tilde{\alpha}(C)\tilde{\alpha}(B) \neq 0$ for

$$C = \begin{pmatrix} 0 & 0 & 0 & 0 \\ 0 & 0 & 1 & 0 \\ 0 & 0 & 0 & 0 \\ 0 & 0 & 0 & 0 \end{pmatrix} \in T_4(R),$$

where $\alpha(e) = e$, by (Abdulhafed, 2019). Thus $\tilde{\alpha}(A)\tilde{\alpha}(T_4(R))\tilde{\alpha}(B) \neq 0$ and so $T_4(R)$is not $\tilde{\alpha}$-quasi-*-IFP. Similarly, it can be proved that $T_n(R)$ is not $\tilde{\alpha}$-quasi-*-IFP for $n \geq 5$.

Furthermore, the class of the α-quasi-*-IFP *-rings is closed under the finite direct sums (with changeless involution). In addition to assume R be a *-ring. Then, both eR and $(1-e)R$ are α-quasi-*-IFP for some projection e in R with $\alpha(e) = e$, if and only if R is α-quasi-*-IFP.

α-reflexive rings with involution

In this section, α-*-reflexive *-rings are introduced as a generalization for *-reflexive and *-rigid *-rings.

Definition 3. A *-endomorphism α of a *-ring R is called **-reflexive* when $aRb = aRb^* = 0$, then, $\alpha(bra) = 0$, for all $a, b, r \in R$ (consequently $\alpha(b^*ra) = 0$). A *-ring R is called α-**-reflexive,* if there exists a *-endomorphism α on R.

Every *-reflexive *-ring is clearly α-*-reflexive, but, on the opposite side it is not true as shown by the following example.

Example 5. The *-ring $R = \begin{pmatrix} \mathbb{Z} & \mathbb{Z} \\ 0 & \mathbb{Z} \end{pmatrix}$, with the adjoint involution * and *-endomorphism $\alpha: R \to R$ is defined by

$$\alpha\left(\begin{pmatrix} a & b \\ 0 & c \end{pmatrix}\right) = \begin{pmatrix} a & 0 \\ 0 & c \end{pmatrix}$$

is α-*-reflexive, since if the matrices

$$A = \begin{pmatrix} a_1 & b_1 \\ 0 & c_1 \end{pmatrix}, B = \begin{pmatrix} a_2 & b_2 \\ 0 & c_2 \end{pmatrix} \in R,$$

satisfy $ARB = ARB^* = 0$, then, we get the equations: $a_1aa_2 = a_1ac_2 = 0, a_1ab_2 +$

ISSN: online 2617-2186 print 2617-2178

$a_1bc_2 + b_1cc_2 = -a_1ab_2 + a_1ba_2 + b_1ca_2 =$ 0 and $c_1cc_2 = c_1ca_2 = 0$, which implies that:

$$\alpha(BrA) = \begin{pmatrix} a_2aa_1 & 0 \\ 0 & c_2cc_1 \end{pmatrix} = 0.$$

Moreover, R is not *-reflexive, since

$$BRA = \begin{pmatrix} 0 & a_2bc_1 + b_2cc_1 \\ 0 & 0 \end{pmatrix} \neq 0.$$

Next, here it is also deduced that, it excluded the identity *-endomorphism I_R, because the *-ring R is I_R-*-reflexive if and only if R is *-reflexive. In general, α-*-reflexive *-ring R is *-reflexive if α is a *-monomorphism on R.

Proposition 5. *Let* R *be an* α-*-*reflexive* *-*ring and* α *is* *-*monomorphism on* R*, then* R *is* *-*reflexive.* It is clearly visible that, there is no connection between either α- reflexive or α-*-rigid and α-*- reflexive *-rings. According to the example 5, there exists an α-*-reflexive *-ring $R = \begin{pmatrix} \mathbb{Z} & \mathbb{Z} \\ 0 & \mathbb{Z} \end{pmatrix}$ which is not α- reflexive. Since

$$BR\alpha(A) = \begin{pmatrix} a_2aa_1 & a_2ab_1 + a_2bc_1 \\ 0 & c_2cc_1 \end{pmatrix} \neq 0,$$

and

$$BR\alpha(A) = \begin{pmatrix} a_2aa_1 & a_2bc_1 + a_2cc_1 \\ 0 & c_2cc_1 \end{pmatrix} \neq 0.$$

Example 6. Consider R = $\mathbb{Z}_8 \oplus \mathbb{Z}_8$ with usual addition and multiplication with exchange involution $(a,b)^* = (a^*, b^*)$, and let α : R → R be an *-endomorphism is defined by $\alpha((a,b)) = (b,a)$. For $a = (4,2), b(2,0) \in \mathbb{Z}_8 \oplus \mathbb{Z}_8$, we get $aRb = aRb^* = 0$.

However, $b\alpha(a) = (4,0) \neq 0$ and $\alpha(b)a = (0,4) \neq 0$, entailing neither $bR\alpha(a) = 0$ and nor $\alpha(b)Ra = 0$. Hence, R is neither right nor left α- reflexive, but, it is α-*-reflexive.

Proposition 6. *Let* R *be a* *-*reflexive* *-*ring. Then the following are equivalent.*

1. R *is* α-*- *reflexive.*
2. *If* arb = 0 = arb* *for all* a, b, r ∈ R, *then* α(arb) = α(arb*) = 0 .

Proof. 1 ⇒ 2. Let $arb = arb^* = 0$, where $a, b, r \in R$, then $\alpha(arb) = \alpha(arb^*) = 0$. Hence, $\alpha(b)\alpha(r)\alpha(a) = 0 = \alpha(b^*)\alpha(r)\alpha(a)$ for all $r \in R$, since R is *-reflexive, then, we get that $\alpha(a)\alpha(r)\alpha(b) = 0 = \alpha(a)\alpha(r)\alpha(b^*)$ which implies $\alpha(aRb) = \alpha(aRb^*)$.

2 ⇒ 1. Let $arb = 0 = arb^*$ for $a, b, r \in R$ which implies by **2** that $\alpha(arb) = \alpha(arb^*) = 0$. Since R is *- reflexive, then $\alpha(bRa) = 0$.

Proposition 7. *Let* α *be a* *-*monomorphism on a* *-*ring* R*. Then,* R *is an* α-*- *reflexive* *-*ring if and only* α(a)α(r)α(b) = 0 = α(a)α(r)α(b*) *if implies* bra = 0 = b*ra *for all* a, b, r ∈ R.

Proof. Let $\alpha(a)\alpha(r)\alpha(b) = 0 = \alpha(a)\alpha(r)\alpha(b^*)$ for $a, b, r \in R$, then

$\alpha(\alpha(b))\alpha(\alpha(r))\alpha(\alpha(a)) = \alpha^2(bra) = 0 = \alpha(\alpha(b^*))\alpha(\alpha(r))\alpha(\alpha(a)) = \alpha^2(b^*ra)$Since, R is α-*-reflexive and α is a *-monomorphism imply $bRa = 0 = b^*Ra$.

Conversely, let $arb = arb^* = 0$, where $a, b, r \in R$, then, $\alpha(arb) = \alpha(a)\alpha(r)\alpha(b) = 0 = \alpha(a)\alpha(r)\alpha(b^*) = \alpha(arb^*)$ by hypothesis so $bRa = 0 = b^*Ra$.

It is easily to show that the class of α-*- reflexive *-rings is closed under finite direct sums (with changeless involution).

Proposition 8. *The class of* α-*- *reflexive* *-*rings is closed under finite direct sums.*

The next step, an example is needed to explain that *-reflexivity is not closed under taking *-subrings. The full matrix ring $\mathbb{M}_n(R)$ over a *-ring R with adjoint involution and the *-endomorphism $\alpha: \mathbb{M}_n(R) \to \mathbb{M}_n(R)$ is defined by

ISSN: online 2617-2186 print 2617-2178

$$\alpha\left(\begin{pmatrix} a & b \\ c & d \end{pmatrix}\right) = \begin{pmatrix} a & -b \\ -c & d \end{pmatrix},$$

It is not α-*-reflexive for $n \geq 2$, according to the following example:

Example 7. The ring $R = \mathbb{M}(\mathbb{Z}_2)$ is prime and *-reflexive. The upper triangular matrix ring $T_2(R) = \begin{pmatrix} \mathbb{Z}_2 & \mathbb{Z}_2 \\ 0 & \mathbb{Z}_2 \end{pmatrix}$ over $\mathbb{Z}_2$ is a *-subring of R. R is clearly α-*-reflexive, but $T_2(R)$ is not, since both matrices $A = \begin{pmatrix} 0 & 0 \\ 0 & 1 \end{pmatrix}$ and $B = \begin{pmatrix} 0 & 1 \\ 0 & 0 \end{pmatrix}$ of R satisfy

$ARB = ARB^* = 0$, but $\alpha(B)R\alpha(A) =$

$$\begin{pmatrix} 0 & -1 \\ 0 & 0 \end{pmatrix}\begin{pmatrix} 1 & -1 \\ 0 & 1 \end{pmatrix}\begin{pmatrix} 0 & 0 \\ 0 & 1 \end{pmatrix} = \begin{pmatrix} 0 & -1 \\ 0 & 0 \end{pmatrix} \neq 0$$

According to the study by [(Abdulhafed, 2019)] every *-reduced equivalence *-rigid, [(Aburawash & Saad, 2016), Example 4.2 and Proposition 4.6] and [(Aburawash & Saad, 2019), Example 7 and Corollary 3], we deduce the following important results.

Corollary 1. Every *-rigid *-ring is α-*- reflexive.

The opposite of the previous **Corollary 1** is not true since, by **Examples 5** it is obtained α-*-reflexive and it is not *-reduced.

Corollary 2. Every *-Baer *-ring is α-*- reflexive.

Corollary 3. *Every *-domain is* α-*- *reflexive.*

Corollary 4. *Every *-ring with semiproper involution is* α-*- *reflexive.*

Now, in contrast to the previous corollary, it is not necessary to be true as shown in the following example.

Example 8. From [(Aburawash & Saad, 2019), Example 9], if $\mathbb{F}$ is a field, then the ring $R = \mathbb{F} \oplus \mathbb{F}^{OP}$, with the exchange involution * is defined by $(a, b)^* = (b, a)$ and the *-endomorphism $\alpha = *$ for all $a, b \in R$, it is obvious that an α *-reflexive but, * is not semiproper. Indeed, the element $0 \neq A = (0, a)$ for some nonzero element a of $\mathbb{F}$ satisfy $ARA^* = 0$.

The following proposition and example show that the class of α-*-reflexive *-rings generalizes strictly that of α-*-reversible *-rings.

Proposition 9. *Every α-*-reversible *-ring is α-*- reflexive.*

Proof. Let $aRb = aRb^* = 0$, then, $ab = ab^* = 0$ implies $rab = rab^* = 0$ for every $r \in R$. So that $\alpha(bra) = \alpha(b^*ra) = 0$, from the α-*-reversibility of R. Thus $\alpha(bRa) = \alpha(b^*Ra) = 0$, hence, R is α-*- reflexive.

The question that, when a α-*-reflexive *-ring is α-*-reversible is answered by the following proposition.

Proposition 10. *A *-ring R is α-*-reversible if and only if R has quasi-*-IFP and α-*- reflexive.*

Proof. The necessity is clear to sufficiency, let's consider $ab = ab^* = 0$, for some $a, b \in R$. Since R has quasi-*-IFP, then, $aRb = aRb^* = 0$. The α-*-reflexivity of R implies $aRb = aRb^* = 0$. Hence $\alpha(ba) = \alpha(b^*a) = 0$, and R is α-*-reversible. By the **Corollary 1**, we can get the following result.

Corollary 5. *Every α-rigid *-ring is α-*- reflexive.*

The following example can show that the converse of **Corollary 5** is not true.

Example 9. By looking to the study [(Başer et al.,2009), Example 2.7 (i)], the trivial extension *-ring $T(\mathbb{Z}_4, \mathbb{Z}_4)$, with the adjoint involution * and the *-endomorphism $\alpha = *$ is not semiprime (so not α-*-rigid), but it is α-*- reflexive.

ISSN: online 2617-2186 print 2617-2178

Proposition 11. *Let's consider* α *to be a *-monomorphism on a *-ring* R*, the following statements are equivalent:*

i. R is α-- reflexive.*
ii. $r_*(aR) = l_*(Ra)$ *for every element* $a \in R$.
iii. For any two nonempty subsets A and B of R, $ARB = ARB^*$ *implies* $\alpha(BRA) = 0$ *(consequently* $\alpha(B^*RA) = 0$*).*

Proof. $(i) \Rightarrow (ii)$. Let $x \in r_*(aR)$, then, $aRx = aRx^* = 0$. Since R is α-*- reflexive, we have $\alpha(x)\alpha(Ra) = \alpha(x^*)\alpha(Ra) = 0$, but α is a *-monomorphism, so $xRa = x^*Ra = 0$, for every $a \in R$. Hence, $xRa = x^*Ra = 0$ implies $x \in l_*(Ra)$, and we get $r_*(aR) \subseteq l_*(Ra)$. Similarly, $l_*(Ra) \subseteq r_*(aR)$ and so $r_*(aR) = l_*(Ra)$ follows.

$(ii) \Rightarrow (iii)$. Let $ARB = ARB^*$for some subsets A and B of R. Then $B \subseteq r_*(AR)$ and so $aRb = aRb^* = 0$ for all $a \in A$ and $b \in B$ and hence $b \in r_*(aR) = l_*(Ra)$ and $bRa = b^*Ra = 0$. which implies $\alpha(BRA) = \alpha(B^*RA) = 0$.

$(iii) \Rightarrow (iv)$. is obvious.

From **Proposition 11**, we have the following corollary.

Corollary 6. *Let* α *be a *-monomorphism of a *-ring*R*, then the following statements are equivalent:*

*i. R is *- reflexive.*
ii. R is α-- reflexive.*
iii. $r_*(aR) = l_*(Ra)$ *for every element* $a \in R$.
iv. For any two nonempty subsets A and B of R, $ARB = ARB^* = 0$ *implies* $\alpha(BRA) = 0$ *(consequently* $\alpha(B^*RA) = 0$*).*

Again, a *-domain *-ring is *- reflexive [(Aburawash & Saad, 2019), Example 4], then, we have:

Corollary 7. *Every *-domain *-ring is α-*- reflexive.*

The converse of **Corollary 7** is not true, since $T(\mathbb{Z}_4, \mathbb{Z}_4)$ is not a domain *-ring in the **Example 9**

Proposition 12. *Let's assume* α *be *-endomorphisms of* a **-ring* R*. If* R *is* α*-*- reflexive *-ring, then* $aRb = 0 = aRb^*$ *for* $a, b \in R$ *implies* $\alpha^k(a)R\alpha^k(b) = 0 = \alpha^k(a)R\alpha^k(b^*)$ *and* $\alpha^k(b)R\alpha^k(a) = 0 = \alpha^k(b^*)R\alpha^k(a)$*for all* $k \geq 1$.

For *-endomorphism α and projection e of a *-ring R such $\alpha(e) = e$, that, we have *-endomorphism $\tilde{\alpha}: eRe \to eRe$ is defined by $\tilde{\alpha}(ere) = e\alpha(r)e$, one can show that *- reflexive property is extended to the *-corner.

Proposition 13. *Let* R *be* a α*-*- reflexive *-ring, then, the *-corner* eRe *for every projection e of* R *is also* α*-*- reflexive.*

Proof. Let R be α-*-reflexive and $a = exe$, $b = eye \in eRe$ such that $a(eRe)b = a(eRe)b^* = 0$. Then $exeReye = exeRey^*e = 0$ implies $\tilde{\alpha}(eye)R\tilde{\alpha}(exe) = \tilde{\alpha}(ey^*e)R\tilde{\alpha}(exe) = 0$, since R is α-*- reflexive. Therefore $\alpha(b)(eRe)\alpha(a) = \alpha(b^*)(eRe)\alpha(a) = 0$ and so eRe is α-*- reflexive.

Proposition 14. *Let* R *be* a **-ring with *-endomorphism* α *such that* $\alpha(e) = e$ *for* $e^2 = ee^* = e \in R$*. If* e *is a central projection* R*, then,* eR *and* $(1 - e)R$ *are* α*-*- reflexive if and only if* R *is* α*-*- reflexive.*

Proof. It is enough to show the necessity by **Proposition 8**. Suppose that eR and $(1 - e)R$ are α-*-reflexive for a central projection $e \in R$. Let $aRb = 0 = aRb^*$ for $a, b \in R$. Then,

$$ea(eR)eb = 0 = ea(eR)eb^*,$$

and

$$(1 - e)a(1 - e)R(1 - e)b = 0 = (1 - e)a(1 - e)R(1 - e)b^*.$$

ISSN: online 2617-2186 print 2617-2178

By hypothesis,

$$0 = \tilde{\alpha}(eb)eR\tilde{\alpha}(ea) =$$

$$e\alpha(b)e\alpha(a) = e\alpha(b)R\alpha(a)$$

and

$$0 = \tilde{\alpha}\big((1-e)b\big)(1-e)R\tilde{\alpha}\big((1-e)a\big) = (1-e)\alpha(b)(1-e)R(1-e)\alpha(a) = (1-e)\alpha(b)R\alpha(a) = 0.$$

For a ring R and an endomorphism, $\alpha: R \to R$ the skew polynomial ring (also called on Ore extension of endomorphism type) $R[x;\alpha]$ of R is the ring that is obtained by giving the polynomial ring over R with the new multiplication $xr = \alpha(r)x$ for all $r \in R$.

Proposition 15. *If R and* $R[x;\alpha]$ *(resp.,* $R[[x;\alpha]]$*) are *- reflexive, then, R is α-*-rigid.*

Proof. Let us consider $a\alpha(a) = a\alpha(a^*) = 0$ and $p = ax, q = a \in R[x;\alpha]$ for $a \in R$, then

$$pRq = axa = a\alpha(a)x = 0, pRq^* =$$

$axa^* = a\alpha(a^*)x = 0$. Since $R[x;\alpha]$ is *- reflexive, hence $\mathrm{qRp} = \mathrm{aax} = \mathrm{a^2x} = 0$

$, q^*Rp = a^*ax = a^*ax = 0$ and so $a^2 = a^*a = 0$. Since R is *-reduced, we get $a = 0$.

According to (Abdulhafed, 2019) and **Proposition 15** the following results are straightforward:

Corollary 8. *If both R and* $R[x;\alpha]$ *(resp.,* $R\big[[x;\alpha]\big]$*) are a reflexive *-ring, then, R is α-*-rigid.*

Corollary 9. *If R is an α-*-rigid *-ring and* $R[x;\alpha]$ *(resp.,* $R\big[[x;\alpha]\big]$*) is a reversible *-ring, therefore, R is *-reflexive.*

Corollary 10. *If R is an α-*-rigid *-ring, then,* $R[x;\alpha]$ *(resp.,* $R\big[[x;\alpha]\big]$*) is *-reflexive.*

If the *-ring $R[x;\alpha]$ is *-reflexive, then, R is *-reflexive and the converse is not correct. Also, the converse of **Corollary 9** is wrong according to studying the example in (Abdulhafed, 2019).

Next, the α-*-reflexivity and α-quasi-*-IFP do not imply each other.

Example 10. For a commutative *-ring R,

$$T_3(R) = \left\{ \begin{pmatrix} a & b & c \\ 0 & a & d \\ 0 & 0 & a \end{pmatrix} \middle| a, b, c, d \in R \right\},$$

it has quasi-*-IFP, but, it does not have *-reflexive by [(Aburawash & Abdulhafed, 2018a), Example 5]. Thus, R is id_R-quasi-*-IFP, but it is not id_R-*-reflexive.

As, a consequence from **Example 10**, $T_n(R)$ is not α-*-reflexive for $n \geq 4$. Clearly, if R is a commutative *-ring, hence, the *-ring:

$$T_n(R) = \left\{ \begin{pmatrix} a & a_{12} & a_{13} & \cdots & a_{1n} \\ 0 & a & a_{23} & \cdots & a_{2n} \\ 0 & 0 & a & \cdots & a_{3n} \\ \vdots & \vdots & \vdots & \ddots & \vdots \\ 0 & 0 & 0 & 0 & a \end{pmatrix} \middle| a, a_{ij} \in R, n \geq 3 \right\}$$

, it is not α-*-reflexive according to (Abdulhafed, 2019) and is quasi-*-IFP. However, it is clearly evident that $T_4(R)$ is not α -quasi-*-IFP and so $T_n(R)$ is not quasi-*-IFP for $n \geq 4$ as reported in **Example 4**.

We get the same results as stated in both studies **[**(Aburawash & Abdulhafed, 2018a), Corollary 11(2)**]** and (Abdulhafed, 2019).

Corollary 11. *If R is a semiprime *-ring, then, the trivial extension* $T(R,R)$*, with adjoint involution is α-*-reflexive.*

Corollary 12. *Let's assume R to be a reduced *-ring and α is the *- endomorphism on R, then, the *-ring* $T(R,R)$*, with componentwise involution * is* $\tilde{\alpha}$*-*-reflexive.*

ISSN: online 2617-2186 print 2617-2178

Corollary 13. *Suppose R* be *an α-rigid *-ring,* then*, the *-ring $T(R,R)$, with componentwise involution* * is *$\tilde{\alpha}$-*-reflexive.*

Corollary 14. Let R be *a rigid *-ring,* then*, the *-ring $T(R,R)$, with componentwise involution* * is *$\tilde{\alpha}$-*-reflexive.*

The trivial extension $T(R,R)$ of a *-ring R can be extended to a *-ring

$$T_3(R)=\begin{pmatrix} a & b & c \\ 0 & a & d \\ 0 & 0 & a \end{pmatrix},$$

and *-endomorphism α of a *-ring R, it also is extended to the *-endomorphism $\tilde{\alpha}: T_3(R) \to T_3(R)$ is defined by $\tilde{\alpha}(a_{ij}) = \left(\alpha(a_{ij})\right)$ with involution defined as:

$$\begin{pmatrix} a & b & c \\ 0 & a & d \\ 0 & 0 & a \end{pmatrix}^{*} = \begin{pmatrix} a & d & c \\ 0 & a & b \\ 0 & 0 & a \end{pmatrix}$$

The following example shows that $T_3(R)$ cannot be $\tilde{\alpha}$-*-reflexive even if R is α-rigid-*-ring.

Example 11. Let R be a commutative α-rigid *-ring. Then, the *-ring $T_3(R)$ is not $\tilde{\alpha}$-*-reflexive, since the matrices

$$A=\begin{pmatrix} 1 & 0 & 0 \\ 0 & 1 & 0 \\ 0 & 0 & 1 \end{pmatrix}, B=\begin{pmatrix} 0 & 0 & 0 \\ 0 & 0 & 1 \\ 0 & 0 & 0 \end{pmatrix} \text{ and}$$

$$C=\begin{pmatrix} 0 & 1 & 0 \\ 0 & 0 & 0 \\ 0 & 0 & 0 \end{pmatrix} \in T_3(R),$$

Satisfy

$$ABC = ABC^{*} = 0,$$

while,

$$\tilde{\alpha}(C)\tilde{\alpha}(B)\tilde{\alpha}(A) \neq 0,$$

where $\alpha(e)=e$, according to (Abdulhafed, 2019).

Extensions of α-quasi-*-IFP and α-*-reflexive *-rings

In this section, recall that R be a *-ring and S be a multiplicatively closed subset of R consisting of nonzero central regular elements, then, the localization of R to S is $S^{-1}R = \{u^{-1}a | u \in S, a \in R\}$, and it also is a *-ring with involution $\diamond$ defined as: $(u^{-1}a)^{\diamond} = u^{-1^{*}}a^{*} = u^{*^{-1}}a^{*}$ see for more details (Aburawash & Abdulhafed, 2018b). A *-endomorphism $\tilde{\alpha}$ on R can be extended to $\tilde{\alpha}$ on $S^{-1}R$, the mapping $\tilde{\alpha}: S^{-1}R \to S^{-1}R$ is defined by $\tilde{\alpha}(u^{-1}a) = \alpha(u^{-1})\alpha(a)$ see [(Abdulhafed, 2019)]. Then, the following proposition is obtained.

Proposition 16. *A *-ring R is α-quasi-*-IFP if and only if $S^{-1}R$ **is** $\tilde{\alpha}$-quasi-*-IFP.*

Proof. Assume that $\beta\gamma = 0 = \beta\gamma^{\diamond}$ with $\beta = u^{-1}a$ and $\gamma = v^{-1}b$, where $a, b \in R$ and $u, v \in S$. Hence,

$$\beta\gamma = u^{-1}av^{-1}b = u^{-1}v^{-1}ab = (\mathrm{vu})^{-1}\mathrm{ab} = 0$$

and

$$\beta\gamma^{\diamond} = u^{-1}a(v^{*})^{-1}b^{*} = u^{-1}(v^{*})^{-1}ab^{*}$$

$$= (v^{*}u)^{-1}ab^{*} = 0,$$

since S exists in the center of R, and so $ab = ab^{*} = 0$. By hypothesis $\mathrm{acb} = 0$ for all $c \in R$, which implies

$$\tilde{\alpha}(\beta\ \xi\ \gamma) = \tilde{\alpha}\left(\mathrm{u}^{-1}\mathrm{aw}^{-1}\mathrm{cv}^{-1}\mathrm{b}\right) = \alpha\left((\mathrm{vwu})^{-1}\right)\alpha(\mathrm{acb}) = 0$$

for every $\xi = w^{-1}c \in S^{-1}R$. The converse is clear.

Proposition 17. *A *-ring R is α -*-reflexive if and only if $S^{-1}R$ is $\tilde{\alpha}$-*-reflexive.*

Proof. It is enough to show that $S^{-1}R$ is $\tilde{\alpha}$ -*-reflexive if R is α *-reflexive. Let R be an α-*-reflexive and $\beta\xi\gamma = 0 = \beta\xi\gamma^{\diamond}$ with

ISSN: online 2617-2186 print 2617-2178

$\beta = u^{-1}a,\ \xi = w^{-1}c$ and $\gamma = v^{-1}b$, where $a, b, c \in R$ and $u, v, w \in S$. Hence,

$\beta\xi\gamma = u^{-1}aw^{-1}cv^{-1}b = u^{-1}w^{-1}v^{-1}acb = (vwu)^{-1}acb = 0,$

and

$\beta\xi\gamma^{\circ} = u^{-1}aw^{-1}c(v^{*})^{-1}b^{*} = u^{-1}w^{-1}(v^{*})^{-1}acb^{*} = (v^{*}wu)^{-1}acb^{*} = 0.$

Since S exists in the central of R so

$acb = 0 = acb^{*}.$

By hypothesis $\alpha(b)\alpha(c)\alpha(a) = 0$, which implies that:

$\tilde{\alpha}(\gamma)\tilde{\alpha}(\xi)\tilde{\alpha}(\beta) = \tilde{\alpha}(v^{-1}b\,)\tilde{\alpha}(w^{-1}c)\tilde{\alpha}(u^{-1}a)$
$= \alpha(v^{-1})\alpha(w^{-1})\alpha(u^{-1})\alpha(b)\alpha(c)\alpha(a)$
$= \alpha((uvw)^{-1})\alpha(b)\alpha(c)\alpha(a) = 0$

It is important here to discuss the *-ring of Laurent polynomials in x, with coefficients in a *-ring R, consists of all formal sums

$$f(x) = \sum_{i=k}^{m} a_i x^i,$$

with obvious addition and multiplication, where $a_i \in R$ and k, m are (possibly negative) integers, and with involution * defined as:

$$f^{*}(x) = \sum_{i=k}^{m} a_i x^i.$$

It is denoted as usual by $R[x; x^{-1}]$. If α is *-endomorphism of a *-ring R, then, the map $\tilde{\alpha}$: $R[x] \to R[x]$ is defined by

$$\tilde{\alpha}\left(\sum_{i=k}^{m} a_i x^i\right) = \sum_{i=k}^{m} \alpha(a_i)\, x^i$$

for all i, is *-endomorphism of the polynomial *-ring $R[x]$, and it is clear this map extends α.

Corollary 15. *Let* R *be a *-ring, then, $R[x]$ is α-quasi-*-IFP* if and only if $R[x; x^{-1}]$ *is $\tilde{\alpha}$-quasi-*-IFP.*

Proof. It is sufficient to show the necessity. Clearly $S = \{1, x, x^2, \ldots\}$ is a multiplicatively closed subset of $R[x]$. Since $R[x; x^{-1}] = S^{-1}R[x]$, it follows that $R[x; x^{-1}]$ is $\tilde{\alpha}$-quasi-*-IFP by **Proposition 16**.

Corollary 16. Let's suppose *R is a *-ring,* then *R[x] is* α -*-*reflexive* if and only if $R[x; x^{-1}]$ *is $\tilde{\alpha}$-*-reflexive.*

Proof. The important thing is to prove the necessity, since $R[x]$ is a *-subring of $R[x; x^{-1}]$. Clearly, $S = \{1, x, x^2, \ldots\}$ is a multiplicatively closed subset of $R[x]$. Since $R[x; x^{-1}] = S^{-1}R[x]$, it follows that $R[x; x^{-1}]$ is $\tilde{\alpha}$-*-reflexive by **Proposition 17**.

A *-ring R is *-Armendariz (resp., quasi-*-Armendariz), when the polynomials

$$f(x) = \sum_{i=0}^{m} a_i x^i$$

and

$$g(x) = \sum_{j=0}^{n} b_j x^j \in R[x],$$

Satisfy

$$f(x)g(x) = f(x)g^{*}(x) = 0$$

(resp., $f(x)R[x]g(x) = f(x)R[x]g^{*}(x) = 0$), then, $a_i b_j = 0$ (resp., $a_i R b_j = 0$) for all i, j (consequently $a_i b_j^{*} = 0$ (resp.; $a_i R b_j^{*} = 0$)).

Theorem 1. *Let R be a *-Armendariz *-ring. Then the following statements are equivalent*

1. *R is α-quasi-*-IFP.*
2. *$R[x]$ is $\tilde{\alpha}$-quasi-*-IFP.*
3. *$R[x; x^{-1}]$ is $\tilde{\alpha}$-quasi-*-IFP.*

ISSN: online 2617-2186 print 2617-2178

Proof. It is enough to prove (1) to obtain (2). Let's consider

$$f(x) = \sum_{i=0}^{m} a_i x^i, g(x) = \sum_{j=0}^{n} b_j x^j \in R[x]$$

Therefore,

$$f(x)R[x]g(x) = 0 = f(x)R[x]g^*(x).$$

By hypothesis,

$$a_i b_j = 0 = a_i b_j^*$$

and

$\alpha(a_i)\alpha(r)\alpha(b_j) \in R$ for all i, j and $r \in R$.

Hence, $\alpha\big(f(x)\big)R[x]\alpha\big(g(x)\big) = 0$, and hence that $R[x]$ is $\tilde{\alpha}$-quasi-*-IFP.

Theorem 2. *Let us assume R is a quasi-*-Armendariz *-ring, then the following statements are equivalent.*

1. *R is α-*-reflexive.*
2. *$R[x]$ is $\tilde{\alpha}$-*-reflexive.*
3. *$R[x; x^{-1}]$ is $\tilde{\alpha}$-*-reflexive.*

Proof. It suffices to show that (1) ⇒ (2). Assume

$$f(x) = \sum_{i=0}^{m} a_i x^i, g(x) = \sum_{j=0}^{n} b_j x^j \in R[x]$$

leads us to obtain:

$$f(x)R[x]g(x) = 0 = f(x)R[x]g^*(x).$$

Since R is quasi-*-Armendariz, it is given $a_i R b_j = 0$ for all i, j. But, R is α-*-reflexive, so $\alpha\big(b_j\big)R\alpha(a_i) = 0$ for all i, j.

Consequently $\alpha(g(x))R[x]\alpha(f(x)) = 0$, and hence $R[x]$ is $\tilde{\alpha}$-*-reflexive.

The following corollaries are obtained by Theorems 1 and 2.

Corollary 17. *Let R be an Armendariz *-ring. Then, the following relations are equivalent:*

1. *R is α-quasi-*-IFP.*
2. *$R[x]$ is $\tilde{\alpha}$-quasi-*-IFP.*
3. *$R[x; x^{-1}]$ is $\tilde{\alpha}$-quasi-*-IFP.*

Corollary 18. *Let R be a quasi-Armendariz *-ring. Then, the following relations are equivalent:*

1. *R is α-*- reflexive.*
2. *$R[x]$ is $\tilde{\alpha}$-*-reflexive.*
3. *$R[x; x^{-1}]$ is $\tilde{\alpha}$-*-reflexive.*

It is known that, *the Dorroh extension* $D(R, Z) = \{(r, n): r \in R, n \in \mathbb{Z}\}$ of a *-ring R is a ring with componentwise addition and multiplication:

$$(r_1, n_1)(r_2, n_2) = (r_1 r_2 + n_1 r_2 + n_2 r_1, n_1 n_2).$$

The involution of R can be extended naturally to $D(R, \mathbb{Z})$ as $(r, n)^* = (r^*, n)$ (see (Aburawash, 1997)). A *-endomorphism α on R can be extended to $\tilde{\alpha}$ on $D(R, \mathbb{Z})$ by $\tilde{\alpha}(r, n) = (\alpha(r), n)$ (see (Başer et al., 2009)).

Proposition 18. A *-ring R is α-quasi-*-IFP with $\alpha(1) = 1$, if and only if its Dorroh extension $D(R, \mathbb{Z})$ is $\tilde{\alpha}$-quasi-*-IFP.

Proof. Let $(r_1, n_1), (r_2, n_2) \in D$ with $(r_1, n_1)(r_2, n_2) = 0 = (r_1, n_1)(r_2^*, n_2)$.

Then,

$r_1 r_2 + n_1 r_2 + n_2 r_1 + n_1 n_2 = 0 = r_1 r_2^* + n_1 r_2^* + n_2 r_1 + n_1 n_2$.

Since $\mathbb{Z}$ is a *-domain, we have $n_1 = 0$ or $n_2 = 0$. If $n_1 = 0$ then $0 = r_1 r_2 + n_2 r_1 = r_1(r_2 + n_2)$ and $0 = r_1 r_2^* + n_2 r_1 = r_1(r_2^* + n_2)$. Since R is α-quasi-*-IFP with $\alpha(1) = 1$, $0 = \tilde{\alpha}(r_1)\tilde{\alpha}(r)\tilde{\alpha}\big((r_2 + n_2)\big) = \alpha(r_1)\alpha(r)\alpha(r_2) + \alpha(r_1)\alpha(r)n_2$ and $0 = \tilde{\alpha}(r_1)\tilde{\alpha}(r)\tilde{\alpha}\big((r_2^* + n_2)\big) = \alpha(r_1)\alpha(r)\alpha(r_2{}^*) + \alpha(r_1)\alpha(r)n_2$ for all $r \in R$. This yields

ISSN: online 2617-2186 print 2617-2178

$0 = \tilde{\alpha}((r_1, n_1))\tilde{\alpha}((r, n))\tilde{\alpha}((r_2, n_2)) =$
$(\alpha(\mathrm{r}_1)\alpha(\mathrm{r}) + \mathrm{n}\alpha((\mathrm{r}_1))\ \alpha(\mathrm{r}_2) +$
$(\alpha(\mathrm{r}_1)\alpha(\mathrm{r}) + n\alpha(r_1))n_2$ for any $(r, n) \in D$, and hence $\tilde{\alpha}((r_1, n_1))D\tilde{\alpha}((r_2, n_2)) = 0$. Now, let $n_2 = 0$. Then, $(r_1 + n_1)r_2 = 0$, and so $0 = (\alpha(r_1) + n_1)R\alpha(r_2) = 0$. It is similar to obtain $\tilde{\alpha}\big((r_1, n_1)\big)D\tilde{\alpha}\big((r_2, n_2)\big) = 0$, and thus, the Dorroh extension $D(R, \mathbb{Z})$ is $\tilde{\alpha}$-quasi-*-IFP.

Proposition 19. *A *-ring R is α-*-reflexive with $\alpha(1) = 1$, if and only if its Dorroh extension $D(R, \mathbb{Z})$ is $\tilde{\alpha}$-*-reflexive.*

Proof. Suppose that $(r_1, n_1), (r_2, n_2) \in D$ with $(\mathrm{r}_1, \mathrm{n}_1)(\mathrm{r}, \mathrm{n})(\mathrm{r}_2, \mathrm{n}_2) = 0 =$ $(\mathrm{r}_1, \mathrm{n}_1)(\mathrm{r}, \mathrm{n})(r_2^*, n_2)$. For any $(r, n) \in D$. The claim here is

$$\tilde{\alpha}\big((r_2, n_2)\big)\tilde{\alpha}\big((r, n)\big)\tilde{\alpha}\big((r_1, n_1)\big) = 0.$$

In fact, we have

$$(r_1 r r_2 + n_1 r r_2 + n r_1 r_2 + n_1 n r_2 + n_2 r_1 r +$$

$$n_1 n_2 r + n n_2 r_1, n_1 n n_2) = 0 = (r_1 r r_2^* + n_1 r r_2^*$$

$$+ n r_1 r_2^* + n_1 n r_2^* + n_2 r_1 r + n_1 n_2 r +$$
$$n n_2 r_1, n_1 n n_2), \qquad r_1 r r_2 + n_1 r r_2 + n r_1 r_2 +$$
$$n_1 n r_2 + n_2 r_1 r + n_1 n_2 r + n n_2 r_1 = 0$$

$$= \mathrm{r}_1 \mathrm{r} r_2^* + \mathrm{n}_1 \mathrm{r} r_2^* + \mathrm{n} r_1 r_2^* + \mathrm{n}_1 \mathrm{n} r_2^* + \mathrm{n}_2 \mathrm{r}_1 \mathrm{r}$$
$$+ n_1 n_2 r + n n_2 r_1$$

and

$$n_1 n n_2 = 0,$$

since $\mathbb{Z}$ is a *-domain $n_1 = 0$, $n = 0$ or $n_2 = 0$. If $n_1 = 0$, then, $r_1 r r_2 + n r_1 r_2 + n_2 r_1 r + n n_2 r_1 = 0$, and so we have:

$$0 = r_1 r r_2 + n r_1 r_2 + n_2 r_1 r + n n_2 r_1 = r_1(r, n)$$

$$(r_2, n_2) = (\alpha(r_2), n_2)(\alpha(r), n)\alpha(r_1) = \alpha(r_2)$$

$\alpha(r)\alpha(r_1) + \alpha(r_2)n\alpha(r_1) + n_2\alpha(r)\alpha(r_1) +$ $\mathrm{n}_2\mathrm{n}\alpha(\mathrm{r}_1)$, since R is $\tilde{\alpha}$-*-reflexive *-ring. This shows that

$$\tilde{\alpha}\big((r_2, n_2)\big)\tilde{\alpha}\big((r, n)\big)\tilde{\alpha}\big((r_1, n_1)\big) =$$
$$\alpha(r_2)\alpha(r)\alpha(r_1) + \alpha(r_2)n\alpha(r_1) +$$
$$n_2\alpha(r)\ \alpha(r_1) + n_2 n\alpha(r_1) =$$
$$\alpha(r_2)\alpha(r)\alpha(r_1) + n_2\alpha(r)\alpha(r_1) +$$
$$n\alpha(r_2)\alpha(r_1) + n_2 n\alpha(r_1) + n_1\alpha(r_2)\alpha(r) +$$
$$n_1 n_2\alpha(r) + n_1 n\alpha(r) = 0,\ n_2 n n_1 = 0.$$

If $n_2 = 0$, then,

$$r_1 r r_2 + n_1 r r_2 + n r_1 r_2 + n_1 n r_2$$
$$= (r_1, n_1)(r, n)r_2 = \alpha(r_2)$$

$$\tilde{\alpha}\big((r, n)\big)\tilde{\alpha}\big((r_1, n_1)\big)$$
$$= \alpha(r_2)\alpha(r)\alpha(r_1)$$
$$+ \alpha(r_2)\alpha(r)n_1 + \alpha(r_2)n\alpha(r_1)$$
$$+ \alpha(r_2)n n_1 =$$

$$\alpha(r_2)\alpha(r)\alpha(r_1) + n_2\alpha(r)\alpha(r_1)$$
$$+ n\alpha(r_2)\alpha(r_1) + n_2 n\alpha(r_1)$$
$$+ n_1\alpha(r_2)\alpha(r) + n_1 n_2\alpha(r)$$
$$+ n_1 n\alpha(r_2) = 0.$$

Therefore, we get $0 = \tilde{\alpha}\big((r_2, n_2)\big)\tilde{\alpha}\big((r, n)\big)$ $\tilde{\alpha}\big((r_1, n_1)\big)$, then, D is $\tilde{\alpha}$-*-reflexive.

Conversely, assume that D is $\tilde{\alpha}$-*-reflexive. Let $\alpha(r_1)R\alpha(r_2) = 0 = \alpha(r_1)R\alpha(r_2^*)$, for $r_1, r_2 \in R$. Then, $\alpha(r_1)(\alpha(r) + n))\alpha(r_2) = 0 = \alpha(r_1)(\alpha(r) + n))\alpha(r_2^*)$ for any$(r, n) \in D$, this implies:

$$0 = \tilde{\alpha}\big((r_1, 0)\big)\tilde{\alpha}\big((r, n)\big)\tilde{\alpha}\big((r_2, 0)\big) =$$
$$\tilde{\alpha}\big((r_1, 0)\big)\tilde{\alpha}\big((r, n)\big)\tilde{\alpha}\big((r_2^*, 0)\big),$$for any $(r, n) \in D$. Since D is $\tilde{\alpha}$-*-reflexive, we have $0 = \tilde{\alpha}\big((r_2, 0)\big)\tilde{\alpha}\big((r, n)\big)\tilde{\alpha}\big((r_1, 0)\big) =$
$$\tilde{\alpha}\big((r_2^*, 0)\big)\tilde{\alpha}\big((r, n)\big)\tilde{\alpha}\big((r_1, 0)\big),$$

and hence, $\alpha(r_2)(\alpha(r) + n)\alpha(r_1) = 0 =$

$\alpha(r_2^*)(\alpha(r) + n)\alpha(r_1)$, thus,

$$\alpha(r_2)R\alpha(r_1) = 0 = \alpha(r_2^*)R\alpha(r_1).$$

Recall that, a ring R is called right Ore, if it is given $a, b \in R$ with b regular, there exist $a_1, b_1 \in R$ with b_1 regular such that: $ab_1 = ba_1$. Left Ore is defined similarly, and R is Ore ring, whether it is both right and left Ore. For

ISSN: online 2617-2186 print 2617-2178

*-rings, right Ore implies left Ore and vice versa. It is a known fact that R is Ore if and only if its classical quotient ring Q of R exists and for *-rings, * can be extended to Q by $(a^{-1}b)^* = b^*(a^*)^{-1}$. A *-automorphism α on Q by $\tilde{\alpha}(ab^{-1}) = \alpha(a)\alpha(b)^{-1}$ (see [(Martindale & 3rd, 1969), Lemma 4], (Hong et al., 2006)). The following theorem is generalized by [(Aburawash & Abdulhafed, 2018a), Theorem 5].

Theorem 3. *Let* R *be an Ore *-ring,* α *the *-automorphism of* R*, and* Q *be its classical quotient *-ring, then,* R *is* α*-*-reflexive if and only if* Q *is* $\tilde{\alpha}$*-*-reflexive.*

Proof. Let R be an α-*-reflexive *-ring and $\beta\gamma\xi = 0 = \beta\gamma\xi^*$ with $\beta = au^{-1}$, $\gamma = bv^{-1}$ and $\xi = cw^{-1} \in Q$. By hypothesis for $a, b, c, d, u, v, w \in R$, there exist $b_1, u_1 \in R$ with u_1 regular

$$ub_1 = bu_1, u^{-1}b = b_1u_1^{-1}, \qquad (1)$$

then, $0 = \beta\gamma\xi = au^{-1}bv^{-1}cw^{-1} = ab_1u_1^{-1}v^{-1}cw^{-1}$. Also, for $c, v \in R$ there exist $c_1, v_1, c_1^* \in R$ with v_1 regular such that:

$$vc_1 = cv_1,\ v^{-1}c = c_1v_1^{-1}$$

and

$$vc_1^* = c^*v_1, v^{-1}c^* = c_1^*v_1^{-1}, \qquad (2)$$

so, we have $0 = \beta\gamma\xi = ab_1u_1^{-1}c_1v_1^{-1}w_1^{-1}$. For $c, u \in R$, there exist $c_1^*, c_2, c_2^*, u_2 \in R$ with u_2 regular such that:

$$u_1c_2 = c_1u_2,\ u_1^{-1}c_1 = c_2u_2^{-1}, \qquad (3)$$

$$u_1c_2^* = c_1^*u_2,\ u_1^{-1}c_1^* = c_2^*u_2^{-1}, \qquad (4)$$

and hence, it is obtained

$$0 = \beta\gamma\xi = ab_1c_2u_2^{-1}v_1^{-1}w^{-1} = ab_1c_2(wv_1u_2)^{-1}$$

which implies $ab_1c_2 = 0$. Similarly,

$$0 = \gamma\beta\xi^* = au^{-1}bv^{-1}(cw^{-1})^* = au^{-1}bv^{-1}(w^*)^{-1}c^* = ab_1u_1^{-1}v^{-1}(w^*)^{-1}c^* = ab_1(w^*vu_1)^{-1}c^*,$$

where $g = w^*vu_1 \in R$. For $c, g \in R$, there exist $g_1, c_2^* \in R$ with g_1 regular such that:

$$gc_2^* = c^*g_1,\ g^{-1}c^* = c_2^*g_1^{-1}.$$

Thus,

$$0 = \gamma\beta\xi^* = ab_1c_2^*g_1^{-1},$$

for which implies that $ab_1c_2^* = 0$, then, $ab_1c_2 = 0 = ab_1c_2^*$. In the following computations, the condition that R is α-*-reflexive can be used freely. Since $ab_1c_2 = 0$, we have $c_2b_1a = 0$, and so $c_2b_1au = 0$. This implies that:

$aub_1c_2 = abu_1c_2 = 0$ by **(1),** then, $u_1c_2ba = 0$, and so $c_1u_2ba = 0$ by **(3)**. This leads to $abc_1u_2 = 0$, and $abc_1 = 0$. Hence, $c_1ba = 0$, and thus $vc_1ba = 0$, so $abcv_1 = 0$. Hence, we get $abc = 0$, and so $cba = 0$. Similarly, $ab_1c_2^* = 0$, we have $c_2^*b_1a = 0$, and so $c_2^*b_1au = 0$. This implies that $aub_1c_2^* = abu_1c_2^* = 0$ by **(1),** then, $u_1c_2^*ba = 0$, and so $c_1^*u_2ba = 0$ **by (4)**. This shows that $abc_1^*u_2 = 0$ and $abc_1^* = 0$. Hence, $c_1^*ba = 0$, and thus $vc_1^*ba = 0$, so $abc^*v_1 = 0$ **by (2)**. Hence, we get $abc^* = 0$ and so c^*ab=0. On the other hand, $\xi\gamma\beta = \tilde{\alpha}(cw^{-1})\tilde{\alpha}(bv^{-1})\tilde{\alpha}(au^{-1})$ and similarly there exist $a_3, a_4, b_3, w_3, v_3, v_4 \in R$ with w_3, v_3, v_4 regular such that:

$$\alpha(w)\alpha(b_3) = \alpha(b)\alpha(w_3), \qquad \alpha(w^{-1})\alpha(b) = \alpha(b_3)\alpha(w_3^{-1}),$$

$$\alpha(v)\alpha(a_3) = \alpha(a)\alpha(v_3), \qquad \alpha(v^{-1})\alpha(a) = \alpha(a_3)\alpha(v_3^{-1})$$

and

$$\alpha(w)\alpha(a_4) = \alpha(a_3)\alpha(v_4), \qquad \alpha(w_3^{-1})\alpha(a_3) = \alpha(a_4)\alpha(v_4^{-1}).$$

Then, we get

$$\xi\gamma\beta = \alpha(c)\alpha(b_3)\alpha(w_3^{-1})\alpha(a_3)\alpha(v_3^{-1})\alpha(u^{-1}) = \alpha(c)\alpha(b_3)\ \alpha(a_4)\alpha(v_4^{-1})\alpha(v_3^{-1})\alpha(u^{-1}) =$$

ISSN: online 2617-2186 print 2617-2178

$\alpha(cb_3a_4)\alpha\left((uv_3v_4)^{-1}\right)$. Since $\alpha(cba)=0$, we obtain $\alpha(w_3)\alpha(cba)=0$, and so

$$\alpha(a)\alpha(b)\alpha(w_3)\alpha(c)=0=\alpha(a)\alpha(w)\alpha(b_3)\alpha(c).$$

This implies that:

$$\alpha(c)\alpha(b_3)\alpha(a)\alpha(w)=0,$$

and thus

$$\alpha(c)\alpha(b_3)\alpha(a)=0.$$

Then,

$$\alpha(c)\alpha(b_3)\alpha(a)\alpha(v_3)=\alpha(c)\alpha(b_3)\alpha(v)\alpha(a_3)=0 \text{ and so, } \alpha(v)\alpha(a_3)\alpha(b_3)\alpha(c)=0.$$

Hence, $\alpha(a_3b_3c)=0=\alpha(cb_3a_3)$ and then

$$\alpha(c)\alpha(b_3)\alpha(a_3)\alpha(v_4)=\alpha(c)\alpha(b_3)\alpha(w)\,\alpha(a_4)=\alpha(wa_4)\alpha(b_3)\alpha(c)=0.$$

It follows that $\alpha(a_4)\alpha(b_3)\alpha(c)=0$ and we get $\alpha(c)\alpha(b_4)\alpha(a_3)=0$. Therefore,

$\xi\gamma\beta=\tilde{\alpha}(cw^{-1}bv^{-1}au^{-1})=\alpha(cb_3a_4)(uv_3v_4)^{-1}=0$.Then Q $\tilde{\alpha}$-*-reflexive.

Finally, according to the study (Abdulhafed, 2019)], [(Aburawash & Abdulhafed, 2018a), Theorem 5], and **Theorem 3**, the following corollaries are deduced.

Corollary 19. *If* R is reflexive **-ring,* then Q *is* $\tilde{\alpha}$-*-*reflexive.*

Corollary 20. *If* Q is reflexive **-ring, then* R *is* α-*-*reflexive.*

Corollary 21. *If* R *is* α-*-*reversible *-ring, then* Q *is* $\tilde{\alpha}$-*-*reflexive.*

Corollary 22. If Q is $\tilde{\alpha}$-*-reversible *-ring, then R is α-*-reflexive.

Conclusion And Future Directions

All the results of the paper are summarized by using a diagram explaining the relations among the corresponding classes.It is possible to follow implications in the class of rings with involution.

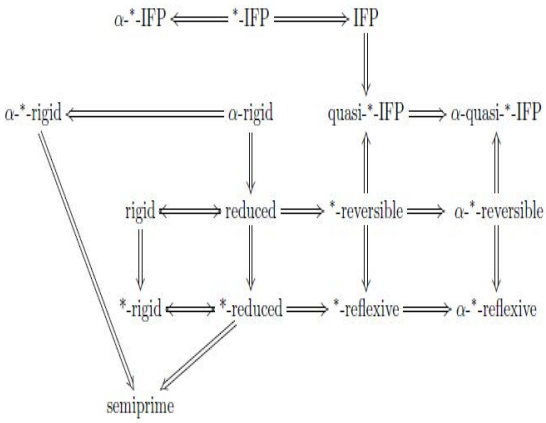

Most importantly, the study has explored the following several new results.

1. Every α-rigid is α-*-*reflexive*.
2. Every *-rigid is α-*-*reflexive*.
3. Every α-*-reversible is α-*-*reflexive*.
4. Each α-*-reversible is α-quasi-*-IFP.

Finally, these results pave the way for further research into some classes of *-rings which generalize that of α-*-reflexive *-rings and investigate their properties.

Based on the above results, we strongly recommend studying the *-rings independently by using both morphisms and structures presiding its involution. However, it is good to join the involutive structures with their non-involutive counterparts. Future work will be concerned with deeper analysis of *-rings, new properties of the created structures and new several structures in the involutive sense. The following questions should be an inception for new works:

1. Studying the extensions over *-Baer *-rings as polynomials, skew polynomials, and matrices is very important. What are the hypotheses needed to do that?
2. How are the extensions of α -*-reflexive possible?
3. Is there a possibility to get a definition for

ISSN: online 2617-2186 print 2617-2178

central α-*-reflexive *-rings analogously to central *-reflexive rings?

REFERENCES

Abdulhafed, M. E. (2019). *A Study of Reflexive and Reversible Rings with Involution* (Unpublished Doctoral dissertation). Faculty of Science -Alexandria University.

Aburawash, U. A. (1997). On Embeding of Involution Rings.pdf. *Mathematica Pannonica*, *8*(2), 245–250.

Aburawash, U. A., & Abdulhafed, M. E. (2018a). On reflexive rings with involution. *International Journal of Algebra*, *12*(3), 115–132. https://doi.org/10.12988/ija.2018.8412

Aburawash, U. A., & Abdulhafed, M. E. (2018b). On reversibility of rings with involution. *East-West J. of Mathematics*, *20*(1), 19–36. https://doi.org/10.2140/pjm.1975.60.131

Aburawash, U. A., & Saad, M. (2014). On Biregular , IFP and Quasi-Baer ∗ -Rings. *East-West J. of Mathematics Mathematics*, *16*(2), 182–192.

Aburawash, U. A., & Saad, M. (2016). *-Baer property for rings with involution. *Studia Scientiarum Mathematicarum Hungarica*, *53*(2), 243–255. https://doi.org/10.1556/012.2016.53.2.1338

Aburawash, U. A., & Saad, M. (2019). Reversible and reflexive properties for rings with involution. *Miskolc Mathematical Notes*, *20*(2), 635–650. https://doi.org/10.18514/MMN.2019.2676

Başer, M., Harmanci, A., & Kwak, T. K. (2008). Generalized semicommutative rings and their extensions. *Bulletin of the Korean Mathematical Society*, *45*(2), 285–297. https://doi.org/10.4134/BKMS.2008.45.2.285

Başer, M., Hong, C. Y., & Kwak, T. K. (2009). On extended reversible rings. *Algebra Colloquium*, *16*(1), 37–48. https://doi.org/10.1142/S1005386709000054

Başer, M., & Kwak, T. K. (2010). Extended semicommutative rings. *Algebra Colloquium*, *17*(2), 257–264. https://doi.org/10.1142/s1005386710000271

Hong, C. Y., Kwak, T. K., & Rizvi, S. T. (2006). Extensions of generalized armendariz rings. *Algebra Colloquium*, *13*(2), 253–266. https://doi.org/10.1142/S100538670600023X

Kim, N. K., & Lee, Y. (2003). Extensions of reversible rings. *Journal of Pure and Applied Algebra*, *185*(1–3), 207–223. https://doi.org/10.1016/S0022-4049(03)00109-9

Martindale, W. S., & 3rd. (1969). Rings with involution and polynomial identities. *Journal, of Algebra*, *11*, 186–194.

Zhao, L., & Zhu, X. (2012). Extensions of α-reflexive rings. *Asian-European Journal of Mathematics*, *5*(1), 1–10.https://doi.org/10.1142/S1793557112500131

ISSN: online 2617-2186 print 2617-2178

مجلة المختار للعلوم 36 (1): 42-56، 2021

تمديد الحلقات الالتفافية الانعكاسية

منى امحمد محمد عبد الحفيظ ، [2] عفاف امحمد محمد عبد الحفيظ

[1] قسم الرياضيات، كلية العلوم، جامعة الزيتونة، ترهونة، ليبيا .
[2] قسم الرياضيات، كلية التربية، جامعة الزيتونة، ترهونة، ليبيا

تاريخ الاستلام: 13 يناير 2021 / تاريخ القبول: 31 يناير 2021
https://doi.org/10.54172/mjsc.v36i1.22:Doi

المستخلص: تقدم الدراسة مفهوم تمديد (خاصية شبة إدراج المعاملات، الانعكاس) للحلقات الالتفافية كونه تعميما على (خاصية شبه إدراج المعاملات، الانعكاس) للحلقات الالتفافية وكل (خاصية شبه إدراج المعاملات، الانعكاس) للحلقات الالتفافية تكون تمديدا (لخاصية شبه إدراج المعاملات، الانعكاس) للحلقات الالتفافية. كما تدرس الشرط الكافي لخاصية شبه إدراج المعاملات والانعكاس لتكون تمديدا (لخاصية شبه إدراج المعاملات، الانعكاس). ويتم أخيرا التحقق من تمديد (لخاصية شبه إدراج المعاملات، الانعكاس) لبعض أنواع الحلقات كثيرات الحدود

الكلمات المفتاحية: الحلقات الالتفافية المختزلة، الحلقات الالتفافية الصلبة، تمديد الحلقات الالتفافية الصلبة، تمديد الحلقات الالتفافية بخاصية إدراج المعاملات، تمديد الحلقات الالتفافية بخاصية شبة إدراج المعاملات، تمديد الحلقات الالتفافية الانقلابية، تمديد الحلقات الالتفافية الانعكاسية.

[1]منى امحمد محمد عبد الحفيظ muna.am2016@gmail.com.قسم الرياضيات، كلية العلوم، جامعة الزيتونة، ترهونة، ليبيا.

Al-Mukhtar Journal of Sciences 36 (1): 57-66, 2021

Aqueous Extract of (*Eruca sativa* Mill) as Growth Stimulant in Enhancing Growth and Yield of Faba Bean (*Vicia faba* L)

Amal F Ehtaiwwesh and Fouziyah Qarimidah

Department of plant science, University of Zawia, Libya

Received: 21 January 2021/ Accepted: 31 January 2021
Doi: https://doi.org/10.54172/mjsc.v36i1.14

Abstract: A field study was conducted in the fall of 2019 to investigate the potential of Arugula (*Eruca sativa* Mill) aqueous extract as a growth stimulant in enhancing the growth and yield of Faba Bean (*Vicia faba* L*)*. The study was conducted using sandy soil at a farm in Abo Esaa town in a plot size of 3X5 m^2 with a row spacing of 25cm,which based on a complete randomized design (RCD) with four replications, three treatments were carried out, including no foliar spray with *E. sativa* extracts (control) and foliar sprayed with 20% and 40% aqueous extracts of *E. sativa*. Accordingly, Faba Bean (*Vicia faba* L) plants were foliar sprayed six times with the aqueous extracts of *E. sativa* at rates of 20 and 40% at vegetative and reproductive stages. The result showed that among these concentrations, the foliar spray of faba bean plants with 40% of *E. sativa* extracts potentially were increased all measured growth and yield traits. The results pointed out that plant height increased by 32%, number of branches by 73%, number of leaves by 95%, number of seeds plant by 89%, leaves, stems, pods and roots dry weight by 92%, 80%, 74%, and 89%, respectively. Thus, the study concluded that *E. sativa* aqueous extracts could potentially be used efficiently by crop producers as a growth enhancer for faba bean crops because of their productivity, great nutritive value, low cost, and environmentally friendly nature.

Keywords*: Vicia faba* L; *Eruca sativa* Mill; Aqueous Extracts; Growth; Yield.

INTRODUCTION

Faba bean (*Vicia faba L)* is a main legume crop grown in Libya due to its high nutritional value of the seeds. Humans in all over the world consume Faba been seeds as a substantial source of vegetable protein (El-Dabaa et al., 2019). Also, some faba bean varieties make significant livestock feed for animal feeding (Crépon et al., 2010; Cherif et al.,2018). Likewise, growing this legume is valuable to other crops as it increases soil fertility by biological nitrogen fixation and increases the soil content of nitrogen (El-Dabaa et al., 2019). In Libya, soil fertility is one of the principal production limitations, especially nitrogen deficiency. Hence, immense quantities of chemical fertilizers are applied for crop production. However, artificial chemical fertilizers are potentially toxic and may harm the environment (Khanh et al., 2004; Macı´as et al., 2006). In addition, over-applying of chemicals may cause human health problems, ground water contamination, and may lead to toxicity in foods (Hong et al., 2004).

Eruca sativa is an herb vegetable and a perennial plant belonging to the Brassicaceae family (Koubaa et al., 2015). Arugula (*Eruca sativa* Mill) is a highly valued plant distributed in many countries worldwide. It has an impressive range of medicinal uses and high nutritional value. The health benefits of *E. sativa* leaves and seeds were widely investigated, however, considering to the literature available, little information is currently available about the biostimulants effect of *E. sativa* on plant growth in general, and on faba bean specifically. Biostimulants are plant extracts that contain some kinds of bioactive compounds that able to im-

***Corresponding Author:** Amal Ehtaiwwesh a.ehtaiweshl@zu.edu.ly , Department of plant science, University of Zawia, Libya.

prove some physiological processes that stimulate growth and development of crops with increasing nutrient use efficiency, and reducing synthetic chemical fertilizers without affecting the quality and crop yield (Bulgari et al., 2015; Elzaawely et al., 2017). Biostimulants possibly offer a new approach for the regulation of physiological processes in plants to stimulate growth, alleviate stress, and increase yield (Yakhin et al., 2017). Foliar application of biostimulants and micronutrients could be a better way of fast action in improving plant growth and yield (Khan et al..,2021). Another work, investigated the effect of some natural plant extracts include garlic, moringa, and licorice extracts on the yield and fruit quality of pear trees. The work is reported that extracts of these plants could be recommended to be used effectively as natural plant extracts for improving the growth of various crops due to its high nutritive value, antioxidant effect, easy preparation, and environmentally friendly (Abd El–Hamied and El-Amary, 2015). To reduce dependence on synthetic chemical fertilizers, an alternative source for nutritional components is required for improving crops and faba bean production that minimizes environmental pollution. Therefore, this study aimed to highlight the potential of arugula (*Eruca sativa* Mill) aqueous extract as a green fertilizer in enhancing the growth and yield of faba bean (*vicia faba* L).

MATERIAL AND METHODS

Plant Materials: Faba bean (*Vicia faba L)* seeds and Arugula (*Eruca sativa* Mill) obtained from the local market.

Experimental and treatment conditions: A field experiment was conducted in sandy soil at a farm in abo Esaa town based on a randomized complete design (RCD) with four replications in a plot size of 3X5 m^2 with a row spacing of 25 cm. Seeds of faba bean were sown in sandy soils in November 2019. Di-Ammonium phosphates ($(NH_4)_2HPO_4$) 46P, 18N were applied twice, the first application was around the vegetative stage, and the second application was around the flowering stage of plant growth. The plants were irrigated as needed and were under monitoring.

***Eruca sativa* extract:** Plant materials were obtained from the local market, and the leaves of the plant were first washed and left to dry. *Eruca sativa* aqueous extract was prepared following modified methods of (Phiri, 2010). Briefly, 100 g of fresh leaves of *E. sativa* were mixed with 100 ml of distilled water in a household blender for 15 minutes. The solution was filtered through filter paper Whatman No. 1 and stored at 4C° until used the next day.

Application of *Eruca sativa* extract: At the spray time, 20% and 40% of plant extract were prepared by taking 20 and 40 ml of plant extract and diluted by adding fresh water to make 100 ml of plant extract, which almost immediately was foliar sprayed to growing faba bean plants. The same procedure was repeated every ten days with a total of six times. The control plants were sprayed with tap water, and plants were harvested after 150 days of sowing.

Data collection: At harvesting, a random sample of four plants were randomly taken from each treatment and the following data were recorded:

1. Plant height (cm)
2. Number of branches / plant.
3. Number of leaves / plant.
4. Number of pods / plant.
5. Number of seeds / pod.
6. Number of seeds / plant.

Subsequently, plants were dried and the following data were recorded:

1. Leave dry weight / plant (g)
2. Stem dry weight / plant (g)
3. Root dry weight / plant (g)
4. Pods dry weight / plant (g)
5. Weight of 10 seeds (g).
6. Yield of seeds (g) / plant.

The 10 seed weight was recorded in g of the weight of 10 randomly selected seeds from

ISSN: online 2617-2186 print 2617-2178

each replication after threshing, and seed yield was calculated. Seeds yield was estimated in g per plant with total weight of seeds after threshing.

Statistical Analysis: The experimental design was a randomized complete design (RCD) with four replications. Analysis of variance performed using generalized linear model (GLM) procedure in SAS 9.4 (SAS Institute Inc., Cary, NC, USA) for growth and yield-related traits. Separation of means was carried out using the least significant differences (LSD; $P < 0.05$). The means were compared using Duncan's multiple range test.

RESULTS

The P-values for growth and yield-related traits obtained with SAS PROC GLM are presented in table 1. The effects of the application of *E. sativa* aqueous extract were significant ($P < 0.05$) on plant height, number of branches, number of leaves, number of pods, number of seeds, leaves, stems, pods, and roots dry weight, dry weight of 10 seeds and yield of seeds (Table 1). Data presented in Table 2 shows the effect of the application of *E. sativa* extract at different concentrations on the growth and yield of faba bean plants.

Table:1. Probability values of the effect of *Eruca sativa* aqueous extract on the growth and yield of faba bean (*Vicia faba* L) Plants

Traits	Treatments
Plant height (cm)	0.0420
Number of branches plant^{-1}	0.0395
Number of leaves plant^{-1}	0.0372
Number of pods plant^{-1}	0.0376
Number of seeds pod^{-1}	0.0467
Number of seeds plant^{-1}	0.0245
Leave dry weight plant^{-1} (g)	0.0460
Stem dry weight plant^{-1} (g)	0.0443
Root dry weight plant^{-1} (g)	0.0478
Pods dry weight plant^{-1} (g)	0.0309
Weight of 10 seeds (g)	0.0455
Yield of seeds plant^{-1}. (g)	0.0013

Table:2. The effect of *(Eruca sativa* Mill*)* aqueous extract on the growth and yield of faba bean (*Vicia faba* L) Plants.

Traits	Treatments		
	Control	20%	40%
Plant height (cm)	55^{b}	56^{b}	73^{a}
Number of branches plant^{-1}	3.7^{b}	5.5^{ab}	6.5^{a}
Number of leaves plant^{-1}	69^{b}	117^{ab}	135^{a}
Number of pods plant^{-1}	9^{b}	10.5^{ab}	14^{a}
Number of seeds pod^{-1}	3.4^{b}	4^{ab}	4.2^{a}
Number of seeds plant^{-1}	31.7^{b}	42^{ab}	60^{a}
Leave dry weight plant^{-1} (g)	5.5^{b}	7.9^{ab}	10.6^{a}
Stem dry weight plant^{-1} (g)	10^{b}	13^{ab}	18^{a}
Root dry weight plant^{-1} (g)	4^{b}	5.6^{ab}	7^{a}
Pods dry weight plant^{-1} (g)	25^{b}	31^{ab}	47^{a}
Weight of 10 seeds (g)	9.7^{b}	13.8^{ab}	16.8^{a}
Yield of seeds plant^{-1}. (g)	32.6^{b}	57.5^{b}	97.8^{a}

* Individual value is the mean of 4 plants under different salinity levels. Values followed by different letters are significantly different according to Duncan's multiple range test ($P < 0.05$

The results were showed that the low concentrations (20%) of *E. sativa* extract did not have a significant effect on the plant height of faba beans. Whereas the high concentrations (40%) of *E. sativa* extract exhibit a significant effect on the plant height of faba bean, which

ISSN: online 2617-2186 print 2617-2178

increased plant height by 32% compared to control plants (Fig. 1A). Concurrently, the number of branches plant-1 increased under both concentrations of *E. sativa* extract. The result indicated that the application of 20% of *E. sativa* extract increased the number of branches plant-1 by 47%, and the application of 40% of *E. sativa* extract increased the number of branches plant-1 was by 73% (Fig. 1B). Likewise, the number of leaves plant-1 was increased by the application of *E. sativa* extract at both concentrations. Figure 1C showed that the number of leaves plant-1 increased by the application of 20% and 40% of *E. sativa* extract by 69% and 95% respectively.

Also, the result indicated that both concentrations of *E. sativa* extract induced a significant increase in the number of pods plant-1 of faba beans. The highest values of the number of pods plant-1 were noted at a concentration of 40% of *E. sativa* extract, which increased plant height by 54% compared to control plants (Fig. 2A). The same trend is found in the number of seeds pod-1 and the number of seeds plant-1. The application of 20% and 40% of *E. sativa* extract increased the number of seeds pod-1 by 19% and 24% respectively Fig. 2B. The number of seeds plant-1 was increased by 33% and 89% as a result of the application of 20% and 40% of *E. sativa* extract respectively Fig 2C.

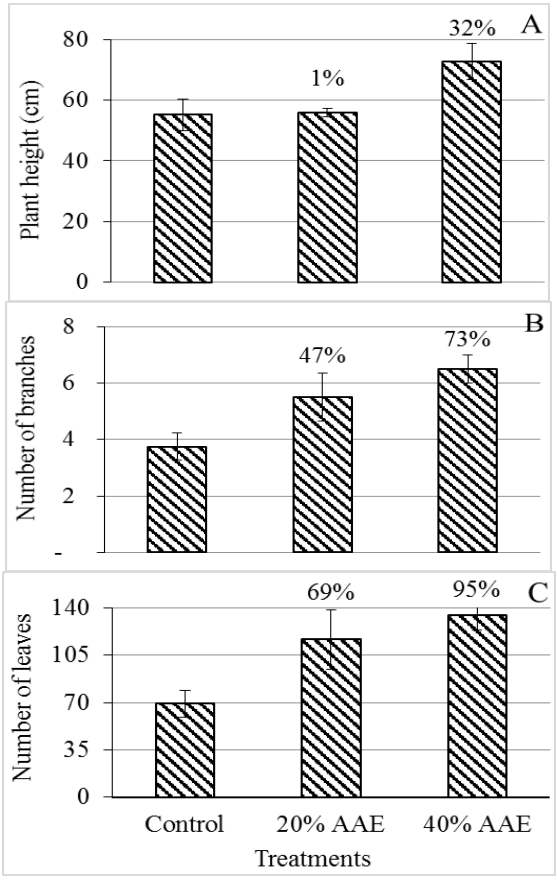

Figure 1. The effect of *Eruca sativa* aqueous extract treatments on (A) plant height (cm), (B) number of branches and (C) number of leaves / plant of faba bean plant. Each datum indicates mean value and vertical lines on top of bars indicate standard error of means (n = 4). Values in parenthesis indicate the percent increase from control.

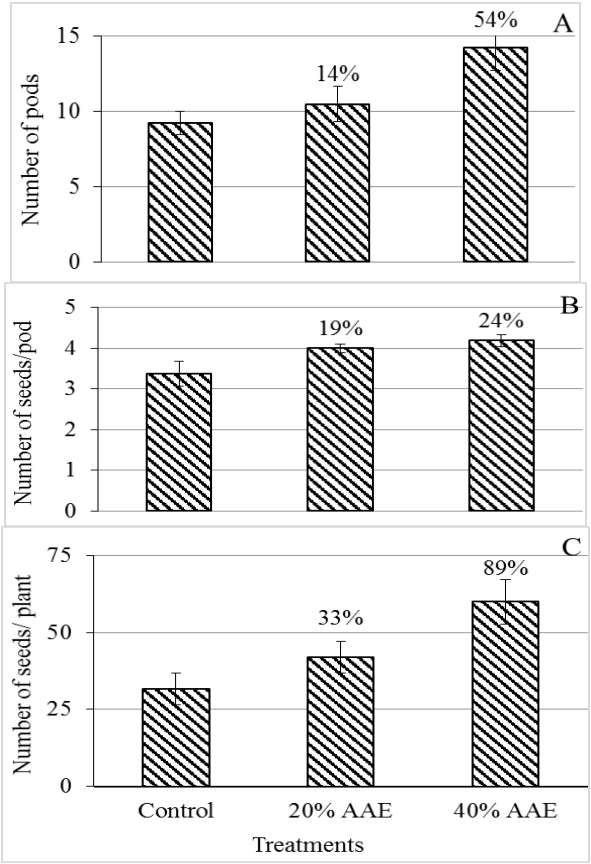

Figure 2. The effect of *Eruca sativa* aqueous extract treatments on (A) Number of pods^{-1} plant, (B) number of seeds pod-1 (C) number of seeds plant^{-1} of faba bean plant. Each datum indicates mean value and vertical lines on top of bars indicate standard error of means (n = 4). Values in parenthesis indicate the percent increase from control.

ISSN: online 2617-2186 print 2617-2178

In addition, *Eruca sativa* aqueous extract treatments created significant stimulation in biomass accumulations plant-1. This stimulation was displayed by an increase in dry weight of the plant's stem, leaves, and roots. Leaves dry weight was increased by 43% and 92% due to the application of 20% and 40% of *Eruca sativa* aqueous extract respectively Fig. 3A. The 20% of *Eruca sativa* aqueous extract treatments increased stems dry weight by 29% and 40% of *Eruca sativa* aqueous extract treatments increased stem dry weight by 80% Fig. 3B. Similarly, the 20% of *Eruca sativa* aqueous extract treatments increased plant roots dry weight by 40% and 74% of *Eruca sativa* aqueous extract treatments Fig. 3C.

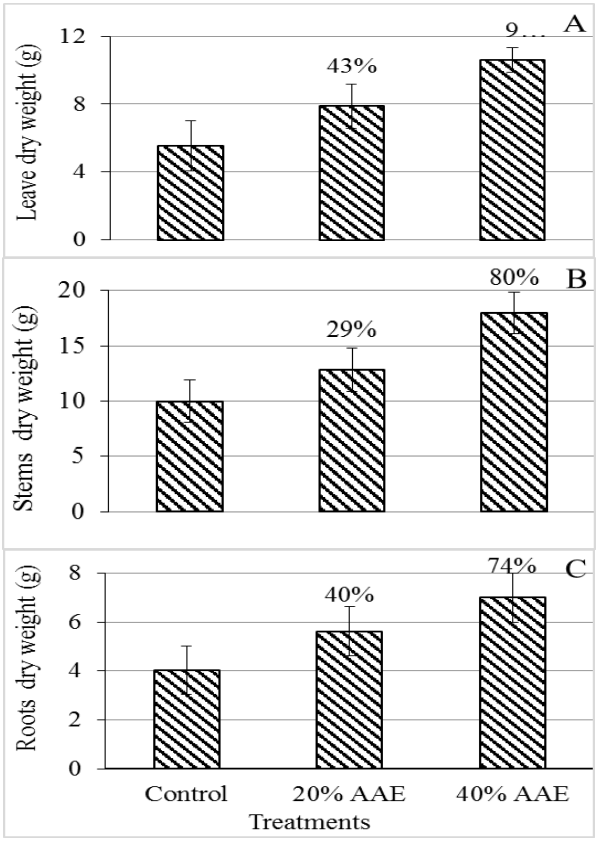

Figure 3. The effect of *Eruca sativa* aqueous extract treatments on (A) leave dry weight (g), (B) stem dry weight (g) (C) roots dry weight (g) of faba bean plant. Each datum indicates mean value and vertical lines on top of bars indicate standard error of means (n = 4). Values in parenthesis indicate the percent increase from control.

Moreover, spraying of faba bean plants with 20% and 40% of *Eruca sativa* aqueous extract resulted in a significant increase in pods dry weight plant-1 (g), weight of 10 seeds, (g) and yield of seeds plant-1 (g) Fig 4.

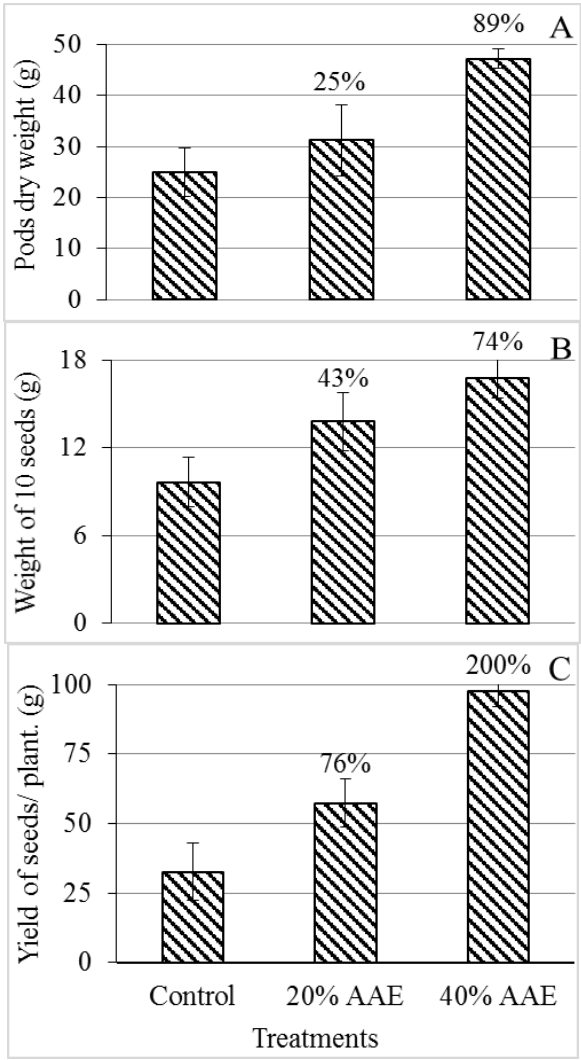

Figure 4. The effect of *Eruca sativa* aqueous extract treatments on (A) pods dry weight plant^{-1} (g), (B) weight of 10 seeds (g) and (C) yield of seeds plant^{-1} (g) of faba bean plant. Each datum indicates mean value and vertical lines on top of bars indicate standard error of means (n = 4). Values in parenthesis indicate the percent increase from control.

The result illustrated that both concentrations of *Eruca sativa* aqueous extract increased pods dry weight plant-1 (g), which was increased by 25% and 89% when plants of faba bean were sprayed by 20% and 40% respectively of *E. sativa* aqueous extract Fig.4A. At

ISSN: online 2617-2186 print 2617-2178

the same time, the weight of 10 seeds (g) as increased by 43% and 74% as a result of the application of 20% and 40% of *E. sativa* aqueous extract respectively Fig.4B. The highest increase was found in the yield of seeds plant-1 (g), which increased by 76% and 200% when faba bean plants were treated with 20% and 40% respectively of *E. sativa* aqueous extract Fig 4C.

DISCUSSION

This work was conducted to study the effect of foliar spray with aqueous extract of *Eruca sativa* Mill plant at concentrations of 20% and 40 % on the growth and yield of faba bean (*Vicia faba* L). The results showed that foliar application with 20 % *Eruca sativa* Mill aqueous extract showed significant effects on vegetative growth and yield components of faba bean. However, foliar application with 40% *Eruca sativa* aqueous extract showed highly significant improvement effects on vegetative growth and yield of faba bean, as shown in table 2. This may be due to the phytochemical properties of *Eruca sativa* aqueous extract and their biostimulate and antioxidant potential (Sadiq et al., 2014). It is noticeable from the results that all implemented concentrations of *Eruca sativa* aqueous extract (20% and 40%) concentrations significantly stimulated the growth and yield components of faba beans.

Currently, concerns are growing about human safety and the environmental impact of conventional synthetic fertilizer commonly used to improve plant growth. Some plant aqueous extracts may enhance plant growth, increase plants' tolerance against biotic and abiotic stresses and improve nutrient use efficiency (Posmyk and Szafrańska, 2016). An increase in growth and yield components of faba bean was achieved when faba bean plants were sprayed with 40% of *Eruca sativa* aqueous extract. This observation is comparable to that reported on the effect of moringa plant extracts on enhancing growth, yield, biochemical, hormonal contents of snap bean plants (Elzaawely et al., 2017). Data also showed that high concentrations of *Eruca sativa* aqueous extract are directly proportional to increased shoot growth. This agree with an early study that concluded the irrigating basil plants with Moringa leaf extracts resulted in an increase of shoot length, shoot fresh weight, and shoot dry weight and recommended Moringa as bio-organic fertilizer for various crops (Abdalla, 2013; Hassanein et al., 2019). According to the results obtained herein, the number of seeds pod-1 was the least affected trait and followed by plant height. Whereas the number of leaves plant-1, leave dry weight, and seed yield plant-1 were the most affected traits.

This finding is in agreement with a study which indicated that *Croton macrostachyus* and *Plectranthus barbatus* leaf extracts increased shoot length and leaf number per plant, and these two plant species were a source of cheap soil nutrients and may substitute the use of inorganic fertilizers (Odhiambo et al., 2019).

In the current study almost all growth and yield traits investigated were significantly improved with the application of *E. sativa* aqueous extract. This outcome was similar to other studies including: Moringa extract improving growth and yield of tomato plants (Culver et al., 2012), *Moringa oleifera* leaf extract improving growth and yield components of snap beans (Emongor, 2015), and foliar application of Moringa leaf extract enhancing growth, yield and nutritional quality of cabbage (Hoque et al., 2020).

The same result was reported in a previous study that showed that the application of mulberry, brassica, and sorghum leaf extracts improved growth and enhanced biochemical and antioxidant activities of radish plants (Ashraf et al., 2016). This improvement of faba bean growth after foliar sprayed with *E. sativa* extracts was because *Eruca sativa* plants have

ISSN: online 2617-2186 print 2617-2178

been reported a rich source of important nutrient elements such as (N, P, K, Ca, Mg, Na, Fe, Cu, Mn, and Zn (Bukhsh et al., 2007; Barlas et al., 2011), that may have benefits in enhancing plant growth. *Eruca sativa* plant may increase plants to uptake more and more valuable elements, which increased the nutrient status and ultimately accomplish optimum growth and yield of faba beans.

CONCLUSIONS

With regard to yield parameters: seed yields^{-1} compared to control were significantly increased, especially that obtained from 40% of *E. sativa*. The study indicated that to improve faba bean production, the application of 40% of *E. sativa* showed the best plant performance. Therefore, using *E. sativa* aqueous extract as commercial fertilizer is recommended for improving the production of faba beans. Plant fertilizers that degrade quickly are safer than persistent synthetic chemical fertilizers, less harmful to the environment, decrease production costs, and are not causing chemical resistance in the environment.

ACKNOWLEDGMENT.

This work was supported by the Department of Plant Science, University of Zawia. Also, the authors want to thank the Qramida family for letting us use their farm and equipment to accomplish the study.

REFERENCES

Abdalla, M. M. (2013). The potential of Moringa oleifera extract as a biostimulant in enhancing the growth, biochemical and hormonal contents in rocket (Eruca vesicaria subsp. sativa) plants. *International journal of plant physiology and biochemistry*, *5*(3), 42-49.

Abd El–Hamied, S. A., & El-Amary, E. I. (2015). Improving growth and productivity of "pear" trees using some natural plants extracts under north sinai conditions. *Journal of Agriculture and veterinary Science*, *8*(1), 1-9.

Ashraf, R., Sultana, B., Iqbal, M., & Mushtaq, M. (2016). Variation in biochemical and antioxidant attributes of Raphanus sativus in response to foliar application of plant leaf extracts as plant growth regulator. *Journal of Genetic Engineering and Biotechnology*, *14*(1), 1-8.

Barlas, N. T., Irget, M. E., & Tepecik, M. (2011). Mineral content of the rocket plant (Eruca sativa). *African Journal of Biotechnology*, *10*(64), 14080-14082.

Bukhsh, E., Malik, S. A., & Ahmad, S. S. (2007). Estimation of nutritional value and trace elements content of Carthamus oxyacantha, Eruca sativa and Plantago ovata. *Pakistan Journal of Botany*, *39*(4), 1181.

Bulgari, R., Cocetta, G., Trivellini, A., Vernieri, P., & Ferrante, A. (2015). Biostimulants and crop responses: a review. Biological Agriculture & Horticulture, 31(1), 1-17.

Cherif, C., Hassanat, F., Claveau, S., Girard, J., Gervais, R., & Benchaar, C. (2018). Faba bean (Vicia faba) inclusion in dairy cow diets: effect on nutrient digestion, rumen fermentation, nitrogen utilization, methane production, and milk performance. *Journal of dairy science*, *101*(10), 8916-8928.

Crépon, K., Marget, P., Peyronnet, C., Carrouee, B., Arese, P., & Duc, G. (2010). Nutritional value of faba bean (Vicia faba L.) seeds for feed and food. *Field Crops Research*, *115*(3), 329-339.

Culver, M., Fanuel, T., & Chiteka, A. Z. (2012). Effect of Moringa extract on growth and yield of tomato. *Greener Journal of Agricultural Sciences*, *2*(5), 207-211.

ISSN: online 2617-2186 print 2617-2178

El-Dabaa, M. A. T., Ahmed, S. A. E., Messiha, N. K., & El-Masry, R. R. (2019). The allelopathic efficiency of *Eruca sativa* seed powder in controlling Orobanche crenata infected *Vicia faba* cultivars. *Bulletin of the National Research Centre*, *43*(1), 37.

Elzaawely, A. A., Ahmed, M. E., Maswada, H. F., & Xuan, T. D. (2017). Enhancing growth, yield, biochemical, and hormonal contents of snap bean (*Phaseolus vulgaris* L.) sprayed with moringa leaf extract. Archives of Agronomy and Soil Science, 63(5), 687-699.

Emongor, V. E. (2015). Effects of moringa (*Moringa oleifera*) leaf extract on growth, yield and yield components of snap beans (Phaseolus vulgaris). *British Journal of Applied Science & Technology*, *6*(2), 114.

Hassanein, R. A., Abdelkader, A. F., & Faramawy, H. M. (2019). Moringa leaf extracts as biostimulants-inducing salinity tolerance in the sweet basil plant. *Egyptian Journal of Botany*, *59*(2), 303-318.

Hong, N. H., Xuan, T. D., Eiji, T., & Khanh, T. D. (2004). Paddy weed control by higher plants from Southeast Asia. *Crop Protection*, *23*(3), 255-261.

Hoque, T. S., Rana, M. S., Zahan, S. A., Jahan, I., & Abedin, M. A. (2020). Moringa leaf extract as a bio-stimulant on growth, yield and nutritional improvement in cabbage. *Asian Journal of Medical and Biological Research*, *6*(2), 196-203.

Khanh, T. D., Xuan, T. D., Hahn, S. J., & Chung, I. M. (2004). Methods to screen allelopathic accessions of wheat, barley, oat, sorghum and cucumber for weed control. *Allelopathy Journal*, *14*(2), 145-165.

Khan, A. U., Ullah, F., Khan, N., Mehmood, S., Fahad, S., Datta, R., Irshad, I., Danish, S., Saud, S., & Alaraidh, I. A. (2021). Production of Organic Fertilizers from Rocket Seed (Eruca Sativa L.), Chicken Peat and Moringa Oleifera Leaves for Growing Linseed under Water Deficit Stress. *Sustainability, 13*(1), 59.

Koubaa, M., Driss, D., Bouaziz, F., Ghorbel, R. E., & Chaabouni, S. E. (2015). Antioxidant and antimicrobial activities of solvent extract obtained from rocket (*Eruca sativa* L.) flowers. *Free Radicals & Antioxidants*, *5*(1).

Macías, F. A., Chinchilla, N., Varela, R. M., & Molinillo, J. M. (2006). Bioactive steroids from Oryza sativa L. *Steroids*, *71*(7), 603-608.

Odhiambo, K., Murungi, J., Wanjau, R., & Naumih, N. (2019). The Effect of Croton macrostachyus, Plectranthus barbatus Leaf Aqueous Extracts and Inorganic Fertilizers on Growth and Nutrients Concentration of Brassica oleracea L. in a Greenhouse at Nairobi. *Asian Journal of Agricultural Extension, Economics & Sociology*. 29(3): 1-10.

Phiri, C. (2010). Influence of Moringa oleifera leaf extracts on germination and early seedling development of major cereals. *Agriculture and Biology Journal of North America*, *1*(5), 774-777.

Posmyk, M. M., & Szafrańska, K. (2016). Biostimulators: a new trend towards solving an old problem. *Frontiers in plant science*, *7*, 748.

Sadiq, A., Hayat, M. Q., & Mall, S. M. (2014). Qualitative and quantitative de-

ISSN: online 2617-2186 print 2617-2178

termination of secondary metabolites and antioxidant potential of Eruca sativa. *Natural Products Chemistry & Research*.

Yakhin, O. I., Lubyanov, A. A., Yakhin, I. A., & Brown, P. H. (2017). Biostimulants in plant science: a global perspective. *Frontiers in plant science*, 7, 2049.

ISSN: online 2617-2186 print 2617-2178

المستخلص المائي لنبات الجرجير (*Eruca sativa Mill*) كمحفز للنمو في تعزيز نمو وإنتاجية نبات الفول (*Vicia faba L*)

امال احتيوش* وفوزية قريميدة

قسم علم النبات، كلية العلوم، جامعة الزاوية، الزاوية، ليبيا

تاريخ الاستلام: 21 يناير 2021 / تاريخ القبول: 31 يناير 2021
Doi:https://doi.org/10.54172/mjsc.v36i1.14

المستخلص:. لمعرفة قدرة المستخلص المائي لنبات الجرجير (*Eruca sativa* Mill) كونه محفزا للنمو في تعزيز نمو وإنتاجية نبات الفول (*Vicia faba* L)، تم إجراء دراسة حقلية خريف 2019. أجريت الدراسة باستخدام تربة رملية في إحدى مزارع منطقة أبوعيسى، وقد اتبعت الدراسة نظام التصميم العشوائي الكامل (RCD) بأربعة مكررات وبمساحة 3x5م^2 وبمسافة 25سم بين الأسطر. وفقا لذلك، تمت معاملة نباتات الفول بثلاث معاملات وتشمل: عدم الرش بالمستخلص المائي لنبات الجرجير (الشاهد)، رش الأوراق بنسبة 20٪، و40٪ من المستخلص المائي لنبات الجرجير *E.sativa*. تم رش اوراق نباتات الفول (*Vicia faba* (L) ست مرات بالمستخلص المائي لنبات الجرجير *E.sativa* بنسبة 20٪، و40٪ في المرحلتين الخضرية والزهرية. أظهرت النتائج أن الرش الورقي لنبات الفول بالمستخلص النباتي لنبات الجرجير بتركيز 40٪ أدى إلى الزيادة في ارتفاع النبات بنسبة 32٪، وعدد الأفرع بنسبة 73٪، وعدد الأوراق بنسبة 95٪، وعدد البذور لكل نبات بنسبة 89٪، ووزن الأوراق والسيقان والقرون والجذور الجافة بمقدار 92٪ ، 80٪ ، 74٪ ، 89٪ على التوالي. واستنتجت الدراسة إمكانية استعمال المستخلص المائي لنبات الجرجير *E. sativa* بكفاءة من قبل منتجي المحاصيل بوصفه محسنا لنمو محاصيل الفول؛ بسبب إنتاجيته الكبيرة، القيمة الغذائية للنبات، وانخفاض التكلفة إضافة إلى كونه مركبا صديقا للبيئة.

الكلمات المفتاحية: الفول *Vicia faba* L، المستخلص المائي، نبات الجرجير *Eruca sativa* Mill ، النمو، إنتاجية المحصول.

*امال احتيوش a.ehtaiweshl@zu.edu.ly قسم علم النبات، كلية العلوم، جامعة الزاوية، الزاوية، ليبيا

Al-Mukhtar Journal of Sciences 36 (1): 67-72, 2021

Optical Soliton Solutions to Gerdjikov-Ivanov Equation Without Four-Wave Mixing Terms in Birefringent Fibers by Extended Trial Function Scheme

Emad E. M. Mikael[1], Abdulmalik.A.Altwaty[2] and Bader R. K. Masry[*1]
[1]*Department of Mathematics, Faculty of Science, University of Tobruk, Tobruk, Libya*
[2]*Department of Mathematics, Faculty of Science, University of Benghazi, AL KUFRA, Libya*

Received: 21 January 2021/ Accepted: 31 January 2021
Doi: https://doi.org/10.54172/mjsc.v36i1.23

Abstract: Without four-wave mixing terms in birefringent fibers, the extended trial function scheme was used to obtain optical soliton solutions for the coupled system corresponding to the Gerdjikov-Ivanov equation. The procedure reveals singular soliton solutions, bright soliton solutions, and highly important solutions in terms of Jacobi's elliptic function. And in the limiting case of the modulus of ellipticity, singular and singular-periodic soliton solutions, along with their respective existence criteria.

Keywords: Birefringent Fibers, The Coupled Gerdjikov-Ivanov Model Without Four-Wave Mixing Terms, Extended Trial Function Scheme, Optical Solutions.

INTRODUCTION

The Gerdjikov-Ivanov (GI) model without four-wave mixing terms (FWM) is one of the varieties of models that study the dynamics of optical soliton propagation for transmission technology, the transcontinental and transoceanic distances, optical fibers, data transmission, and the telecommunications industry. This model has been studied for polarization-preserving fibers along with strategic algorithms such as modified simple equation scheme, the csch method, the extended $\tanh - \coth$ method, $\frac{G'}{G^2}$-expansion method, sine-cosine method, trial, and the extended trial equation method, trial equation integration architecture, extended Kudryashov's method, and the $\exp(-(\phi))$-expansion method (Arshed, 2018; Arshed et al., 2018; Biswas, Ekici, Sonmezoglu, Majid, et al., 2018; Biswas, Ekici, Sonmezoglu, Triki, et al., 2018; Biswas, Yildirim, Yasar, Triki, et al., 2018a, 2018b; Biswas, Yıldırım, et al., 2018; Ekici et al.,2017; Jawad et al.,2018; Kadkhoda, N.; Jafari, 2016; Yildirim, 2019d, 2019a, 2019b, 2019c) and the extended simplest equation method (Hassan & Altwaty, 2020). Although there are many advancements, the solitons were taken into account only along one model component. The extended trial function scheme has been applied to the coupled GI model without FWM given in two-component forms in birefringent fibers which gives rise to improving the model further. The strategy of the method reveals singular and bright soliton solutions. Furthermore, highly important solutions in terms of Jacobi's elliptic function, and in the limiting case of the modulus of ellipticity, singular and singular-periodic soliton solutions have been gained and listed with their respective existence criteria.

GOVERNING MODEL

The (GI) equation (Arshed, 2018; Arshed et al., 2018; Biswas, Ekici, Sonmezoglu, Majid, et al., 2018; Biswas, Ekici, Sonmezoglu, Triki, et al., 2018; Biswas, Yildirim, Yasar, Triki, et al., 2018b, 2018a; Biswas, Yıldırım, et al., 2018; Jawad et al., 2018; Yildirim, 2019d, 2019b, 2019c) is represented as

$$i\,\psi_t + a\,\psi_{xx} + b\,|\psi|^4\,\psi + i\,c\,\psi^2\,\psi_x^* = 0 \qquad (1)$$

***Corresponding Author:** Bader R. K. Masry bader.masry@tu.edu.ly , Department of Mathematics, Faculty of Science, University of Tobruk, Tobruk, Libya.

The first term is referred to as the temporal evolution of pulses when the existence of group velocity dispersion is supplied by the coefficient of a in this quite important governing model. The complex-valued function $\psi(x,t)$ is referred to as the wave profile. The coefficient of b is named as the nonlinear term that signifies quintic nonlinearity. Once and for all the existence of a form of dispersive phenomenon is ensured with the coefficient of c.

The GI model without FWM in birefringent fibers (Yildirim, 2019) is described by

$$i\psi_t + a_1\psi_{xx} + (b_1|\psi|^4 + c_1|\psi|^2|\phi|^2 + d_1|\phi|^4)\psi + i(\beta_1\psi^2 + \gamma_1\phi^2)\psi_x^* = 0,$$
$$i\phi_t + a_2\phi_{xx} + (b_2|\phi|^4 + c_2|\phi|^2|\psi|^2 + d_2|\psi|^4)\phi + i(\beta_2\phi^2 + \gamma_2\psi^2)\phi_x^* = 0. \quad (2)$$

The coefficients of a_j correspond to group velocity dispersion when the coefficients of b_j stem from self-phase modulation in this coupled GI system. Once and for all, the coefficients of c_j as well as d_j correspond to cross-phase modulation, whilst the coefficients of β_j, γ_j account for other forms of dispersive phenomenon along with $j = 1,2$.

MATHEMATICAL PRELIMINARIES

The starting hypothesis for solving the considered coupled system is given by

$$\psi(x,t) = w_1(\zeta(x,t))e^{i\theta(x,t)}, \quad (3)$$
$$\phi(x,t) = w_2(\zeta(x,t))e^{i\theta(x,t)}, \quad (4)$$

where w_j represent the amplitude component of the soliton and θ_j for $j = 1,2$ is the phase component of the soliton that is described as

$$\zeta(x,t) = k_1x - \nu t, \quad (5)$$
$$\theta(x,t) = -k_2x + \mu t + k_3. \quad (6)$$

Here, ν is the velocity of the soliton, k_2 is the frequency of the solitons in each of the two components while w is the soliton wave number and k_3 is the phase constant. By putting (4) and (5) into (2) we get:

$$-(\mu + a_1k_2^2)w_1 + a_1k_1^2w_1'' + b_1w_1^5 + c_1w_1^3w_2^2 + d_1w_1w_2^4 - k_2\beta_1w_1^3 - k_2\gamma_1w_2^2w_1 + i(-\nu - 2a_1k_1k_2 + k_1\beta_1w_1^2 + k_1\gamma_1w_2^2)w_1' = 0, \quad (7)$$

$$-(\mu + a_2k_2^2)w_2 + a_2k_1^2w_2'' + b_2w_2^5 + c_2w_2^3w_1^2 + d_2w_1^4w_2 - k_2\beta_2w_2^3 - k_2\gamma_2w_1^2w_2 + i(-\nu - 2a_2k_1k_2 + k_1\beta_2w_2^2 + k_1\gamma_2w_1^2)w_2' = 0. \quad (8)$$

Equation (7) and (8) can be gathered as

$$-(\mu + a_jk_2^2)w_j + a_jk_1^2w_j'' + b_jw_j^5 + c_jw_j^3w_l^2 + d_jw_jw_l^4 - k_2\beta_jw_j^3 - k_2\gamma_jw_l^2w_j + i(-\nu - 2a_jk_1k_2 + k_1\beta_jw_j^2 + k_1\gamma_jw_l^2)w_j' = 0, \quad (9)$$

where $j = 1,2$ and $l = 3 - j$, using the balancing principle we get $w_j = w_l$

$$-(\mu + a_jk_2^2)w_j + a_jk_1^2w_j'' + (b_j + c_j + d_j)w_j^5 - k_2(\beta_j + \gamma_j)w_j^3 + i(-\nu - 2a_jk_1k_2 + k_1(\beta_j + \gamma_j)w_j^2)w_j' = 0, \quad (10)$$

Splitting into real and imaginary parts we get:

$$-(\mu + a_jk_2^2)w_j + a_jk_1^2w_j'' + (b_j + c_j + d_j)w_j^5 - k_2(\beta_j + \gamma_j)w_j^3 = 0, \quad (11)$$
$$-\nu - 2a_jk_1k_2 + k_1(\beta_j + \gamma_j)w_j^2 = 0. \quad (12)$$

Equation (12) presents the velocity of the soliton solution, balancing w'' with w^5 in equation (11) gives $N = \frac{1}{2}$,

since N is not real, we set $w_j = \sqrt{\varphi_j}$. Substituting into (11) and multiplying by $4\varphi_j\sqrt{\varphi_j}$ we get

$$\sigma_{(1,j)}\varphi_j^2 + \sigma_{(2,j)}\varphi_j\varphi_j'' + \sigma_{(3,j)}(\varphi_j')^2 + \sigma_{(4,j)}\varphi_j^4 + \sigma_{(5,j)}\varphi_j^3 = 0, \quad (13)$$

where $\sigma_{(1,j)} = -4(\mu + a_jk_2^2)$, $\sigma_{(2,j)} = 2a_jk_1^2$, $\sigma_{(3,j)} = -a_jk_1^2$, $\sigma_{(4,j)} = 4(b_j + c_j + d_j)$, $\sigma_{(5,j)} = -4k_2(\beta_j + \gamma_j)$.

Balancing $\varphi_j\varphi_j''$ with φ^4 gives $N = 1$

EXTENDED TRIAL EQUATION SCHEME

The traveling wave solution with extended trial function scheme is:

$$\varphi_j = \sum_{i=0}^{N} A_{i,j}u^i, \quad j = 1,2, \quad (14)$$

where

$$(u')^2 = \Gamma(u) = \frac{\Theta(u)}{\Upsilon(u)} = \frac{\sum_{i=0}^{\tau}\lambda_iu^i}{\sum_{i=0}^{\rho}\chi_iu^i}, \quad (15)$$

ISSN: online 2617-2186 print 2617-2178

where λ_i, χ_i, $A_{i,j}$ are constants and λ_τ, χ_ρ, $A_{N,j}$ are non-zero. Equation (15) can be formulated as

$$\pm(\zeta-\zeta_0)=\int\frac{du}{\sqrt{\Gamma(u)}}=\int\sqrt{\frac{\Upsilon(u)}{\Theta(u)}}du, \quad (16)$$

The balancing principle applied to (13) implies

$$\tau=\rho+2N+2, \quad (17)$$

Since $N=1$ and setting $\rho=0$, we get $\tau=4$ consequently, from (14) we have

$$\varphi_j=A_{0,j}+A_{1,j}u, \quad (18)$$

$$(\varphi_j')^2=\frac{(A_{1,j})^2\sum_{i=0}^{4}\lambda_i u^i}{\chi_0}, \quad (19)$$

$$\varphi_j''=\frac{(A_{1,j})\sum_{i=0}^{4}i\lambda_i u^{i-1}}{2\chi_0}, \quad (20)$$

where $\lambda_4\neq0$ and $\chi_0\neq0$. Substituting Eqs. $(18)-(20)$ into Eq. (13), we obtain a system of algebraic equations. Solving the system, we get

$\lambda_0=\lambda_0$, $\lambda_1=\lambda_1$, $A_{0,j}=A_{0,j}$, $A_{1,j}=A_{1,j}$, $\chi_0=\chi_0$, $\lambda_2=$

$$\frac{A_{0,j}^4\chi_0\left(4b_j-2+4c_j+4d_j\right)+2A_{0,j}^3k_2\chi_0\left(\beta_j+\gamma_j\right)+A_{1,j}a_jk_1^2\left(A_{0,j}\lambda_1-A_{1,j}\lambda_0\right)}{A_{0,j}a_jk_1^2}$$

$$,\ \lambda_3=\frac{6A_{1,j}k_2\chi_0(\beta_j+\gamma_j)-4A_{0,j}A_{1,j}\chi_0}{3a_jk_1^2},\ \lambda_4=-\frac{A_{1,j}^2\chi_0}{3a_jk_1^2},$$

$$\mu=\frac{4A_{0,j}^4\chi_0(b_j+c_j+d_j)-4A_{0,j}^3k_2\chi_0(\beta_j+\gamma_j)+A_{1,j}a_jk_1^2(A_{0,j}\lambda_1-A_{1,j}\lambda_0)-4A_{0,j}^2a_jk_2^2\chi_0}{4A_{0,j}^2\chi_0}$$

Substituting into (15) and (16), we get

$$\pm(\zeta-\zeta_0)=Q\int\frac{du}{\sqrt{\Gamma(u)}}, \quad (21)$$

where $Q=\sqrt{\frac{\chi_0}{\lambda_4}}$, $\Gamma(u)=\sum_{i=0}^{4}\frac{\lambda_i}{\lambda_4}u^i$.

Therefore the traveling wave solutions to Eq.(2) are

When $\Gamma(u)=(u-\vartheta_1)^4$

$$\psi(x,t)=\sqrt{A_{0,1}+A_{1,1}\vartheta_1\pm\frac{A_{1,1}Q}{k_1x-2a_1k_1k_2t-\zeta_0}}\times e^{i(-k_2x+\mu t+k_3)}, \quad (22)$$

$$\phi(x,t)=\sqrt{A_{0,2}+A_{1,2}\vartheta_1\pm\frac{A_{1,2}Q}{k_1x-2a_2k_1k_2t-\zeta_0}}\times e^{i(-k_2x+\mu t+k_3)}. \quad (23)$$

When $\Gamma(u)=(u-\vartheta_1)^3(u-\vartheta_2)$, and $\vartheta_2>\vartheta_1$

$$\psi(x,t)=\sqrt{A_{0,1}+A_{1,1}\vartheta_1+\frac{4A_{1,1}Q^2(\vartheta_2-\vartheta_1)}{4Q^2-[(\vartheta_1-\vartheta_2)(k_1x-2a_1k_1k_2t-\zeta_0)]^2}}\times e^{i(-k_2x+\mu t+k_3)}, \quad (24)$$

$$\phi(x,t)=\sqrt{A_{0,2}+A_{1,2}\vartheta_1+\frac{4A_{1,2}Q^2(\vartheta_2-\vartheta_1)}{4Q^2-[(\vartheta_1-\vartheta_2)(k_1x-2a_2k_1k_2t-\zeta_0)]^2}}\times e^{i(-k_2x+\mu t+k_3)} \quad (25)$$

When $(u-\vartheta_1)^2(u-\vartheta_2)^2$

$$\psi(x,t)=\sqrt{A_{0,1}+A_{1,1}\vartheta_L+\frac{(-1)^{L+1}A_{1,1}(\vartheta_1-\vartheta_2)}{e^{\frac{(\vartheta_1-\vartheta_2)(k_1x-2a_1k_1k_2t-\zeta_0)}{Q}}-1}}\times e^{i(-k_2x+\mu t+k_3)}, \quad (26)$$

$$\phi(x,t)=\sqrt{A_{0,2}+A_{1,2}\vartheta_L+\frac{(-1)^{L+1}A_{1,2}(\vartheta_1-\vartheta_2)}{e^{\frac{(\vartheta_1-\vartheta_2)(k_1x-2a_1k_1k_2t-\zeta_0)}{Q}}-1}}\times e^{i(-k_2x+\mu t+k_3)}. \quad (27)$$

where $L=1,2$.

When $\Gamma=(u-\vartheta_1)^2(u-\vartheta_2)(u-\vartheta_3)$,and $\vartheta_1>\vartheta_2>\vartheta_3$

$$\psi(x,t)=\sqrt{A_{0,1}+A_{1,1}\vartheta_1-\frac{2A_{1,1}(\vartheta_1-\vartheta_2)(\vartheta_1-\vartheta_3)}{\mathrm{R1}}}\times e^{i(-k_2x+\mu t+k_3)}, \quad (28)$$

$$\phi(x,t)=\sqrt{A_{0,2}+A_{1,2}\vartheta_1-\frac{2A_{1,2}(\vartheta_1-\vartheta_2)(\vartheta_1-\vartheta_3)}{\mathrm{R1}}}\times e^{i(-k_2x+\mu t+k_3)}. \quad (29)$$

Where $\mathrm{R1}=2\vartheta_1-\vartheta_2-\vartheta_3+(\vartheta_3-\vartheta_2)\times\cosh\left(\frac{(k_1\sqrt{(\vartheta_1-\vartheta_2)(\vartheta_1-\vartheta_3)})(k_1x-2a_1k_1k_2t-\zeta_0)}{Q}\right)$.

When $\Gamma=(u-\vartheta_1)(u-\vartheta_2)(u-\vartheta_3)(u-\vartheta_4)$, and $\vartheta_1>\vartheta_2>\vartheta_3>\vartheta_4$

$$\psi(x,t)=\sqrt{A_{0,1}+A_{1,1}\vartheta_2+\frac{2A_{1,1}(\vartheta_1-\vartheta_2)(\vartheta_4-\vartheta_2)}{\mathrm{R2}}}\times e^{i(-k_2x+\mu t+k_3)}, \quad (30)$$

$$\phi(x,t)=\sqrt{A_{0,2}+A_{1,2}\vartheta_2+\frac{2A_{1,2}(\vartheta_1-\vartheta_2)(\vartheta_4-\vartheta_2)}{\mathrm{R2}}}\times e^{i(-k_2x+\mu t+k_3)}, \quad (31)$$

Where

$$R2=\vartheta_4-\vartheta_2+\frac{(\vartheta_1-\vartheta_4)sn^2\left(\pm\sqrt{(\vartheta_1-\vartheta_3)(\vartheta_2-\vartheta_4)}\left(k_1x-2a_1k_1k_2t-\zeta_0\right),m\right)}{2Q},$$

and $m^2=\frac{(\vartheta_2-\vartheta_3)(\vartheta_1-\vartheta_4)}{(\vartheta_1-\vartheta_3)(\vartheta_2-\vartheta_4)}$.

Note that ϑ_i, $i=1,\ldots,4$ are the roots of $\Gamma(u)=0$.

When $A_{0,j}=-A_{1,j}\vartheta_1$ and $\zeta_0=0$, the solutions $(22)-(31)$ are reduced to the following plane wave solutions:

$$\psi(x,t)=\sqrt{\pm\frac{A_{1,1}Q}{k_1x-2a_1k_1k_2t}}\times e^{i(-k_2x+\mu t+k_3)}, \quad (32)$$

$$\phi(x,t)=\sqrt{\pm\frac{A_{1,2}Q}{k_1x-2a_1k_1k_2t}}\times e^{i(-k_2x+\mu t+k_3)}, \quad (33)$$

$$\psi(x,t)=\sqrt{\frac{4A_{1,1}Q^2(\vartheta_2-\vartheta_1)}{4Q^2-[(\vartheta_1-\vartheta_2)(k_1x-2a_1k_1k_2t)]^2}}\times e^{i(-k_2x+\mu t+k_3)}, \quad (34)$$

$$\phi(x,t)=\sqrt{\frac{4A_{1,2}Q^2(\vartheta_2-\vartheta_1)}{4Q^2-[(\vartheta_1-\vartheta_2)(k_1x-2a_1k_1k_2t)]^2}}\times e^{i(-k_2x+\mu t+k_3)}, \quad (35)$$

ISSN: online 2617-2186 print 2617-2178

singular soliton solutions:

$$\psi(x,t) = \sqrt{\frac{A_{1,1}(\vartheta_2-\vartheta_1)}{2}(1 \mp \coth(X))} \times e^{i(-k_2x+\mu t+k_3)}, \quad (36)$$

$$\phi(x,t) = \sqrt{\frac{A_{1,2}(\vartheta_2-\vartheta_1)}{2}(1 \mp \coth(X))} \times e^{i(-k_2x+\mu t+k_3)}, \quad (37)$$

and bright soliton solutions:

$$\psi(x,t) = \left(\frac{D}{\sqrt{C+\cosh(B(k_1x-2a_1k_1k_2t-\zeta_0))}}\right) \times e^{i(-k_2x+\mu t+k_3)}, \quad (38)$$

$$\phi(x,t) = \left(\frac{D}{\sqrt{C+\cosh(B(k_1x-2a_1k_1k_2t-\zeta_0))}}\right) \times e^{i(-k_2x+\mu t+k_3)}, \quad (39)$$

where $D = \sqrt{\frac{2A_{1,j}(\vartheta_1-\vartheta_2)(\vartheta_1-\vartheta_3)}{(\vartheta_3-\vartheta_2)}}$, $B = \frac{\sqrt{(\vartheta_1-\vartheta_2)(\vartheta_1-\vartheta_3)}}{Q}$, $C = \frac{2\vartheta_1-\vartheta_2-\vartheta_3}{\vartheta_3-\vartheta_2}$, $j = 1,2$.

The amplitude of the soliton is given by D where the inverse width of the soliton is given by B. The solitons will exist for $A_{1,j} < 0$. Furthermore, when $A_{0,j} = -A_{1,j}$ and $\zeta_0 = 0$, Jacobi's elliptic function solutions (30), (31) are written as:

$$\psi(x,t) = \left(\frac{D_1}{\sqrt{C_1+sn^2(B_L(k_1x-2a_1k_1k_2t-\zeta_0))}}\right) \times e^{i(-k_2x+\mu t+k_3)}, \quad (40)$$

$$\phi(x,t) = \left(\frac{D_1}{\sqrt{C_1+sn^2\left(B_L(k_1x-2a_1k_1k_2t-\zeta_0)\right)}}\right) \times e^{i(-k_2x+\mu t+k_3)}, \quad (41)$$

where $D_1 = \sqrt{\frac{A_{1,j}(\vartheta_1-\vartheta_2)(\vartheta_4-\vartheta_2)}{(\vartheta_1-\vartheta_4)}}$, $B_L = \frac{(-1)^L\sqrt{(\vartheta_1-\vartheta_3)(\vartheta_2-\vartheta_4)}}{2Q}$, $C_1 = \frac{2\vartheta_4-\vartheta_2}{\vartheta_1-\vartheta_4}$, and $L = 1,2$.

Remark-1: When the modulus $m \to 1$, the singular optical soliton solutions are obtained as:

$$\psi(x,t) = \left(\frac{D_1}{\sqrt{C_1+\tanh^2(B_L(k_1x-2a_1k_1k_2t-\zeta_0))}}\right) \times e^{i(-k_2x+\mu t+k_3)}, \quad (42)$$

$$\phi(x,t) = \left(\frac{D_1}{\sqrt{C_1+\tanh^2(B_L(k_1x-2a_1k_1k_2t-\zeta_0))}}\right) \times e^{i(-k_2x+\mu t+k_3)}, \quad (43)$$

where $\vartheta_3 = \vartheta_4$.

Remark-2: When the modulus $m \to 0$, singular-periodic solutions are obtained as:

$$\psi(x,t) = \left(\frac{D_1}{\sqrt{C_1+\sin^2(B_L(k_1x-2a_1k_1k_2t-\zeta_0))}}\right) \times e^{i(-k_2x+\mu t+k_3)}, \quad (44)$$

$$\phi(x,t) = \left(\frac{D_1}{\sqrt{C_1+\sin^2(B_L(k_1x-2a_1k_1k_2t-\zeta_0))}}\right) \times e^{i(-k_2x+\mu t+k_3)}, \quad (45)$$

where $\vartheta_2 = \vartheta_3$.

CONCLUSION

The coupled system corresponding to the Gerdjikov-Ivanov equation, without FWM in birefringent fibers, was considered on account of acquiring optical soliton solutions. Bright soliton, and singular soliton solutions, were presented by the extended trial function scheme. Additional solutions, which are singular and singular-periodic soliton solutions, were obtained using the limiting of the modulus of ellipticity of the Jacobi elliptic function. Subsequently, by virtue of this paper, four-wave mixing terms (FWM) will be added to the model discussed in this article, and results will be reported accordingly.

REFERENCES

Arshed, S. (2018). Two reliable techniques for the soliton solutions of perturbed Gerdjikov–Ivanov equation. *Optik*, *164*, 93–99.

Arshed, S., Biswas, A., Abdelaty, M., Zhou, Q., Moshokoa, S. P., & Belic, M. (2018). Optical soliton perturbation for Gerdjikov–Ivanov equation via two analytical techniques. *Chinese Journal of Physics*, *56*(6), 2879–2886.

Biswas, A., Ekici, M., Sonmezoglu, A., Majid, F. B., Triki, H., Zhou, Q., … Belic, M. (2018). Optical soliton perturbation for Gerdjikov–Ivanov equation by extended trial equation method. *Optik*, *158*, 747–752.

Biswas, A., Ekici, M., Sonmezoglu, A., Triki, H., Alshomrani, A. S., Zhou, Q., … Belic, M. (2018). Optical solitons for Gerdjikov–Ivanov model by extended trial equation scheme. *Optik*, *157*, 1241–1248.

Biswas, A., Yildirim, Y., Yasar, E., Triki, H., Alshomrani, A. S., Ullah, M. Z., … Belic, M. (2018a). Optical soliton perturbation with full nonlinearity for Gerdjikov–Ivanov equation by trial

ISSN: online 2617-2186 print 2617-2178

equation method. *Optik*, *157*, 1214–1218.

Biswas, A., Yildirim, Y., Yasar, E., Triki, H., Alshomrani, A. S., Ullah, M. Z., … Belic, M. (2018b). Optical soliton perturbation with Gerdjikov–Ivanov equation by modified simple equation method. *Optik*, *157*, 1235–1240.

Biswas, A., Yıldırım, Y., Yaşar, E., Zhou, Q., Alshomrani, A. S., Moshokoa, S. P., & Belic, M. (2018). Solitons for perturbed Gerdjikov–Ivanov equation in optical fibers and PCF by extended Kudryashov's method. *Optical and Quantum Electronics*, *50*(3), 149.

Ekici, M., Zhou, Q., Sonmezoglu, A., Moshokoa, S. P., Ullah, M. Z., Biswas, A., & Belic, M. (2017). Optical solitons with DWDM technology and four-wave mixing. *Superlattices and Microstructures, 107,* 254-266.

Hassan, S. M., & Altwaty, A. A. (2020). Optical solitons of the extended Gerdjikov-Ivanov equation in DWDM system by extended simplest equation method. *Applied Mathematics and Information Sciences 14, No. 5,* 901-907

Jawad, A. J. M., Biswas, A., Abdelaty, M., Zhou, Q., Moshokoa, S. P., & Belic, M. (2018). Chirped singular and combo optical solitons for Gerdjikov–Ivanov equation using three integration forms. *Optik*, *172*, 144–149.

Kadkhoda, N., & Jafari, H. (2016). Kudryashov method for exact solutions of isothermal magnetostatic atmospheres. *Iranian Journal of Numerical Analysis and Optimization, 6(1),* 43-53.

Yildirim, Y. (2019a). Bright, dark and singular optical solitons to Kundu–Eckhaus equation having four-wave mixing in the context of birefringent fibers by using of modified simple equation methodology. *Optik*, *182*, 110–118.

Yildirim, Y. (2019b). Optical solitons of Gerdjikov–Ivanov equation in birefringent fibers with modified simple equation scheme. *Optik*, *182*, 424–432.

Yildirim, Y. (2019c). Optical solitons of Gerdjikov–Ivanov equation with four-wave mixing terms in birefringent fibers by modified simple equation methodology. *Optik*, *182*, 745–754.

Yildirim, Y. (2019d). Optical solitons to Gerdjikov–Ivanov equation in birefringent fibers with trial equation integration architecture. *Optik*, *182*, 349–355.

ISSN: online 2617-2186 print 2617-2178

الحلول البصرية اللامتغيرة زمنيا لمعادلة جيردجيكوف ايفانوف بدون تداخل رباعي الموجات في الألياف ثنائية الانكسار باستخدام طريقة الدالة التجريبية الممتدة

عماد اغنيوة مكائيل[1]، عبد المالك عبدو التواتي[2] وبدر رمضان مصري[1*]

[1]قسم الرياضيات، كلية العلوم، جامعة طبرق، طبرق– ليبيا

[2]قسم الرياضيات، كلية العلوم، جامعة بنغازي، الكفرة– ليبيا

تاريخ الاستلام: 21 يناير 2021/ تاريخ القبول: 31 يناير 2021

Doi:https://doi.org/10.54172/mjsc.v36i1.23

المستخلص: بدون تداخل رباعي الموجات، طريقة الدالة التجريبية الممتدة استخدمت للحصول على حلول بصرية لا متغيرة زمنيا للنظام المزدوج المقابل لمعادلة جيردجيكوف ايفانوف. الإجراء يكشف حلول بصرية مفردة، حلول بصرية ساطعة، وحلول في غاية الأهمية في صيغة دالة جاكوبي الإهليجية، وفي نهايات الدالة الإهليجية نحصل على حلول بصرية مفردة، وحلول بصرية مفردة دورية جنبا إلى جنب مع معايير وجودها.

الكلمات المفتاحية: ألياف ثنائية الانكسار، نموذج جيردجيكوف ايفانوف المزدوج بدون تداخل رباعي الموجات، طريقة الدالة التجريبية الممتدة، حلول بصرية.

*بدر رمضان مصري bader.masry@tu.edu.ly قسم الرياضيات، كلية العلوم، جامعة طبرق، طبرق– ليبيا.

Al-Mukhtar Journal of Sciences 36 (1): 73-79, 2021

Performance Metrics in Cognitive Radio Networks

Mahmoud Ali Ammar
Department of Computer Engineering, University of Zawia, Zawia, Libya

Received: 25 January 2021/ Accepted: 31 January 2021
Doi: https://doi.org/10.54172/mjsc.v36i1.21

Abstract: In Cognitive Radio Networks (CRN), the main aim is to allow the secondary users (SUs) to identify the empty bands and use them to transmit or receive data opportunistically. Primary users (PUs) have the priority to use a channel, while the secondary users must vacant this channel once a primary user requests it. An attack known in cognitive radio networks as a Primary User Emulation Attack (PUEA) aims to prevent the SU from using the empty bands. In this paper, an analytical and experimental approach is presented to mitigate the PUEA. This approach is based on obtaining the Probability Density Functions (PDFs) of the received powers at the secondary users from malicious nodes and also from the primary transmitter in the cognitive network. Then, these obtained PDFs are used in Neyman-Pearson composite hypothesis test to measure the performance metrics (probability of false alarm and miss detection in the network). The results proved that the performance metrics were greatly influenced by the network area, where the secondary user is located, and the threshold value λ used in the decision rule. Also, there are boundaries for the λ choices that cannot be overtaken.

Keywords: Cognitive Radio (CR); Probability Density Function (PDF); Primary User Emulation Attack (PUEA).

INTRODUCTION

The four main functions of cognitive radio are spectrum sensing, spectrum decision, spectrum sharing, and spectrum mobility. Via these functions the secondary users in the CR must be able to distinguish between the available channels and used channels. For example, if a TV transmitter acts as a primary user, then the users that can use the white spaces (available channels) in the TV band are called cognitive users (Buddhikot & Ryan, 2005).

The major challenge in spectrum sensing is the ability of the cognitive radio to recognize the spectrum bands that are not used by the primary users so the secondary users can coexist with the primary users without any interference to their communication. Recently the operational aspects of CR and its security aspects have gained a great deal of attention (FCC 2003). The reasons that make the cognitive radio vulnerable to new kind of security threats are as follows :-

- The open and dynamic features of the cognitive radio network make the CR systems more vulnerable to various malicious attacks. The new threats such as jamming, primary user emulation (PUE), and Spectrum Sensing Data Falsification (SSDF) (Jin et al., 2009).
- Because the cognitive radio network shares some features of the conventional wireless networks, we have to deal with the conventional wireless security risks in addition to the threats targeting the cognitive radio features. The conventional risks include MAC spoofing, Denial of Service …etc. (Akyildiz et al., 2006).

Based on these vulnerabilities, countermeasures are needed to make the cognitive radio networks robust and secure against any type of threat.

***Corresponding Author:** Mahmoud Ali Ammar m.ammar@zu.edu.ly , Department of Computer Engineering, University of Zawia, Zawia, Libya

Cooperative spectrum sensing can be vulnerable when some malicious nodes share false local sensing reports with others. In such cases, the fused decision may be altered, hence the reliability of cooperative spectrum sensing. Such phenomenon where local sensing results are manipulated is known as spectrum sensing data falsification or Byzantine attack. A malicious radio can advertise 'occupied' as 'available' inducing a policy violation or advertise 'available' as 'occupied' causing a denial of spectrum usage. The environment and changing the parameters in order to improve the quality of service are achieved based on the main functions of the cognitive radio. In adversarial, military, and heterogeneous competitive networks, such actions are not surprising where an adversary wants to cripple the operation of others in the network. Apart from this, there are also cases where a node's permanent spatial orientation is such that its reports are not suitable for use by other nodes. The adversary may vary attack strategies based on different objectives. Hence there is a need to evaluate the trustworthiness of radios before considering their local spectrum sensing reports (Chen & Park, 2006).

The main aim of this research is to obtain the performance metrics in cognitive radio networks. These metrics are crucial in the spectrum detection process to mitigate the attacks that are presented in the cognitive radio networks. Mitigating these attacks leads to improving the spectrum sensing in the cognitive radio network.

OBJECTIVE OF ADVERSARIAL ATTACKERS

The objectives of an attacker have a direct correlation with the way the attacks are launched, and therefore they determine the nature of attacks. Selfish attacks The attacker's motive is to acquire more spectrum for its own use by preventing others from competing for the channels and unfairly occupying their share. In this type of attack, adversaries will defy the protocols and policies only if they are able to benefit from them (Bhattacharjeea 2013; Mathur & Subbalakshmi, 2007).

Malicious attacks: The attackers' only objective is to create hindrance for others and does not necessarily aim at maximizing their own benefits. They do not have any rational objective and identify protocols and policies to just induce losses to others (Jakimoski & Subbalakshmi, 2008).

IMPACT OF PUE ATTACKS ON CR NETWORKS

The presence of PUE attacks causes several problems for CR networks. The list of potential consequences of PUE attacks is:

1. Bandwidth waste: The ultimate objective of deploying CR networks is to address the spectrum under-utilization that is caused by the current fixed spectrum usage policy. By dynamically accessing the spectrum "holes", the SUs are able to retrieve these otherwise wasted spectrum resources (Cabric et al., 2004).

2. QoS degradation: The appearance of a PUE attack may severely degrade the Quality-of-Service (QoS) of the CR network by destroying the continuity of secondary services (Cabric et al., 2004).

3. Connection unreliability: If a real-time secondary service is attacked by a PUE attacker and finds no available channel when performing spectrum handoff, the service has to be dropped. This real-time service is then terminated due to the PUE attack. In principle, the secondary services in CR networks inherently have no guarantee that they will have stable radio resources because of the nature of dynamic spectrum access. The existence of PUE attacks significantly increases the connection unreliability of CR networks.

ISSN: online 2617-2186 print 2617-2178

SIMULATION MODEL

In practice, the SU aims to identify the signal source, whether it is from a primary transmitter (PT) or malicious users. This scenario model is simulated using Matlab software. Figure 1 shows the cognitive radio network users' distributions where the SUs and malicious users are located in a circular area with radius R.

Some assumptions are considered as follows: The primary user is at a distance d_p from the secondary user. The malicious users are distributed randomly around the good user, as in Figure 1. This model aims to analyze the performance metrics under long-distance d_p = 160 km to the SU. At the same time, the network radios R and R_o are too small, R = 300 m and R_0 = 30 m. such parameters for analysis in CR networks are chosen as a novel study of the model under these low - parameters to prove the efficiency of the analytical model.

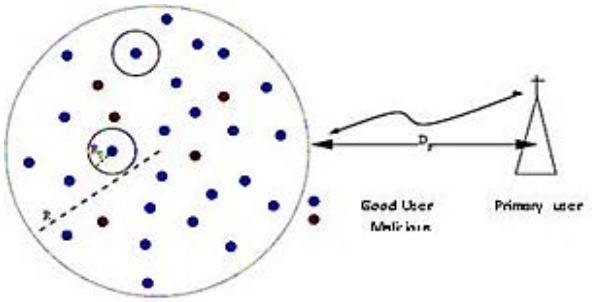

Figure: (1). Radio network users' distributions

If M denotes the number of malicious users in the system, P_t: Primary transmission power, P_m: Malicious transmission power, σ_p: Variance of Primary users, σ_m: Variance of Malicious users. The simulation model novel parameters are as in Table 1 below.

Table: (1). The simulation model parameters

Parameter	d_p	R	R_o	M	P_t	P_m	σ_p	σ_m
Value	160 KM	300 m	30 m	20	100 KW	10 W	8 dB	5.5 dB

MATHEMATIC FUNCTIONS OF THE RECEIVED SIGNALS

To calculate the probability density functions PDFs and use them in the simulated model. The received power Pr is determined first based on the relation below:

$$P_r \propto d^{\gamma} \quad (1)$$

γ is the path loss exponent. Thus, the received power from the primary is:

$$P_r^{(P)} = P_t\, d_p^{-2k} \quad (2)$$

Where k is the path loss $K = 10^{\varepsilon p/10}$

Thus the probability density function of the received power is:

$$P^{\Pr}(x) = \frac{1}{A\sigma_p\sqrt{2\pi x}} \exp\left(-\frac{(10\log_{10} x - \mu_p)^2}{2\sigma_p^2}\right) \quad (3)$$

μ_p, σ_p are the mean and variance of the distribution and given by

$$\mu_p = 10\log_{10} P_t - 20\log_{10} d_p$$

Secondly, the received power from each malicious user $P^{(mi)}$ at the secondary user is calculated according to the equation below:

$$P^{(mi)} = (P_T)_{mi}\, d_i^{-4}\, K \quad (4)$$

Where k is the path loss. d_i is the distance from the secondary user.

Based on the above equations, the decision variable Λ that is used to find the false alarm and miss detection probabilities can be calculated as follows:

$$\Lambda = P^m(\chi) \,/\, P^{\Pr}(\chi) \quad (5)$$

Where $P^{\Pr}(\chi)$ and $P^m(\chi)$ are the pdf of received powers from the primary and all malicious users respectively.

After performing Λ, it is compared with a threshold λ that can be chosen to guarantee a fine false alarm and miss detection probabili-

ISSN: online 2617-2186 print 2617-2178

ties as follows:
IF $\Lambda \leq \lambda$ then
The decision is that the transmission is from a primary user.
IF $\Lambda > \lambda$ then
The decision is that the transmission is from a malicious user.

RESULTS DISCUSSION AND ANALYSIS

The results obtained using Matlab simulation are presented in this section. The performance of the cognitive network under the PUE attack is studied in terms of probability of miss detection and false alarm.

Both the probability of miss detection and false alarms are calculated for 1000 times of simulations to be averaged to offer accurate results. The result obtained first was based on the threshold value λ=0.45. The network is assumed to be under a high number of malicious attackers M=20. In this case, it is noticed that when λ is too small, the achieved false alarm probability is very small, which in this case is about 0.05 as shown in Figure 2 below. At the same time, the miss detection probability is high and is about 0.325, as shown in Figure 3. These values are averaged out of 1000 runs.

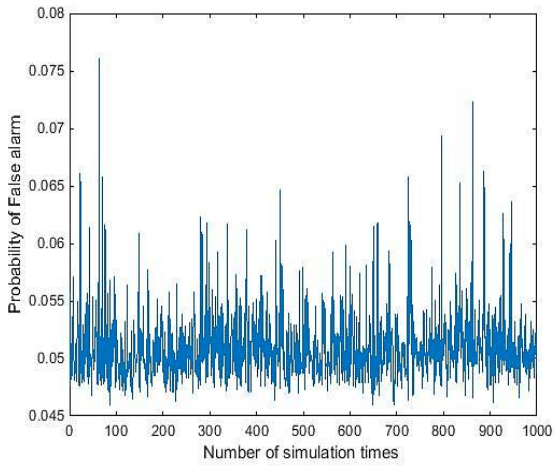

Figure :(2). False alarm probability for λ=0.45

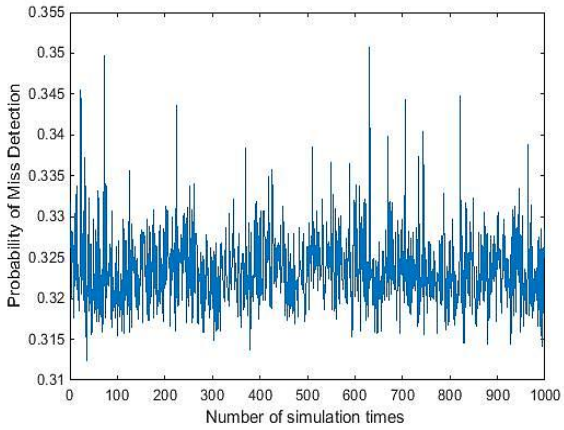

Figure: (3). Miss detection probability for λ=0.45

Furthermore, the model is justified under a high value of λ, λ=2.2. Thus the false alarm probability is high, which in this case is 0.43, opposed to the miss detection probability which is very small and is 0.17. These results are summarized in Table 2 as follows.

Table: (2). Miss detection and false alarm for different λ

Parameter	False Alarm Probability Averaged for 1000 runs	Miss Detection Probability Averaged for 1000 runs
λ =0.45	0.05	0.325
λ =2.2	0.43	0.17

These results mean that the threshold value of the simulated mathematics model must be chosen so that it doesn't exceed 2.2 and not less than 0.45. These boundaries of the threshold value λ can guarantee acceptable values of the performance metrics (miss detection and false alarm). In addition, it has proved that at least one of these performance metrics is low because of the mathematic relationship, which forms an inverse correlation. Specifically, there is an inverse correlation between λ and miss detection, while a positive correlation exists between λ and the false alarm, i.e. as λ decreases, false alarm decreases, and miss detection increases.

To sum up, choosing the value λ out of the

ISSN: online 2617-2186 print 2617-2178

boundaries leads to increasing one of these probabilities, which leads to a wrong decision about the presence of the primary user.

CDF OF FALSE ALARMS AND MISSED DETECTIONS

In order to testify these results, the cumulative distribution function (CDF) is calculated to display both the false alarms and the missed detection probabilities on the same graph as shown in Figure 4. Notably, the CDF plot is a non-decreasing function, and this indicates that the parameters and assumptions that were considered in the simulation are well-chosen and the results are accurate because these cumulative distributions functions in Figure 4 match and follow the general appearance of the CDF of the continuous variable of the simulated model.

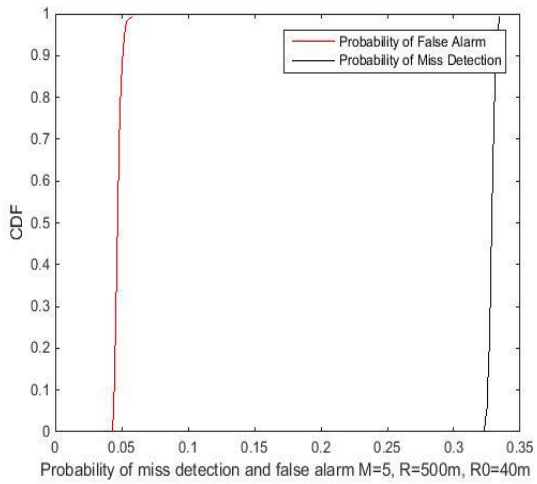

Figure: (4). Cumulative distribution functions for miss detection and false alarm

CONCLUSION

Due to the limitations and problems in the conventional spectrum sensing and radio network approaches, this paper focused on one of the major threats in the radio networks which is the primary user emulation attack. In this proposed model and using an analytical approach, the security against primary user emulation attacks in radio networks was discussed. The proposed analytical model and its impact on the PUEA attack were investigated.

The performance metrics results (the probability of false alarm and missed detection in the network) proved that the number of malicious nodes in the system has a great impact on the network, and this has led to a reduction in the quality of service due to the transmission from a high number of malicious users.

Also, it has proved that at least one of the performance metrics is low as a result of the inverse correlation between λ and miss detection probability. In other words, there is an inverse correlation between λ and miss detection, while a positive correlation exists between λ and the false alarm. This means if λ decreases, false alarm decreases and miss detection increases. For each model, there is a boundary for the value of λ depending on the parameters used in the model.

REFERENCES

Akyildiz, I. F., Lee, W.-Y., Vuran, M. C., & Mohanty, S. (2006). NeXt generation/dynamic spectrum access/cognitive radio wireless networks: A survey. *Computer networks, 50*(13), 2127-2159.

Bhattacharjeea, S. (2013). In cognitive radio networks. The International Journal for the Computer and Telecommunications, 01(36) 1387-1398 .

Buddhikot, M. M., & Ryan, K. (2005). Spectrum management in coordinated dynamic spectrum access based cellular networks. First IEEE International Symposium on New Frontiers in Dynamic Spectrum Access Networks, 2005. DySPAN 2005.,

Cabric, D., Mishra, S. M., & Brodersen, R. W. (2004). Implementation issues in

ISSN: online 2617-2186 print 2617-2178

spectrum sensing for cognitive radios. Conference Record of the Thirty-Eighth Asilomar Conference on Signals, Systems and Computers, 2004.,

Chen, R., & Park, J.-M. (2006). Ensuring trustworthy spectrum sensing in cognitive radio networks. 2006 1st IEEE Workshop on Networking Technologies for Software Defined Radio Networks,

Federal Communications Commission FCC. (2003). NPRM - Facilitating Opportunities for Flexible, Efficient, and Reliable Spectrum Use Employing Cognitive Radio Technologies. FCC, 03-322.

Jakimoski, G., & Subbalakshmi, K. (2008). Denial-of-service attacks on dynamic spectrum access networks. ICC Workshops-2008 IEEE International Conference on Communications Workshops,

Jin, Z., Anand, S., & Subbalakshmi, K. (2009). Detecting primary user emulation attacks in dynamic spectrum access networks. 2009 IEEE International Conference on Communications,

Mathur, C. N., & Subbalakshmi, K. (2007). Security issues in cognitive radio networks. *Cognitive Networks, 25*, 272-290.

ISSN: online 2617-2186 print 2617-2178

مقاييس الاداء في شبكات الراديو المعرفية

محمود علي عمار

قسم الحاسوب، كلية الهندسة، جامعة الزاوية، ليبيا

تاريخ الاستلام: 25 يناير 2021 / تاريخ القبول: 31 يناير 2021

Doi:https://doi.org/10.54172/mjsc.v36i1.21

المستخلص: في شبكات الراديو المعرفية Cognitive Radio Networks(CRN) الهدف الرئيسي هو السماح للمستخدمين الثانويين Secondary users (SUs) بتحديد النطاقات الفارغة، واستخدامها لنقل البيانات، أو استقبالها بشكل انتهازي. يتمتع المستخدمون الأساسيون Primary Users (Pus) بالأولوية في استخدام قناة أو تردد ما بينما يجب على المستخدمين الثانويين إخلاء هذه القناة بمجرد أن يطلبها المستخدم الأساسي. هناك هجوم أمني يُعرف في الراديو المعرفي بأنه هجوم محاكاة المستخدم الأساسي Primary user emulation attack (PUEA) ، ويهدف إلى منع SU من استخدام النطاقات الفارغة. في هذا البحث ، تم تقديم نهج تحليلي وتجريبي للتخفيف من PUEA ، ويستند هذا النهج إلى الحصول على وظائف الكثافة الاحتمالية Probability Density Function (PDF) للطاقة المتلقية للمستخدمين الثانويين من قبل العقد الخبيثة في الشبكة وكذلك من المرسل الاساسي في الشبكة المعرفية. بعد ذلك يتم استخدام ملفات PDF التي تم الحصول عليها في اختبار الفرضية المركبة Neyman-Pearson لقياس مقاييس الأداء (احتمال الإنذار الخاطئ، واكتشاف الأخطاء الخاطئ في الشبكة). أثبتت النتائج أن مقاييس الأداء تتأثر بشكل كبير بموقع الشبكة، موقع المستخدم الثانوي، وقيمة العتبة المستخدمة في قاعدة القرار. كما أن هناك حدودًا للاختيارات لا يمكن تجاوزها.

الكلمات المفتاحية: الراديو المعرفي CR؛ دالة الكثافة الاحتمالية (PDF)؛ هجوم محاكاة المستخدم الأساسي (PUEA).

* محمود علي عمار m.ammar@zu.edu.ly قسم الحاسوب ، كلية الهندسة ، جامعة الزاوية ، ليبيا

مجلة المختار للعلوم 36 (1): 80-97، 2021

تقييم جودة المياه الجوفية في جنوب طرابلس وملاءمتها للري باستخدام مؤشر جودة مياه الري (IWQI)

أحمد إبراهيم خماج[1*] وعبد الرحمن أحمد الرياني[2] و محمد ميلاد دليوم[3]

[1] قسم التربة والمياه، كلية الزراعة، جامعة طرابلس، ليبيا

[2] المعمل المتقدم للتحاليل الكيميائية، هيئة أبحاث العلوم الطبيعية والتكنولوجيا. طرابلس، ليبيا

[3] مركز أبحاث شجرة الزيتون، هيئة أبحاث علوم الطبيعية والتكنولوجيا طرابلس، ليبيا.

تاريخ الاستلام: 13 يناير 2021/ تاريخ القبول: 31 يناير 2021

https://doi.org/10.54172/mjsc.v36i1.12:Doi

المستخلص: تمثل المياه الجوفية أحد أهم المحددات الرئيسية في تطور، ونجاح استدامة النشاط الزراعي في ليبيا. كما أن الإدارة الجيدة، والتخطيط السليم لهذا المورد يستوجب معرفة نوعية المياه للحد من المشكلات التي قد تواجه مستعملي تلك المياه. تهدف هذه الدراسة إلى التعرف على التركيب الكيميائي للمياه الجوفية في منطقة جنوب طرابلس، وتقييم جودة المياه الجوفية لأغراض الري. ولتحقيق أهداف هذه الدراسة تم تجميع 31 عينة من مياه آبار جوفية منتشرة في جنوب طرابلس خلال شهر يوليو 2016. أجريت العديد من التحاليل الكيميائية على تلك العينات لتقدير درجة التوصيل الكهربي، ودرجة التفاعل، وتركيز بعض الأيونات الذائبة التي تضمنت كل من الصوديوم، والبوتاسيوم، والكالسيوم، والماغنيسيوم، والكلوريدات، والبيكربونات، والكبريتات، بالإضافة إلى حساب نسبة الصوديوم المدمص. تم تحديد مؤشر جودة مياه الري ذي الخمس معلمات، والتي تشمل كل من (درجة التوصيل الكهربي، الصوديوم، الكلوريدات، البيكربونات، نسبة ادمصاص الصوديوم المعدلة). استخدمت طريقة مقلوب المسافة الوزنية بأس 2، للحصول على خرائط التوزيع المكاني للخصائص الكيميائية، ولمؤشر جودة مياه الري. أظهرت النتائج ارتفاع قيم درجة التوصيل الكهربي عند منتصف منطقة الدراسة، وانخفاضها عند شرقها، وغربها، وأن نمط التوزيع المكاني لها مشابه إلى حد كبير لنمط التوزيع المكاني لكل من أيون الصوديوم، والكلوريد. كما دلت النتائج على أن متوسط الوفرة النسبية للأنيونات الذائبة معبراً عنه بوحدات (ملليمكافيء/ لتر) كانت 65.8، 20.4، 13.8% وذلك للكلوريدات، والكبريتات، والبيكربونات على التوالي. في حين كان متوسط الوفرة النسبية للكاتيونات الذائبة 49.3، 28.1، 21.7، 0.9% وذلك للصوديوم، والماغنيسيوم، والكالسيوم، والبوتاسيوم على التوالي. تراوحت قيم مؤشر جودة مياه الري بين 41.2 و76.6. كما بينت خريطة التوزيع المكاني لمؤشر جودة مياه الري أن 62 % من مساحة منطقة الدراسة صنفت على أنها ذات قيود، ومحددات معتدلة للاستخدام في أغراض الري، وأن 37.5% صنفت على أنها ذات قيود ومحددات مرتفعة.

الكلمات المفتاحية: المياه الجوفية، نموذج ميرلسIWQI، مقلوب المسافة الوزنية، جنوب طرابلس.

المقدمة

تعد المياه الجوفية أحد أكثر عناصر الدورة الهيدرولوجية أهمية في المناطق الجافة، وشبه الجافة لما لها من أهمية في نجاح أي استثمار زراعي مرتبط بإنتاج المحاصيل لضمان الأمن الغذائي. في العديد من المناطق الجافة وشبه الجافة التي تعتمد على المياه الجوفية مصدرا وحيدا لعمليات الري الزراعي، أدت عمليات الاستنزاف المستمر للمياه الجوفية في تلك المناطق إلى انخفاض مستوياتها، وانخفاض معدلات التغذية، وارتفاع ملوحتها ومن ثم تدني نوعيتها خصوصا في المناطق المتاخمة للبحر. تؤثر نوعية المياه الجوفية المستخدمة لأغراض الري على معدلات رشح التربة، بناء التربة، تطور مشاكل الصودية، والملوحة، مشاكل البيكربونات والمشاكل المرتبطة بنوعية الأملاح. وعلى الرغم من أن تلك التأثيرات مرتبطة بالخصائص الكيميائية، والطبيعية للتربة إلا أنها تنعكس بدورها على معدلات إنتاج المحاصيل الزراعية

[1*]أحمد إبراهيم خماج، ekhmaj@gmail.com ،قسم التربة والمياه، كلية الزراعة، جامعة طرابلس

(Simsek and Gunduz، 2007). كما تكمن التأثيرات السلبية لانخفاض نوعية مياه الري أيضاً في تزامن التأثير الأسموزي الناشئ عن ارتفاع الملوحة، مع التأثير السمي لبعض الأيونات الذائبة على المحاصيل الزراعية (Arnon،1972).

لقد تم تطوير العديد من مؤشرات جودة مياه الري التي تؤثر على مدى صلاحيتها للمساهمة في الحد من الآثار السلبية التي قد تنشأ عن استخدام مياه الري على كل من التربة، والمحصول على حد سواء. تساعد تلك المؤشرات عبر تحويل البيانات المتعلقة بنوعية مياه الري إلى معلومات مهمة لمتخذي القرار، وأصحاب المصلحة في معالجة القضايا المتعلقة بالبيئة، والزراعة، وإدارة مياه الري (Mohammed،2011).

تتميز مؤشرات نوعية مياه الري عن بقية أنظمة تصنيف نوعية مياه الري في أنها ذات قيمة مفردة (Single value)، تمكن من الحكم على نوعية مياه الري. تختزل تلك القيمة أهمية المعلمات المختلفة المستخدمة في تصنيف نوعية مياه الري عند مكان معين، وفي زمن محدد (Brhane، 2016). وعلى الرغم من أن تلك المؤشرات قد لا تتضمن حساباتها كل المعلمات ذات العلاقة بنوعية مياه الري، إلا أن احتواءها على أكثر المعلمات أهمية قد يوفر دليلاً بسيطاً، وفعالاً للحكم على نوعية مياه الري.

تتفق أغلب مؤشرات نوعية مياه الري المختلفة في اتباعها منهجية متقاربة تعتمد على إعطاء أوزان محددة للمعلمات المختلفة بناء على أهميتها إلا أنها تتباين في ماهية تلك المعلمات وعددها. علاوة على ذلك، فإنه من المهم الإشارة إلى اختلاف مفهوم جودة مياه الري مع اختلاف المواقع المستهدفة بعملية الري، حيث تختلف أنماط المحاصيل المزروعة، و ظروف التربة، والمناخ (Babiker وآخرون، 2007). فلقد اقترح (Simsek و Gunduz، 2007) مؤشراً لنوعية مياه الري تم تطبيقه في سهل سيماف بتركيا. اعتمد المؤشر المقترح على ضوابط، واشتراطات تصنيف نوعية مياه الري الصادرة عن منظمة الأغذية، والزراعة (Ayers و Westcot، 1999) والتي تأخذ في اعتبارها معلمات تعكس مخاطر الملوحة، والرشح، والنفاذية، والسمية النوعية لبعض الأيونات، والتأثيرات العرضية التي تسببها مياه الري على المحاصيل.

صنفت نوعية مياه الري وفقاً للمؤشر المقترح إلى مياه منخفضة، ومعتدلة، وعالية الجودة. كما استخدم (Misaghi وآخرون،2017) معلمات تمثلت في الصوديوم (Na^+)، الكلوريد (Cl^-)، درجة التفاعل (pH)، نسبة الصوديوم المدمص (SAR)، والأملاح الكلية الذائبة (TDS)، وقد صنفت مياه الري وفقاً لذلك إلى مياه رديئة جداً، رديئة، معتدلة، جيدة، عالية الجودة. اقترح (Meireles وآخرون، 2010)، مؤشراً جديداً لنوعية مياه الري (IWQI) باستخدام تقنية تحليل المتغيرات المتعددة (Multivariate Statistical Analysis). اقتصرت المعلمات المستخدمة كمدخلات في حسابات هذا المؤشر على ما تضمنه نظام مختبر الملوحة الأمريكي (Richards، 1954) ومنظمة الأغذية، والزراعة (Ayers و Westcot، 1999).

اشتملت تلك المعلمات في مجملها على كل من درجة التوصيل الكهربي، والصوديوم، والكلوريد، والبيكربونات، ونسبة الصوديوم المدمص المعدلة (SAR^o). كل هذه المعلمات تعكس تأثيرات كل من الخطورة الناشئة عن ملوحة مياه الري، وانخفاض معدلات الرشح، ومشاكل السمية على النبات. تكمن أهمية مؤشر (Meireles وآخرون، 2010) مقارنة بغيره من المؤشرات في كونه قد طور لغرض تحديد نوعية مياه الري، وذلك على النقيض من المؤشر المستخدم من قبل (Misaghi وآخرون،2017)، والذي تبنى مؤشر WQI-NSF والمطور من قبل المؤسسة الدولية للتطهير للولايات المتحدة الأمريكية، والمستهدف لتقييم نوعية مياه الشرب المنتجة من عمليات معالجة مياه الصرف الصحي.

كما أن اعتماد حسابات مؤشر (Meireles وآخرون، 2010) على تصنيف مختبر الملوحة الأمريكي (Richards، 1954 ;Ayers و Westcot، 1999). اللذان يعتبران من أكثر أنظمة تصنيف مياه الري استعمالا، وانتشاراً، مع محدودية عدد المعلمات، وتوفر بياناتها، وسهولة الحصول على تقديراتها، بالإضافة إلى حداثته النسبية، جعله محل دراسة العديد من الباحثين، والمهتمين بقضايا نوعية مياه الري. فلقد استخدم

ISSN: online 2617-2186 print 2617-2178

مؤشر IWQI في تقييم نوعية مياه الري لحوض حلبجة سيد صادق بالعراق خلال موسمين رطب، وجاف من قبل (Abdullah وآخرون، 2016)، وفي جنوب الصحراء الشرقية بمصر للعديد من الخزانات الجوفية في حلايب، وشلاتين (Heba وآخرون، 2016)، وفي شمال غربي محافظة المنيا بمصر من قبل (Abdulhady، 2018)، وفي مناطق شابهار، وسيستان، وبلوشستان، في جنوب شرقي إيران من قبل (Abbasina وآخرون، 2018)، وفي المكسيك، في مناطق Ikhueniro و Okhuah .

محلياً، وعلى الرغم من أهمية استخدام مؤشر IWQI لتقييم نوعية مياه الري، إلا أن أغلب الدراسات المتعلقة بتقييم نوعية مياه الري اقتصرت على التصنيفات المقترحة من قبل مختبر الملوحة الأمريكي، ومنظمة الأغذية، والزراعة، وعلى سبيل المثال لا الحصر (عبد العزيز وآخرون، 2009 ;الصادي وآخرون، 2019). تهدف هذه الدراسة إلى التعرف على التركيب الكيميائي للمياه الجوفية، وتقييم نوعية المياه الجوفية باستخدام مؤشر (Meireles وآخرون، 2010) للخزانات الجوفية الضحلة جنوب طرابلس.

المواد وطرق البحث

وصف منطقة الدراسة: تقع منطقة الدراسة بين دائرتي عرض 32.757° و 32.890° شمالا و بين خطي طول 13.043° و 13.338° شرقاً و وتغطي مساحة 340.90 كم^2 تقريباً، وذلك كما هو موضح في الشكل (1). تتصف تضاريس منطقة الدراسة بأنها على درجة كبيرة من الاستواء، وتتدرج في الارتفاع عن مستوى سطح البحر نحو الجنوب. شهدت منطقة الدراسة تطوراً عمرانياً ملحوظاً، خصوصاً في شمالها، كما تنتشر فيها الكثير من الحيازات الزراعية. تمتاز المنطقة مناخياً، بنمط نطاق مناخ البحر المتوسط.

تصل معدلات الأمطار السنوية بين 288 ملم في محطة الإرصاد المناخية بمطار طرابلس الواقع جنوب منطقة الدراسة، و337 ملم بمحطة مدينة طرابلس الواقعة شمال منطقة طرابلس (الميلودي، 2018). تعد المياه الجوفية المصدر الوحيد للإمدادات المائية اللازمة لمختلف الاستعمالات الزراعية، والصناعية، ولأغراض الشرب. وقد أدى حفر المزيد من الآبار، واستخدام المضخات ذات القدرات العالية لسحب المياه الجوفية بمعدلات تفوق كميات التغذية السنوية إلى إحداث خلل في الموازنة المائية للخزان الجوفي، وارتفاع ملوحة المياه المستخرجة منها (Ekhmaj وآخرون، 2014). يدل السجل الجيولوجي في منطقة الدراسة، الموضح في الشكل (1) على أن الطبقات الحاملة للمياه الجوفية غير المقيدة تتبع الخزان الرباعي (Quaternary Aquifer) والمكون من تداخلات من الرمل، والحصى، والحجر الرملي، والحجر الجيري (Flogel، 1979). يتراوح عمق مستوى الماء الجوفي في الخزان الجوفي غير المقيد بين 10 و 160 متر تحت مستوى سطح الأرض، وبسمك مشبع يتراوح من 10 إلى 90 متر. كما تتراوح إنتاجية أغلب آبار منطقة الدراسة بين 20 و 50 م^3/ ساعة (Floegel، 1979).

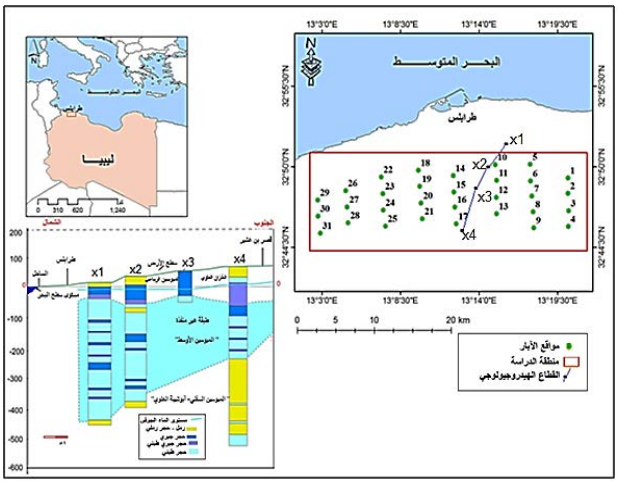

شكل (1) الموقع الجغرافي والقطاع الهيدروجيولوجي لمنطقة الدراسة

الوصف العام لنموذج IWQI: اعتمدت طريقة (Meireles وآخرون، 2010) لتحديد جودة مياه الري، والتي تستخدم بدرجة رئيسية في تقييم المياه في الأغراض الزراعية على تقنية تحليل المتغيرات المتعددة (Multivariant analysis). ولكي يتم حساب الأوزان النسبية للعوامل المختلفة في هذه الطريقة، يجب استخدام قيم تلك المعلمات المشتقة من بيانات نوعية مياه الري وفقا لما اقترحته مستشارية لجنة جامعة كاليفورنيا (UCC) بالإضافة إلى ما ورد من خصائص مياه الري من قبل(Ayers و Westcot، 1999)، وتتلخص هذه الطريقة في التعرف على قيم المعلمات التي لها السيادة في

ISSN: online 2617-2186 print 2617-2178

أداء الدور المهم في نوعية المياه للأغراض الزراعية. تتضمن هذه المعلمات كل من التوصيل الكهربي(EC)، معبرا عنها بوحدات ميكروسيمنز/ سم، وبعض الأيونات الذائبة في مياه الري معبرا عنها بالملي مكافئ/ لتر، والتي اشتملت على كل من الصوديوم الذائب (Na^+)، الكلوريدات (Cl^-) والبيكربونات الذائبة (HCO_3^-)، بالإضافة إلى نسبة ادمصاص الصوديوم المعدلة (SAR^o)، المقترحة من قبل (Suarez, 1981) ، والتي تم حسابها وفقا لما أشار إليه (Lesch و Suarez، 2009) على النحو الموضح في المعادلة (1).

$$SAR^o = \frac{Na^+}{\sqrt{\frac{Ca^{2+}_{eq}+Mg^{2+}}{2}}} \quad (1)$$

حيث يمثل Na^+ تركيز الصوديوم الذائب في مياه الري، Ca^{2+}_{eq} تركيز الكالسيوم المعدل الذائب في مياه الري، Mg^{2+} تركيز الماغنيسيوم الذائب في مياه الري. وفقاً لمؤشر جودة المياه المقترح، فإن الوحدات المستخدمة في وصف تركيزات العناصر الداخلة في حساب SAR^o هي وحدات الملي مكافئ/لتر.

يتم تحديد مساهمة كل معلمة على حدة عند حساب مؤشر جودة مياه الري، بحيث تشمل هذه المساهمة كل من قيم نوعية المياه المقدرة (q_i) والوزن النسبي (w_i)، كما تستخدم المعادلة (2) في حساب قيم (q_i) وذلك على النحو التالي:

$$q_i = q_{max} - \left(\frac{q_{iamp}\times(x_{ij}-x_{inf})}{x_{amp}}\right) \quad (2)$$

حيث تمثل q_{max} القيمة العظمى لكل صنف، x_i تمثل القيمة المقاسة لكل معلمة، x_{inf} تمثل قيمة الحد الأدنى للصنف الذي تتبعه المعلمة، q_{iamp} تمثل سعة الصنف، x_{amp}تمثل القيمة المناظرة لسعة الصنف والذي تتبعه المعلمة. يوضح الجدول (1) قيم q_i والتي تمثل نوعية المياه المقدرة بالنسبة للمعلمة الواحدة المحددة. تعكس قيم w_i الوزن المعياري للمعلمات، ويرتبط بأهميته في تفسير التغير الكلي في نوعية المياه والموضح في الجدول (2). تحدد قيم مؤشر جودة المياه لأغراض الري IWQI من المعادلة (3) التي يمكن كتابتها على النحو التالي:

$$IWQI = \sum_{i=1}^{n} q_i w_i \quad (3)$$

طبقاً للمعادلة (3)، فإن المؤشر IWQI هو مؤشر لا وحدات له، وتتراوح قيمته من 0 إلى 100. إن الاختلاف في التقسيمات المختلفة لمياه الري الموضحة في الجدول (3)،تم تنفيذها مع الأخذ في الاعتبار مخاطر مشاكل الملوحة، الانخفاض في معدلات تخلل ماء التربة، بالإضافة إلى تأثيرات السمية على النبات.

جدول (1) قيم نوعية المياه المقدرة (q_i) وفقا لقيم المعلمات المختلفة.

q_i	EC(ميكروسيمنز/سم)	SAR^o	Na^+(ملليمكافئ/ لتر)	Cl^-(ملليمكافئ/ لتر)	HCO_3^-(ملليمكافئ/ لتر)
85−100	[200، 750)	[2-3)	[2، 3)	4 >	[1، 1.5)
60 −85	[750، 1500)	3[،6)	[3، 6)	[4، 7)	[1.5، 4.5)
35−60	[1500، 3000)	[6,12)	[6، 9)	[7، 10)	[4.5، 8.5)
أقل من 35	200≥ أو 3000≤	SAR^o<2 SAR^o≥12	2≥ أو 9≤	10≤	1> أو 8.5≤

ISSN: online 2617-2186 print 2617-2178

جدول (2) الأهمية الوزنية (w_i) للمعلمات المختلفة

المعلمة	القيمة (w_i)
درجة التوصيل الكهربي (EC) "ميكروسيمنز/ سم"	0.211
الصوديوم (Na^+) "ملليمكافئ/ لتر"	0.204
البيكربونات (HCO_3^-) "ملليمكافئ/ لتر"	0.202
الكلوريد (Cl^-) "ملليمكافئ/ لتر"	0.194
نسبة ادمصاص الصوديوم المعدلة (SAR^o)	0.189
الإجمالي	1

تمثل تلك التقسيمات قيود ومحددات استخدام مياه الري والتي تم تصنيفها بالاستعانة بما توصل إليه كل من (Bernardo, 1995) و (Holand و Amorim، 1997). تجدر الإشارة هنا إلى أن القيم الصغرى في هذا النموذج تمثل نوعية المياه الرديئة، وأن نوعية المياه تتحسن مع الارتفاع في قيم IWQI.

تجميع البيانات: لإنجاز هذا العمل تم تجميع 31 عينة مياه من الآبار في منطقة الدراسة خلال شهر يوليو 2016. وتم تحديد مواقع آبار أخذ العينات بالاستعانة بجهاز (GPS). تراوح عمق الماء الساكن في الآبار من 24 إلى 120 متر تحت مستوى سطح الأرض. كما تم تجميع بيانات كاملة عن البئر من حيث تاريخ الحفر، والعمق. تضمنت التحاليل الكيميائية التي أجريت على مياه الآبار، تقدير كل من التوصيل الكهربي (EC)، درجة التفاعل (pH)، وبعض الأيونات الرئيسية الذائبة والتي شملت كل من الكالسيوم (Ca^{2+}) والماغنيسيوم (Mg^{2+}) الصوديوم (Na^+)، والبوتاسيوم (K^+)، والبيكربونات (HCO_3^-)، والكلوريدات (Cl^-)، والكبريتات (SO_4^{2-}). أجريت التحاليل الكيميائية على عينات المياه في معمل تحليل التربة والمياه بقسم التربة، والمياه بكلية الزراعة– جامعة طرابلس، وفقاً للطرق المشار إليها من قبل (APHA وآخرون، 1992). كما تم حساب الأملاح الكلية الذائبة (TDS) كدالة لدرجة التوصيل الكهربي باستخدام العلاقة المقترحة من قبل (Albu وآخرون، 1997)على النحو التالي:

$$TDS\ (mg/l) \approx EC(\mu S/cm) \times 0.640 \quad (4)$$

كما تم الاستعانة ببرنامج Rockware 14 للتعرف على هيدروكيميائية المياه الجوفية عبر التمثيل البياني للتحاليل الكيميائية للمياه الجوفية (مخطط بايبر) المقترح من قبل (Piper، 1944).

.جدول (3) محددات وقيود استخدام مياه الري وفقا لمؤشر جودة مياه الريMeireles وآخرون (2010)

IWQI	محددات وقيود الاستخدام	التوصيات	
		التربة	النبات
85-100	لا توجد	بالإمكان استخدامها لجميع أنواع الترب. قد تتعرض التربة إلى مخاطر منخفضة من الصودية والملوحة.	لا توجد خطورة للسمية على أغلب المحاصيل
70 – 85	منخفضة	بالإمكان استخدامها للترب خفيفة القوام، أو متوسطة النفاذية. ولاستبعاد مخاطر الصودية في الترب ثقيلة القوام ينصح بإجراء عمليات الغسيل	ارتفاع خطورة الملوحة على المحاصيل الحساسة للملوحة.
55-70	معتدلة	من الأفضل استخدامها للتربة متوسطة، وعالية النفاذية. كما ينصح بإجراء عمليات الغسيل المتوسط للأملاح لمنع تدهور التربة.	بالامكان استخدامها لري المحاصيل متوسطة التحمل للملوحة
40–55	مرتفعة	بالإمكان استخدام هذا النوع من المياه للترب عالية النفاذية، والتي لا تحوي طبقات منضغطة. كما يتطلب أن يكون تكرار الري مرتفعا.	ملائمة لري المحاصيل من متوسطة إلى عالية التحمل للملوحة مع عمليات تحكم خاصة في الملوحة عدا تلك المياه التي
0-40	عالية	لا يجب استخدام هذه المياه لأغراض الري تحت الظروف الاعتيادية.	تصلح للمحاصيل عالية التحمل للملوحة، عدا تلك المياه التي تحوي قيم منخفضة من الصوديوم والكلوريدات والبيكربونات.

ISSN: online 2617-2186 print 2617-2178

خرائط التوزيع المكاني للخصائص الكيميائية: تم الحصول على خرائط التوزيع المكاني المختلفة باستخدام طريقة مقلوب المسافة الوزنية (IDW) ضمن بيئة نظم المعلومات الجغرافية عبر استخدام برنامج ArcGis10.4 وملحقاته، والمطور من قبل معهد بحوث النظم البيئية (ESRI.، 2012) تصنف طريقة مقلوب المسافة الموزونة IDW على أنها أحد طرق الاستنباط .التقديرية (deterministic) التي تنتج سطوحاً تقديرية بشكل أفضل عند محدودية عدد النقاط، وانتظام توزيعها. كما تم وصفها من قبل (Azpurua و Dos Ramos،2010) بأنها طريقة دقيقة، وحدسية. (Intuitive) بالإمكان كتابة الصيغة الرياضية التي تصف طريقة مقلوب المسافة الموزونة على النحو التالي:

$$z(x_0) = \frac{\sum_{i=1}^{n} \frac{x_i}{h_{ij}^{\beta}}}{\sum_{i=1}^{n} \frac{1}{h_{ij}^{\beta}}} \qquad (5)$$

تمثل $z(x_0)$ القيمة المتنبأ بها للخاصية موضوع الدراسة عند الموقع x_0، كما تمثل n العدد الكلي للبيانات المتوفرة (في هذه الدراسة 31 نقطة)، و x_i قيمة الخاصية عند الموقع i، تمثل h المسافة الفاصلة بين النقطة المراد التنبؤ بالخاصية عندها، والنقطة معلومة التقدير، β تشير إلى أس المسافة. على الرغم من أن قيمة الأس تساوي أي قيمة أعلى من الصفر، إلا أنه في هذه الدراسة تم اختيار قيمة للأس مساوية 2. فلقد أشار (Babak، و Deutsch، 2008) إلى أن هذه القيمة هي الأكثر استخداماً عند تطبيق طريقة مقلوب المسافة الموزونة في التقديرات المكانية.

النتائج والمناقشة

الخصائص الكيميائية للمياه الجوفية: يوضح الجدول (4) أرقام الآبار، ومواقعها، ونتائج تحليل الخواص الكيميائية للمياه الجوفية. أظهرت النتائج المتحصل عليها أن متوسط عمق منسوب الماء الساكن تحت مستوى سطح الأرض (WSL) في منطقة الدراسة بلغ 77.5 متر، وأن أقل عمق تم تسجيله 24 متر كان في البئر رقم 14 الواقع في شمال منتصف منطقة الدراسة. في حين سجل أقصى عمق120 متر وذلك عند البئر رقم 25 الواقع في الجنوب الغربي من منطقة الدراسة.

يوضح الجدول (5) بعض الخصائص الإحصائية للخواص الكيميائية للمياه الجوفية في منطقة الدراسة. أظهرت النتائج أن قيم درجة التفاعل (pH) تراوحت بين 7 و8، وبمعامل اختلاف منخفض نسبياً (3%)، كما أنها تقع ضمن المدى الطبيعي المسموح به لمياه الري (6.5–8.4). والموصى به من قبل (Ayers وWestcot،1999) .

يُظهر الشكل (2) أن هناك ارتفاعاً نسبياً في قيم درجة التفاعل عند الحدود الشمالية الشرقية من منطقة الدراسة مقارنة ببقية المناطق. كما يمكن ملاحظة أن المنطقة الشمالية الشرقية تنخفض فيها تركيزات البيكربونات الذائبة، وذلك وفقاً للتوزيع المكاني للبيكربونات الذائبة الموضح في الشكل (3).

تتفق هذه النتائج مع ما خلص إليه (Srinithi وRamesh، 2014) حيث تنخفض قيم pH مع الزيادة في تركيز البيكربونات في المياه الجوفية. تتميز المياه بخاصية التوصيل الكهربي؛ لاحتوائها على أيونات تزيد من قدرتها على التوصيل الكهربي (Richards، 1954). أظهرت النتائج تفاوتاً كبيراً في قيم درجة التوصيل الكهربي في عينات المياه. فلقد تراوحت بين 490 ميكروسيمنز/ سم، و7700 ميكروسيمنز /سم، بانحراف معياري، ومعامل اختلاف مقداره 1797 ميكروسيمنز/سم و 81% على التوالي. فلقد كانت القيم المرتفعة لدرجة التوصيل الكهربي في الآبار هي تلك الواقعة في مشروع الهضبة الزراعي عند مركز منطقة الدراسة (الآبار 19و20و21)، وذلك على النحو الموضح في الشكل (4).

تشير هذه النتائج إلى أن تعاظم كميات السحب من الخزانات الجوفية، في تلك المنطقة أدى إلى حدوث تلوث للمياه الجوفية بمياه البحر(Ekhmaj، وآخرون، 2014)، والذي يعد أحد أسباب ارتفاع كمية الأملاح الكلية الذائبة في المياه الجوفية. حيث يشير ارتفاع قيم التوصيل الكهربي في عينات المياه إلى ارتفاع كمية الأملاح الكلية الذائبة، وتباياتها أيضاً، وذلك على النحو الموضح في الجدول (5).

ISSIN: online 2617-2186 print 2617-2178

توضح الأشكال (3،4، 5، 6، 7) أن نمط التوزيع المكاني للأيونات الذائبة مشابه إلى حد بعيد مع نمط التوزيع المكاني لدرجة التوصيل الكهربي، حيث تشكل مجموعة الآبار (19،20،21) بؤرة ترتفع فيها تركيزات الأيونات الذائبة، وفي اتجاهها. تظهر قيم معامل الاختلاف في تركيز الأيونات الرئيسة الذائبة التباينات الواضحة بين مياه الآبار الجوفية في محتواها من تلك الأيونات وذلك كما هو موضح في الجدول (5).

ففي حين كانت أيونات البيكربونات هي الأقل اختلافا (21%) فإن تركيزات الصوديوم، والكلوريدات كانت الأكثر اختلافاً بنسبة 106%، و 111% على التوالي. من ناحية أخرى، تمثل أيونات الصوديوم، والكلوريدات النسبة الأكبر لمكونات الأملاح الكلية الذائبة بنسبة 18% و 36% على التوالي. كانت مساهمة بقية الأيونات في مكونات الأملاح الكلية الذائبة 7، 5، 0.5، 13، 15% وذلك للكالسيوم، والماغنيسيوم، والبوتاسيوم، والبيكربونات، والكبريتات على التوالي. إن ارتفاع تركيز الكلوريدات في المياه الجوفية مقارنة ببقية الأيونات الذائبة، يوفر المؤشر الأكثر بساطة لحدوث ظاهرة تلوث الخزانات الجوفية بمياه البحر (Mercado وآخرون،2006; El Moujabber1985،) تكمن أهمية تقدير الكلوريدات الذائبة في المياه

ISSN: online 2617-2186 print 2617-2178

جدول (4). أرقام الآبار ومواقعها ونتائج تحليل الخواص الكيميائية للمياه الجوفية

البئر	خط الطول (درجة شرقاً)	خط العرض (درجة شمالاً)	WSL (متر)	pH	EC (ميكرو سيمينز/متر)	TDS (ملجم/لتر)	Ca^{2+} (ملجم/لتر)	Mg^{2+} (ملجم/لتر)	Na^{+} (ملجم/لتر)	K^{+} (ملجم/لتر)	HCO_3^{-} (ملجم/لتر)	Cl^{-} (ملجم/لتر)	SO_4^{2-} (ملجم/لتر)	SAR^{o}
1	13.33748	32.82008	90	7.8	580	371	32	26.4	48.3	3.9	140.3	71	80.6	1.5
2	13.33759	32.80269	90	8	550	352	26.4	26.2	36.8	2.7	134.2	63.9	73	1.2
3	13.33829	32.78288	75	7.9	570	365	28	28.8	44.9	3.5	134.2	71	78.7	1.4
4	13.3379	32.76506	65	7.6	800	512	44	37.2	65.6	4.7	195.2	106.5	102.7	1.9
5	13.29324	32.83579	90	7.8	650	416	36	31.2	54.5	4.7	134.2	85.2	95	1.6
6	13.29381	32.81699	95	7.9	490	314	27.2	22.1	33.6	2.3	103.7	56.8	70.1	1.1
7	13.29525	32.79973	95	7.4	1860	1190	84	52.8	239.9	6.6	134.2	390.5	178.6	5.3
8	13.29664	32.78174	90	7.5	1100	704	61.6	49.4	99.1	5.5	140.3	184.6	143	2.4
9	13.29742	32.76349	90	7.7	670	429	36.8	30.7	52.9	4.3	207.4	92.3	53.8	1.6
10	13.25248	32.83554	60	7.3	5100	3264	144	163.2	864.1	10.9	183	1491	399.4	12.4
11	13.25412	32.81757	55	7.3	3900	2496	184	112.8	503.9	9.8	244	994	383	8.4
12	13.25378	32.79813	75	7.6	880	563	48	40.8	72	4.7	225.7	142	89.3	2
13	13.25414	32.77949	65	7.7	960	614	52.8	45.1	80	5.1	219.6	177.5	95	2.1
14	13.20343	32.82279	24	7.5	4820	3085	268	132	592	8.2	250.1	1207	536.6	8.9
15	13.20431	32.80435	65	7.3	4200	2688	184	144	520	7.8	231.8	1065	481.9	7.9
16	13.20515	32.78694	75	7	2920	1869	144	110.4	319.9	7	219.6	692.3	340.8	5.5
17	13.20687	32.76797	90	7.8	1310	838	64	55.2	127.9	7.8	256.2	241.4	112.3	3.1
18	13.16281	32.8291	27	7.4	3140	2010	172	105.6	336	7	189.1	816.5	269.8	5.6
19	13.16426	32.81062	65	7.5	4100	2624	192	134.4	512	9.4	195.2	1100.5	441.6	7.8
20	13.1659	32.79174	75	7.5	5500	3520	204	171.6	816	16	195.2	1739.5	369.6	11.2
21	13.16736	32.77372	65	7	7700	4928	288	242.4	1136	35.1	189.1	2591.5	395.5	13.2
22	13.11915	32.82137	50	7.5	1540	986	88	98.4	72	5.5	201.3	276.9	213.1	1.3
23	13.12138	32.8022	90	7.6	1870	1197	76	60	239.9	7.4	170.8	426	221.8	5.3
24	13.12144	32.78383	85	7.3	3140	2010	184	24	431.9	12.1	189.1	710	370.6	10.1
25	13.12413	32.76543	120	7.7	1840	1178	72	84	196	6.6	195.2	390.5	174.7	3.9
26	13.0776	32.80561	65	7.5	1060	678	48	72	65.6	5.9	231.8	177.5	105.6	1.5
27	13.07944	32.78724	90	7.4	1450	928	56	79.2	128.1	7	231.8	213	239	2.7
28	13.08064	32.76919	120	7.3	1490	954	57.2	83.3	131.3	6.2	225.7	248.5	245.8	2.7
29	13.04511	32.79514	75	7.4	1140	730	76	31.2	120.1	6.2	183	213	127.7	3.3
30	13.04558	32.77667	90	7.6	1550	992	80	76.8	123.3	8.2	237.9	284	183.4	2.6
31	13.04801	32.75744	95	7.3	1910	1222	108	81.6	180.1	10.9	225.7	319.5	299.5	3.6

ISSIN: online 2617-2186 print 2617-2178

جدول (5) الخصائص الإحصائية لمستوى الماء الجوفي الساكن، ولبعض الخواص الكيميائية للمياه الجوفية.

البارامتر	المتوسط الحسابي	القيمة الصغرى	القيمة القصوى	الانحراف المعياري	معامل الاختلاف(%)
WSL (متر)	77.5	24	120	21.5	28
pH	7.5	7	8	0.26	3
EC (ميكروسيمينز/سم)	2219	490	7700	1797	81
TDS(ملجم/لتر)	1420	314	4928	1150	81
Ca^{2+}(ملجم/لتر)	102	26	288	73	72
Mg^{2+}(ملجم/لتر)	79	22	242	53	67
Na^{+}(ملجم/لتر)	266	34	1136	281	106
K^{+}(ملجم/لتر)	7.83	2.3	35.1	5.8	74
HCO_3^{-}(ملجم/لتر)	194	104	256	40.6	21
Cl^{-}(ملجم/لتر)	537	57	2592	594	111
SO_4^{-}(ملجم/لتر)	225	54	537	141	63
SAR^{O}	4.61	1.09	13.24	3.60	78

الجوفية في إمكانية الاعتماد عليها في وصف المياه الجوفية، وذلك وفقا لاختلاف تركيزاتها. فلقد أشار (Alfarrah وآخرون، 2011) إلى أن المياه الجوفية يمكن تصنيفها بناء على محتواها من الكلوريدات الذائبة، بحيث تكون عذبة عندما يقل تركيزها عن 150 ملجم/ لتر، وخليط بين عذبة، وآسنة عندما يتراوح تركيزها بين 150 و 300 ملجم/لتر، وآسنة عندما يتراوح تركيزها بين 300 و 1000 ملجم/ لتر، وبين آسنة ومالحة عندما يتراوح تركيزها بين 1000، و10000 ملجم/لتر. وفقاً لهذا التصنيف فإن الآبار (1–6، 9، 12) وهي آبار تقع شرق منطقة الدراسة، توصف على أنها عذبة، وأن الآبار (8، 13،17، 22، 26– 30) توصف على أنها مياه خليط بين عذبة، وآسنة. كما توصف مياه الآبار (11، 16، 18، 23، 24، 25، 31) على أنها آسنة، أما بقية الآبار (10، 14، 15، 19، 20، 21) فإنها مياه آسنة، ومالحة.

يوضح الشكل (8) أن المياه الآسنة المالحة يرتكز وجودها في منطقة مشروع الهضبة الزراعي، ويمتد أثرها نحو الشمال الشرقي. كما يتضح أن نمط التوزيع المكاني لكل من الكلوريدات، والكبريتات متشابهان (الشكل 8 و9) إلى حد كبير، خصوصا وأن التركيزات المرتفعة من الكبريتات مرتبطة بدرجة أساسية بعمليات الخلط التي تحدث للمياه الجوفية مع المياه المالحة ذات المنشأ البحري، وأن ارتباط كل من الكلوريدات مع الكبريتات غالباً ما يحدث في الخزان الجوفي العلوي المتأثر بعمليات تداخل مياه البحر بالمياه الجوفية (Alfarrah وآخرون، 2011).

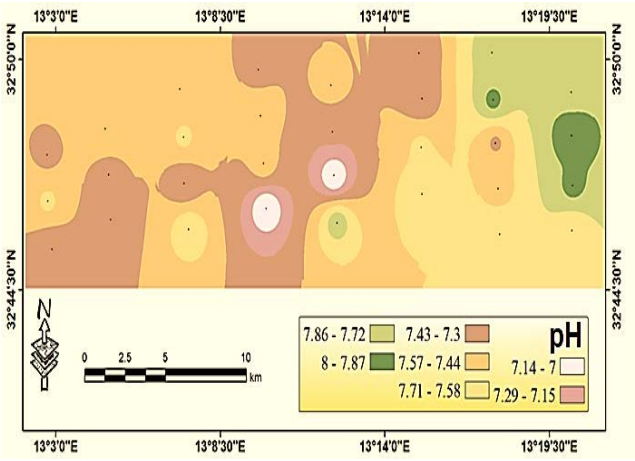

شكل (2) التوزيع المكاني لدرجة التفاعل لمياه آبار منطقة الدراسة.

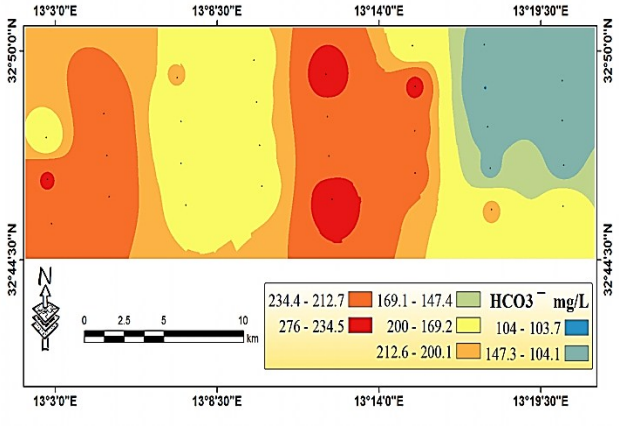

شكل (3) التوزيع المكاني للبيكربونات الذائبة (ملجم/لتر) في مياه آبار منطقة الدراسة.

ISSIN: online 2617-2186 print 2617-2178

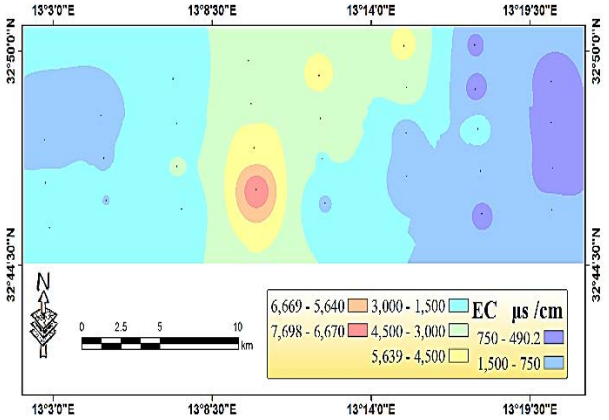

شكل (4) التوزيع المكاني لدرجة التوصيل الكهربي (ميكرو سيمينز/سم) لمياه آبار منطقة الدراسة.

يوضح الجدول (5) أن قيم نسبة الصوديوم المدمص المعدلة SAR^o تتراوح بين 1.09 و13.24، بمتوسط مقداره 4.61، وبمعامل اختلاف 78%. وفقا لتصنيف منظمة الأغذية والزراعة (Ayer وWestcot، 1985) فإن أغلب مياه آبار منطقة الدراسة تقل فيها قيم نسبة ادمصاص الصوديوم المعدلة عن 3، وبالتالي فإنه لا يتوقع عند استخدامها ظهور مشاكل متعلقة بنسبة ادمصاص الصوديوم المعدلة.في حين تتراوحت قيم نسبة ادمصاص الصوديوم المعدلة في المياه بين 3، و 9، وهي المياه التي يتوقع عند استخدامها ظهور مشاكل النفاذية في التربة، وهو ما اتصفت به مياه الآبار (7، 11، 14–16، 18، 19، 23، 25). إن القيم المرتفعة لنسبة الصوديوم المعدلة في المياه، والتي ينتج عند استخدامها ظهور مشاكل حادة (SAR^o أكبر من 9) كانت في الآبار 10، 20، 21، 24. يظهر الشكل (10) التوزيع المكاني لقيم SAR^o المعدلة، حيث ترتفع قيم SAR^o عند منتصف منطقة الدراسة مقارنة بما هو في شرقها، وغربها. يعزى نمط هذا التوزيع إلى ارتفاع قيم الصوديوم في مياه آبار تلك المنطقة، والذي قد تعطي دلالة أيضا على وجود اتصال هيدرولوليكي مباشر بين آبار تلك المنطقة. إن الأثر الضار المتوقع حدوثه عند استعمال مياه مرتفعة SAR^o يتمثل في ادمصاص الصوديوم على الأسطح الغروية في التربة (الطين) واحلاله محل الماغنيسيوم، وبقية الكاتيونات، مسببا انخفاض معدل نفاذية التربة (Todd، 1980)، وتصلب التربة عند السطح، و الضرر على عمليات الإنبات (Ayer وWestcot، 1985).

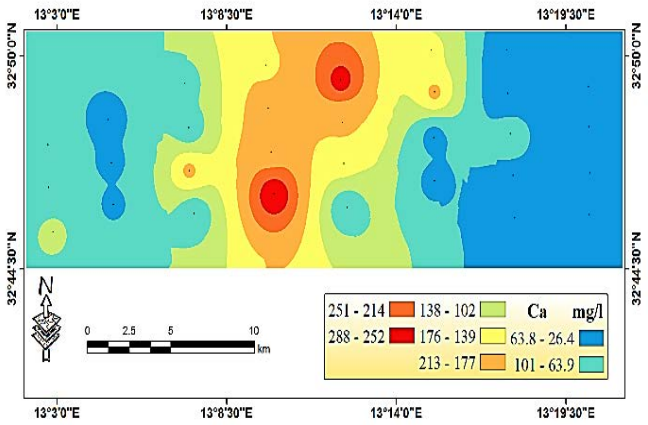

شكل (5) التوزيع المكاني للكالسيوم الذائب (ملجم/لتر) في مياه آبار منطقة الدراسة.

الارتباط بين الخصائص الكيميائية المختلفة للمياه الجوفية:

لقد تم تقدير معامل بيرسون للارتباط لقياس درجة الارتباط بين الخصائص الكيميائية المختلفة. على الرغم من أن العمليات الهيدروكيميائية للمياه الجوفية بالغة التعقيد، إلا أن مثل هذا التحليل قد يسمح بفهم بعض أوجه تلك العمليات (Ekhmaj، وآخرون، 2014).

يوضح الجدول (5) مصفوفة الارتباط للعلاقات الخطية بين الخصائص الكيميائية المختلفة للمياه الجوفية. أظهرت النتائج أن هناك ارتباطا سالباً، ومعنوياً عند مستوى 0.05 بين درجة التفاعل وبقية الخصائص الكيميائية. كانت قيم معامل الارتباط لدرجة التفاعل أكثر سالبية مع الكالسيوم (−0.67) ومع الكبريتات (−0.70). كما كان الارتباط موجباً ومرتفعاً عند مستوى معنوية 0.05 بين درجة التوصيل الكهربي ومحتوى المياه من الكلوريدات (0.99)، والصوديوم (0.99)، وبدرجة أقل مع الكالسيوم (0.95)، والماغنيسوم (0.93)، والكبريتات (0.87)، والبوتاسيوم (0.82) وبدرجة أدنى مع البيكربونات (0.28). يعطي ارتفاع قيم معامل الارتباط بين درجة التوصيل الكهربي، ومحتوى المياه من الأيونات الذائبة دلالة على تحكم تلك الأيونات في قيم درجة التوصيل الكهربي (Sundaray، 2010). كما أظهرت النتائج ارتباطاً موجباً وعالياً بين الكلوريدات مع الصوديوم (0.99) مما يدل على حدوث عمليات تلوث المياه الجوفية بمياه البحر (Panteleit، وآخرون، 2001).

ISSN: online 2617-2186 print 2617-2178

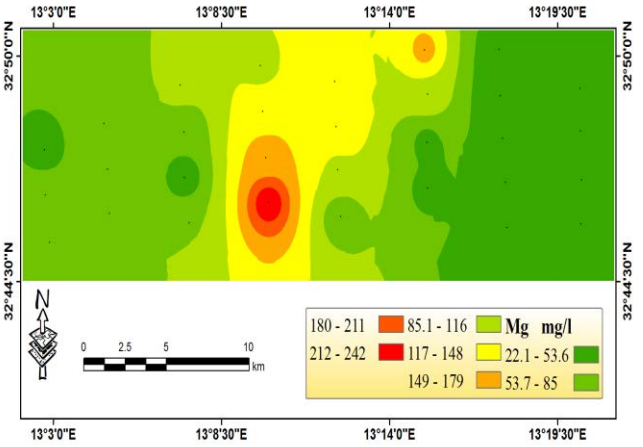

شكل (6) التوزيع المكاني للماغنيسيوم الذائب (ملجم/لتر) في مياه آبار منطقة الدراسة.

كما يؤكد حدوث مثل هذا التلوث أن كل من أيونات الكلوريدات، والكبريتات كانت أكثر ارتباطاً معنوياً بالكاتيونات مقارنة بأيون البيكربونات، والتي كان ارتباطها مع الكاتيونات منخفضاً، وغير معنوي عند مستوى 0.05. إن الكلوريدات، والكبريتات أكثر وفرة من البيكربونات في مياه البحر (Appelo و Postma، 1996).

كما أشارت دراسة (El-Trriki، 2006) إلى أن حدوث تلوث الخزانات الجوفية المتاخمة للبحر بمياه البحر، مرتبط بعمليات تداخل مياه البحر، والذي يحدث نتيجة لانخفاض ضغط المياه العذبة حول منطقة الضخ للبئر، وباستمرار الضخ من البئر فإن المياه المالحة تتحرك إلى أعلى في شكل مخروط تحت منطقة الضخ مما يسبب في تلوث المياه الجوفية بالمياه المالحة للبحر. إن العلاقات الموجبة عالية الارتباط بين أيوني الكالسيوم، والماغنيسيوم، تدل على حدوث عمليات الإذابة، والترسيب لمعدني الدولوميت، والكالسيت (Aris وآخرون، 2007)، خصوصاً وأن الارتباط بينهما مع أيون البيكربونات مرتفع نسبيا عند مقارنته مع الارتباط بأيوني الصوديوم، والبوتاسيوم

السيادة النوعية النسبية للأيونات الذائبة في مياه الآبار:

إن متوسط الوفرة النسبية للأيونات الذائبة في مياه آبار منطقة الدراسة، معبرا عنه بوحدات (ملليمكافيء/لتر) كانت 65.8، 20.4، 13.8% وذلك للكلوريدات، والكبريتات، والبيكربونات، على التوالي. تشير هذه النتيجة إلى ارتفاع قيم تركيز الكلوريدات الذائبة في تلك المياه.

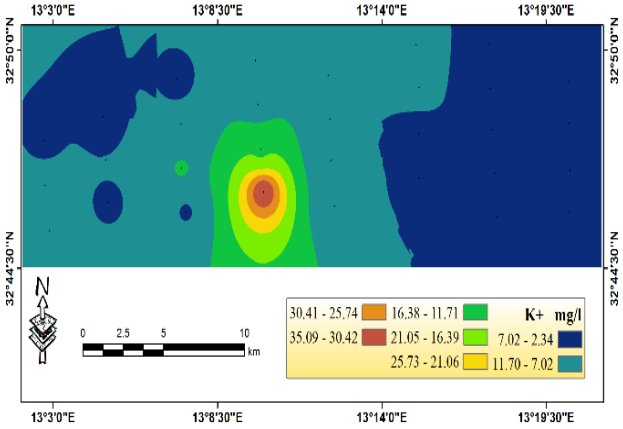

شكل (7) التوزيع المكاني للبوتاسيوم الذائب (ملجم/لتر) في مياه آبار منطقة الدراسة.

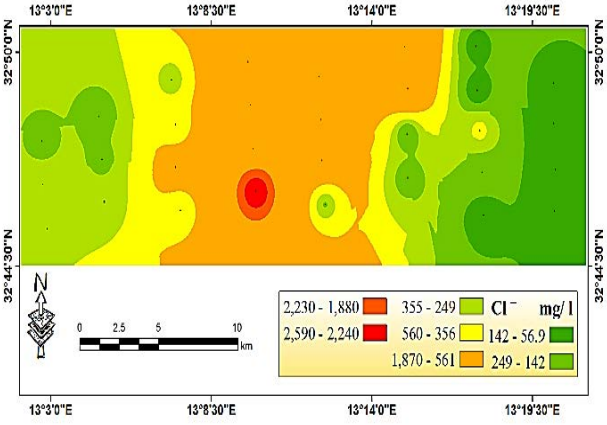

شكل (8) التوزيع المكاني للكلوريد الذائب (ملجم/لتر) في مياه آبار منطقة الدراسة.

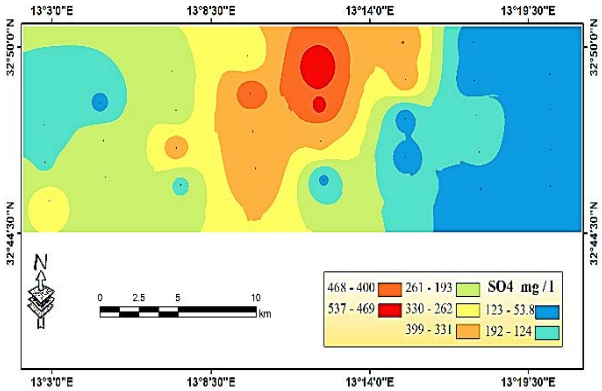

شكل (9). التوزيع المكاني لتوزيع الكبريتات الذائبة (ملجم/لتر) في مياه آبار منطقة الدراسة.

ISSN: online 2617-2186 print 2617-2178

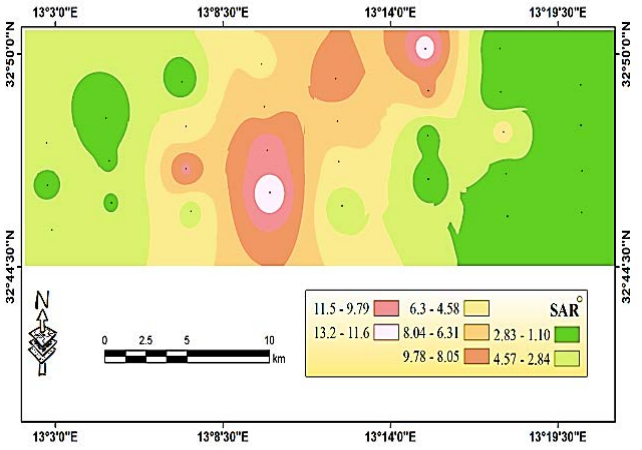

شكل (10) التوزيع المكاني لنسبة ادمصاص الصوديوم المعدلة (SAR^o) في مياه آبار منطقة الدراسة.

جدول (5) معامل بيرسون للارتباط للخصائص الكيميائية المختلفة.

	pH	EC	Ca^{2+}	Mg^{2+}	Na^+	K^+	HCO_3^-	Cl^-	SO_4^{2-}
EC	-0.66								
Ca^{2+}	-0.67	0.95							
Mg^{2+}	-0.65	0.93	0.83						
Na^+	-0.62	0.99	0.90	0.89					
K^+	-0.61	0.82	0.74	0.78	0.83				
HCO_3^-	-0.43	0.28*	0.35*	0.36*	0.19*	0.19*			
Cl^-	-0.62	0.99	0.91	0.92	0.99	0.86	0.20*		
SO_4^{2-}	-0.70	0.87	0.91	0.79	0.82	0.55	0.41	0.80	
SAR^o	-0.63	0.95	0.90	0.80	0.97	0.76	0.20*	0.94	0.85

*الارتباط غير معنوي عند مستوى 0.05

كما يتضح من الشكل (11) فإن السيادة النوعية للأنيونات كانت كلوريدية وذلك وفقا للتوزيع النسبي لها على مثلث الأنيونات حيث تتراوحت نسبها بين 50-86 (ملليمكافئ/لتر،%)، وذلك للآبار (7، 14،11،10-25، 29، 30)، كما كانت السيادة النوعية المرتفعة للكبريتات في الآبار (27، 28، 31)، بنسبة سيادة 33، 32، 33 ملليمكافئ/ لتر (%)، على التوالي.وعلى الرغم من أن السيادة النوعية لأيون البيكربونات للبئر 9 كانت الأعلى وبقيمة 49 ملليمكافيئ/ لتر (%)، إلا أن مياه بقية الآبار تميزت بانخفاض نسب البيكربونات فيها، حيث تراوحت تلك النسبة ما بين 4 و39 ملليمكافئ/ لتر (%). أما بالنسبة للكاتيونات الذائبة، فإن متوسط الوفرة النسبية لها، معبرا عنه بوحدات (ملليمكافيء/ لتر) كانت 49.3، 28.1، 21.7، 0.9% وذلك للصوديوم، والماغنيسيوم، والكالسيوم، والبوتاسيوم على التوالي. يظهر التوزيع النسبي لتلك الأيونات على مثلث الكاتيونات أن السيادة كانت لأيوني الصوديوم، والبوتاسيوم بحيث تجاوزت 50 ملليمكافئ/ لتر % وذلك في الآبار(7، 10، 11، 14، 15، 19، 20، 21، 23، 25)، ويجدر الإشارة هنا إلى ملاحظة انخفاض نسبة مساهمة البوتاسيوم الذائب في تلك النسبة المئوية، وذلك كما هو موضح في الشكل (11).

كما يشير مثلث الكاتيونات إلى ارتفاع محتواها النسبي من الماغنيسيوم بحيث تفوق 40 ملليمكافئ/ لتر % وذلك للآبار 2، 3، 23، 26، 27، 28، 30. أما بالنسبة لمحتوى المياه من الكالسيوم فإن هناك انخفاضاً ملحوظاً في نسبة وجوده النسبي حيث لم تتعد نسبته في المياه 30 ملليمكافئ/لتر % في جميع الآبار عدا البئرين 24، 29. إن اختلاف التوزيع النسبي للأيونات الذائبة في المياه الجوفية تخضع للعديد من العوامل أهمها عمليات الإذابة، والخلط بمياه البحر بالإضافة

ISSN: online 2617-2186 print 2617-2178

إلى حدوث تفاعلات التبادل الكاتيوني (Pulido ، 2004 Walraevens; و VanCamp،2005). تظهر تأثيرات هذه العمليات في نوعية المياه على شكل معين بايبر. يوضح الشكل (11) أن نوعية المياه في الآبار 7، 10، 11، 15، 19، 20، 21، 23، 24 يسود فيها كلوريد الصوديوم المكون الرئيسي لمياه البحر، وهذا يعطي دلالة على حدوث خلط لمياه تلك الآبار بمياه البحر. كما أن بقية مياه الآبار تسود فيها كلوريدات، وكبريتات الكالسيوم، والماغنيسيوم، والتي تميز حدوث عمليات الملوحة، وتفاعلات التبادل الكاتيوني (Alfarrah وآخرون،2011).

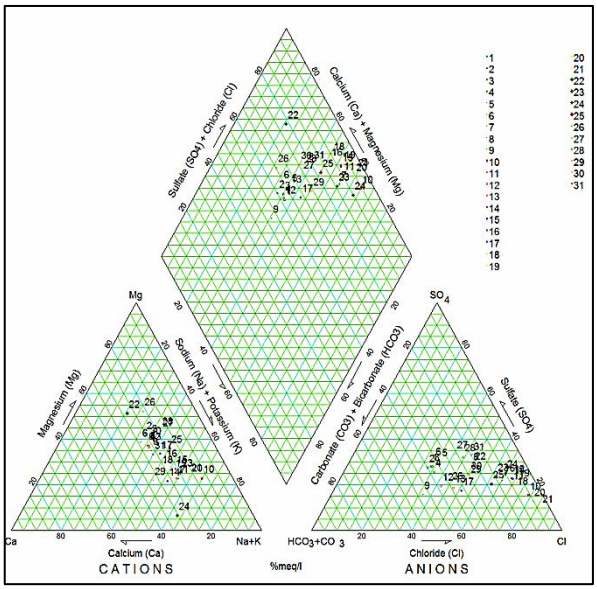

شكل (11) مخطط بايبر لتحديد السيادة النوعية للكاتيونات والأنيونات الذائبة

مؤشر جودة مياه الري: لقد تم استخدام قيم درجة التوصيل الكهربي، الصوديوم، الكلوريد البيكربونات، ونسبة ادمصاص الصوديوم المعدلة في تقدير مؤشر جودة مياه الري، وذلك على النحو الذي اقترحه Meireles، وآخرون (2010). تظهر الأشكال (12و 13و 14و 15و 16) التوزيع المكاني لمساهمة درجة التوصيل الكهربي، الصوديوم، الكلوريد البيكربونات، ونسبة ادمصاص الصوديوم في قيم مؤشر جودة مياه الري على التوالي. وفقاً لما أشار إليه Meireles، وآخرون (2010)، فإنه كلما ارتفعت قيم المساهمة تحسنت جودة مياه الري. يلاحظ من خلال الشكل(12، 13، 14) التشابه الكبير في نمط التوزيع المكاني لمساهمة درجة التوصيل الكهربي، والصوديوم، و الكلوريد. يمكن أن يعزى هذا التشابه إلى أن درجة التوصيل الكهربي مرتبطة بالأملاح الكلية الذائبة والتي يشكل فيها الصوديوم، والكلوريد أكثر مكوناتها خصوصا في المياه عالية الملوحة في المناطق القريبة من البحر(Ekhmaj وآخرون، 2014). كما أن قيم الأهمية النسبية لكل من درجة التوصيل الكهربي، والصوديوم، والكلوريد متقاربة، وذلك كما هو موضح في الجدول (2)، مما قد يفسر أيضا تشابه نمط التوزيع المكاني لهذه الأيونات. يظهر الشكل (15) ارتفاع قيم مساهمة البيكربونات في الشمال الشرقي من منطقة الدراسة، وتناقصها في اتجاه الغرب، ومن ثم ارتفاعها مجدداً، يعزى هذا الاختلاف في التوزيع المكاني لمساهمة البيكربونات بدرجة رئيسية إلى اختلاف تركيز البيكربونات في المياه الجوفية نتيجة لتفاعلات الإذابة للحجر الجيري في الطبقات الحاوية للمياه (Appelo، 1994).

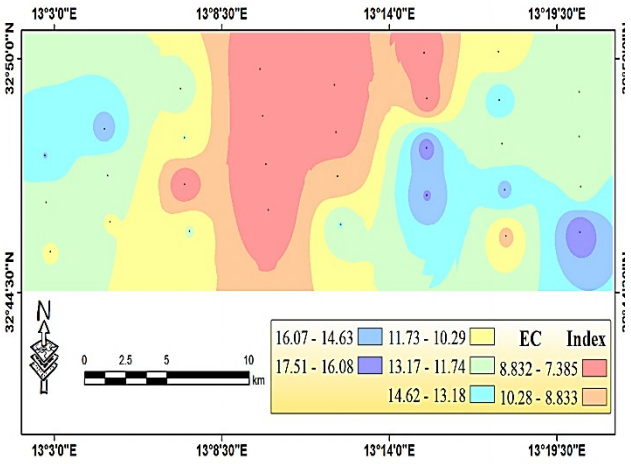

شكل (12) التوزيع المكاني لمساهمة درجة التوصيل الكهربي في قيم مؤشر جودة مياه الري

إن عمليات الإذابة التي تتم في الخزانات الجوفية المحتوية على الحجر الجيري يلاحظ تأثيرها في ارتفاع قيم الكالسيوم، والماغنيسيوم الذائبين خصوصا في غرب منطقة الدراسة حيث تنخفض بدورها قيم مساهمة نسبة الصوديوم المدمص المعدلة مقارنة ببقية منطقة الدراسة وذلك على النحو الموضح في الشكل (16).

ISSN: online 2617-2186 print 2617-2178

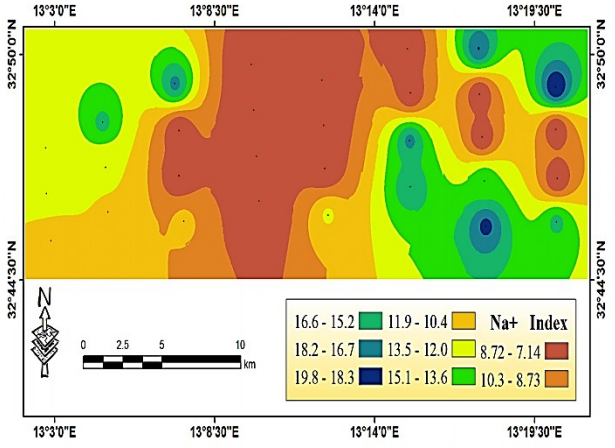

شكل (13) التوزيع المكاني لمساهمة الصوديوم في قيم مؤشر جودة مياه الري

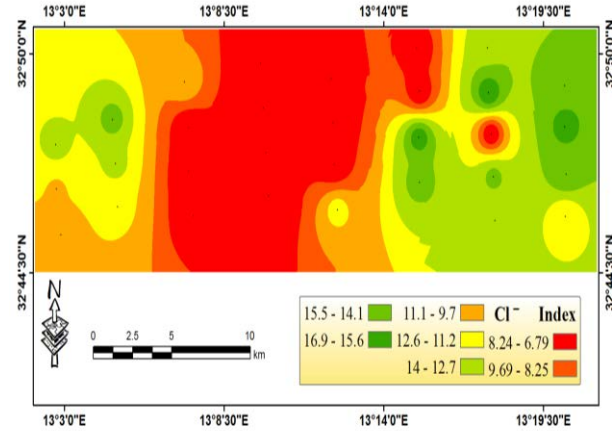

شكل (14) التوزيع المكاني لمساهمة الكلوريد في قيم مؤشر جودة مياه الري

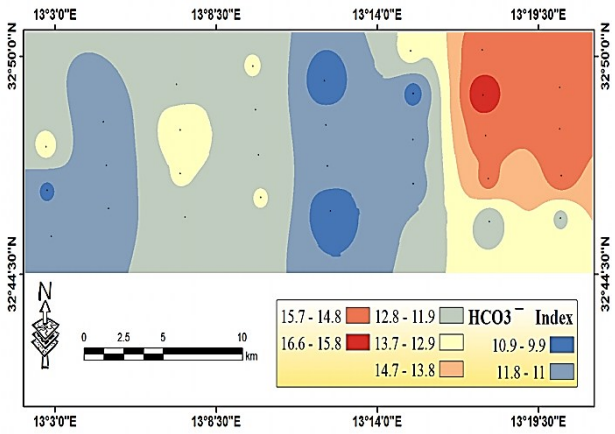

شكل (15) التوزيع المكاني لمساهمة البيكربونات في قيم مؤشر جودة مياه الري

تم حساب مؤشر جودة مياه الري باستخدام المعادلة (3) وذلك بالأخذ في الاعتبار العوامل المختلفة، وأهميتها الوزنية النسبية. وبالاعتماد على محددات، وقيود الاستخدام الموضحة في الجدول (3) فإن مياه 12 بئراً (هي الآبار7، 10، 11، 14-16، 18-21، 23، 24) ذات قيود استخدام مرتفعة، بقيم مؤشر جودة تتراوح من 40 إلى 55.

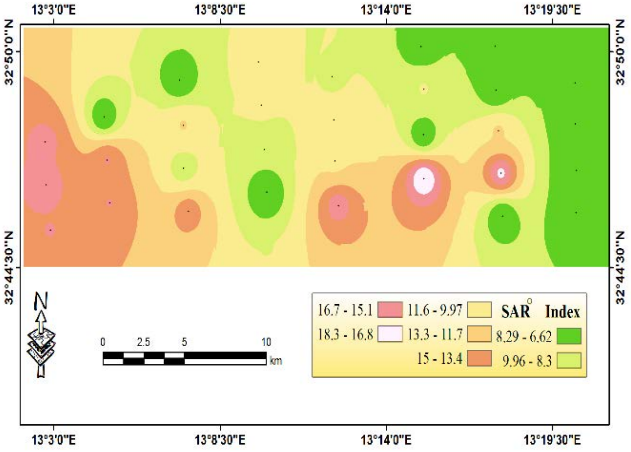

شكل (16) التوزيع المكاني لمساهمة نسبة ادمصاص الصوديوم المعدلة في قيم مؤشر جودة مياه الري

والتي يمكن استخدامها في الترب عالية النفاذية، والتي لا تحوي طبقات منضغطة مما يتطلب حراثتها دورياً، ويجب أن تتم عملية الري بتكرار مرتفع، كما أنها ملائمة لري المحاصيل من متوسطة إلى عالية التحمل للملوحة. بالإضافة إلى ذلك فإن مياه 17 بئرا صنفت على أن قيود استخدامها معتدلة، حيث كانت قيم مؤشر جودة مياه الري فيها بين 55 و 70. إن مثل هذه النوعية من المياه تصلح لري المحاصيل متوسطة التحمل للملوحة، والتي تتم زراعتها في تربة متوسطة، وعالية النفاذية. مع إجراء عمليات الغسيل المتوسط للأملاح لمنع تدهور التربة. كما بينت النتائج أن هناك بئرين هما البئران رقم 8، و13 واللذان كانت مياههما ذات مواصفات منخفضة القيود للاستخدام لأغراض الري، حيث تراوحت قيمة مؤشر جودة المياه بين 70 و 85. هذه النوعية من المياه تصلح لري النباتات الحساسة للملوحة مع مراعاة استخدامها للترب خفيفة القوام، أو متوسطة النفاذية.

يوضح الشكل (17) التوزيع المكاني لمؤشر جودة مياه الري في منطقة الدراسة. يتبين من خلال الأشكال (12، 13، 14) التأثير الكبير لمساهمة درجة التوصيل الكهربي، والصوديوم، والكلوريد على نمط التوزيع المكاني لمؤشر جودة مياه الري، الشكل (17). ينخفض مؤشر جودة مياه الري عند منتصف

ISSN: online 2617-2186 print 2617-2178

منطقة الدراسة مقارنة بشرقها، وغربها. كما أن انخفاض قيمة الأهمية الوزنية لكل من البيكربونات، ونسبة الصوديوم المدمص يجعل من مساهمتهما في قيم مؤشر جودة مياه الري منخفضة نسبياً. توضح النتائج المتحصل عليهما من التوزيع المكاني لمؤشر جودة مياه الري أن 62% من مساحة منطقة الدراسة تصنف على أنها ذات مياه ذات قيود معتدلة الاستخدام لأغراض الري، وأن 37.5% منها تصنف على وجوب تقييد استخدامها بدرجة مرتفعة، في حين كانت 0.5% من مساحة منطقة الدراسة ذات مياه منخفضة القيود للاستخدام في أغراض الري.

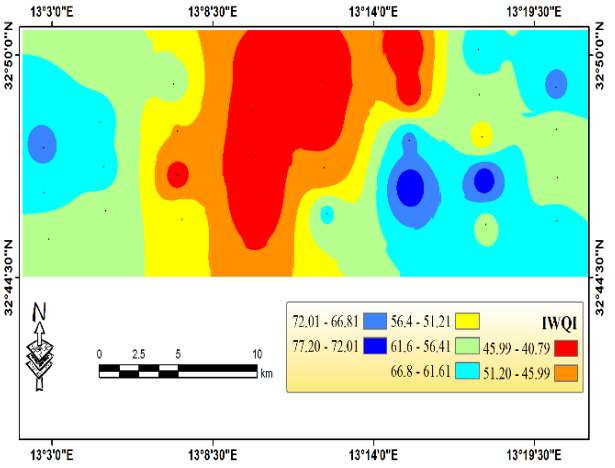

شكل (17) التوزيع المكاني لقيم مؤشر جودة مياه الري

الاستنتاجات

أظهرت نتائج التحليل الكيميائي لمياه الآبار في منطقة الدراسة أن درجة التوصيل الكهربي كانت مرتفعة في منتصف منطقة الدراسة بحيث أخذ نمط هذا الارتفاع شريطا يمتد من الشمال إلى الجنوب. كما أن نمط التوزيع المكاني لكل من أيوني الصوديوم، والكلوريدات الذائبة مشابه إلى حد كبير لنمط التوزيع المكاني لدرجة التوصيل الكهربي، مما يعطي دلالة كبيرة على أن المكون الرئيس للأملاح الذائبة في أغلب مياه الآبار في منطقة الدراسة هو ملح كلوريد الصوديوم مع بعض الاستثناءات في جنوب غربي منطقة الدراسة، حيث يرتفع فيها تركيز البيكربونات. كانت الوفرة النسبية للكاتيونات الذائبة الرئيسية هي للصوديوم، يليه الماغنيسيوم، ثم الصوديوم، وأخيرا البوتاسيوم. أما بالنسبة للأنيونات الذائبة الرئيسية فكانت السيادة للكلوريدات، فالكبريتات، ثم البيكربونات. أوضحت نتائج استخدام مؤشر جودة مياه الري أنه بالإمكان تصنيف أغلب مياه آبار منطقة الدراسة على أنها ذات قيود معتدلة، ومتوسطة. تمكن النتائج المتحصل عليها من المساهمة في إنجاح برامج الري في منطقة الدراسة بحيث تراعى فيها نوعية المياه المستخدمة بالإضافة إلى اختيار نوعية التربة، والمحاصيل الملائمة للري بمثل هذه المياه.

شكر وتقدير

يتقدم الباحثون بالشكر والامتنان إلى المهندس حسام حسن شحادة ، مساعد باحث بقسم التربة والمياه، كلية الزراعة، جامعة طرابلس، على مساعدته القيمة في إجراء التحاليل الكيميائية التي أجريت في هذه الدراسة.

المراجع

الصادي بشير يوسف، رأف الله عطية محمد، بن زقطة، مصطفى محمد والجائر محمد منصور. (2020). دراسة جودة مياه الري بالمشاريع الزراعية بمنطقة مصراتة. مجلة جامعة مصراتة للعلوم الزراعية. 1(2): 465-478.

الميلودي، عبير مصطفى (2018). *تحديد مؤشرات الجفاف المناخي المعتمدة على الهطول لمنطقة سهل الجفارة*. رسالة ماجستير غير منشورة. كلية الزراعة. جامعة طرابلس، ليبيا، طرابلس.

عبد العزيز، عبد الرزاق مصباح الصادق، أحمد إبراهيم خماج وصلاح عبد المولى أبوخذير (2009). رصد نوعية المياه الجوفية بتاجوراء- ليبيا. *مجلة الإسكندرية للتبادل العلمي* 30.(4)، 260-280 .

Abbasnia A, Alimohammadi M, Mahvi A. H, Nabizadeh.R, Yousef. M, Mohammadi. H Passalari. Hand Mirzabi. H. M. (2018). Assessment of groundwater quality and evaluation of scaling and corrosiveness potential of drinking water samples in villages of Chabahr city, Sistan and Baluchistan province in Iran. *Data Brief* 16:182–92.

Abdulhady, Y., Zaghlol, E. and Gedamy, Y, (2018). Assessment of the groundwater

ISSN: online 2617-2186 print 2617-2178

UFPB. Studies FAO Irrigation and Drainage paper No. 29. FAO: Rome.

Azpurua. M and Dos Ramos. K (2010). A comparison of Spatial Interpolation Methods for Estimation of Average Electromagnatic Field Magnitude. *Progress InElectromagnetic Research* (14), 135-145.

Babiker, I.S. M.ohamed, M. A A. and Hiyama, T. (2007). Assessing groundwater quality using GIS.*Water Resource Manag*. (21): 699-715.

Babak. O. and Deutsch. C. V (2008). Statistical Approach to inverse distance interpolation. *Stoch. Res. Risk. Assess*. 23(5), 543-553

Bernardo, S. (1995). Manual of Irrigation. (4 th ed), *Vicosa*: Federal University of Vicosa, Brazil.

Brhane, G.K. (2016). Irrigation Water Quality Index and GIS Approach based Groundwater Quality Assessment and Evaluation for Irrigation Purpose in Ganta Afshum Selected Kebeles, Northern Ethiopia. *International Journal of Emerging Trends in Science and Technology*, 3(09), 4624-4636.

Ekhmaj, I. A, Ezlit, Y., and Elaalem, M (2014). The Situation of Seawater Intrusion in Tripoli, Libya. *International Conference on Biological, Chemical and Environmental Sciences (BCES-2014)* June 14-15, 2014 Penang -Malaysia.

El Moujabber M, Bou Samra B, Darwish T, Atallah T (2006). Comparison of different indicators for groundwater contamination by seawater intrusion on the Lebanese coast. *Water Resource Manage* (20), 161–180.

El-Trriki, N. A. (2006). Groundwater Salinization in the Coastal area of Jifara Plain, *NW-Libya.* MSc. Belgium. University of Ghent.

ESRI. (2012). ArcGIS Desktop. Environmental Systems Research Institute. Redlands, California. USA.

quality of the QuaternaryAquifer in reclaimed areas at the Northwestern El-Minya Governorate- Egypt, using the water quality index. *International Journal of Recent Scientific Research* 9(1), 23033-23047.

Abdullah, T.O., Ali, S. S. and Al Ansari, N. A. (2016). Groundwater assessment of Halabja Saidsadiq Basin, Kurdistan region, NE of Iraq using vulnerability mapping. *Arab J Geosci* 9(3), 223.

Alfarrah, N., Martens K. and Walraevens, K (2011). Hydrochemistry of the Upper Miocene-Pliocene-Quaternary aquifer complex of Jifarah Plain, NW-Libya. GeologicaBelgica, 14(3–4), 159–174.

Albu, M., Banks, D. and Nash, H. (1997). Mineral and Thermal Groundwater Resources. *Springer, Dordrecht*.

APHA. (1992). Standard Methods for Examination of Water and Wastewater. 18th Edition. *American Public Health Association.* Washington DC.

Appelo C. A. J. and D. Postma (1996). Geochemistry, Ground-water and Pollution. A.A. *Balkema Publishers*, Rotterdam.

Appelo, C.A.J.(1994). Cation and proton exchange, pH variations, and carbonate reactions in a freshening aquifer. *Water Resource. Res*. 30, 2793–2805.

Aris, Z. A. M. H. Abdllah, Ahmed.A. and. Woong.K. K. (2007). Controlling factors of groundwater hydrochemistry in a small island's aquifer," *Int. J. Env. Sci and Tech.* 4 (4), 441- 450.

Arnon, I. (1972). Crop production in dry regions London, *leonardHill. United Kingdom.*

Ayers. R. S. and Westcot. D. W. 1985. Irrigation water quality. FAO, Rome.pp. 174.

Ayers, R. S and Westcot, D.W (1999). Water quality for agriculture.2nd Campina Grand:

ISSN: online 2617-2186 print 2617-2178

Aquifers- Monitoring, Modeling and Management, Essaouira, Morroco, 23-25.

Piper, A.M. (1944) A graphic procedure in the Geochemical interpretation of water analysis. *Transactions. American Geophysical Union*, 25, 914 -928.

Pulido-Leboeuf,P.(2004) Seawater intrusion and associated processes in a small coastal complex aquifer (Castell de Ferro, Spain). *Applied Geochemistry* (19), 1517–1527.

Ramesh, and Srinithi, K. (2014). Hydrochemical Characteristics of Groundwater in Mayiladuthurai Block of Nagapattinam District, Tamil Nadu. International *Journal of ChemTech Research.* 6 (14), 5698-5708.

Richards LA (1954).Diagnosis and improvement of saline and alkaline soils. United States Salinity Laboratory, US Department of Agriculture*, Agri Hand book 60 Washington. USA.*

Simsek, C. and Gunduz, O. (2007). IWQ index: A GIS integrated technique to assess irrigation water quality. *EnvironmentalMonitoring and Assessment* (128) 277–300.

Suarez, D. L. (1981). Relation between pHc and sodium adsorption ratio (SAR) and an alternative method of estimating SAR of soil and drainage waters. SSSA J. 45(3): 469-475.

Sundaray, S. K. (2010). Application of Multivariate Statistical techniques in hydrological studies- A case study of Brahmani- Koel River (India). *Environ. Monit. Assess* 164, 297-310

Todd, D.K. (1980) *Groundwater Hydrology*; Wiley: Hoboken, NJ, USA.

Walraevens K and Van Camp M. (2005) Advances in understanding natural groundwater quality controls in coastal aquifers. *In: 18 Salt Water Intrusion Meeting (SWIM). Cartagena 2004, Spain*, 451–460.

Flogel, H. (1979). Seawater Intrusion Study. SARALD/FAO project. Unpublished Report. Tripoli, 56p.5 tables, 26 fig. and 3 maps.(AW-295).

Heba. S.A, Hassan. A. A. and Faid. A. M, (2016). Assessment of Groundwater Quality for Different Aquifers in Halaib and Shalatien at South Eastern Desert of Egypt. *Journal of Soil Sciences and Agricultural Engineering*, *Mansoura Univ*. 11(6), 203-214.

Holanda, J. S. and Amorim, J. A. (1997). Management and control salinity and irrigated agriculture water, Congresso Brasileiro de Engenharia setting, 26, Campina Grande: 137-169.

Lesch, S. M., and D. L. Suarez. (2009). A short note on calculating the adjusted SAR index. *Transactions of the ASABE* 52 (2), 493–496.

Meireles, A. C. M., Andrade, E. M., Chaves, L. C. G., Frischkorn, H., and Crisostomo, L. A. (2010). A new proposal of the classification of irrigation water. *Revista Ciência Agronômica,*(41), 349–357.

Mercado, A., (1985). The use of hydro geochemical patterns in carbonate sand and sandstone aquifers to identify intrusion and flushing of old saline water. *Ground Water*(23), 635–644.

Misaghi, F. (2017) .Introducing a water quality index-dor assessing water for irrigation purposes: a case study of the ghezelozan River. *Sci Total Envi-rov* (589), 107-116.

Mohammed, M.N. (2011). Quality assessment of Tigris river by using water quality index for irrigation purpose. *European Journal of Scientific Research* 57 (1): 15-28.

Panteleit, B., Kessels, W., Kantor, W., Schulz, H. (2001). Geochemical Characteristics of Salinization- Zones in the Coastal Aquifer Test Field (Cat-Field) in North-Germany. In Proceeding of 5th *International Conference on Saltwater Intrusion and Coastal*

ISSN: online 2617-2186 print 2617-2178

Evaluation of Groundwater Quality in the South of Tripoliand its suitability for Irrigation Using Irrigation Water Quality Index (IWQI)

Ahmed Ibrahim Ekhmaj*[1], Abdul Rahman Ahmed Alriyani[2] and Mohamed Melad Dulayoum[3]

[1]Soil and water Department, Faculty of Agriculture, University of Tripoli.*
[2]Advanced Laboratory of Chemical Analysis, Authority of Natural Science Research and Technology, Tripoli, Libya.
[3]Olive tree research center, Authority of Natural Science Research and Technology, Tripoli, Libya.,

Received: 13 January 2021/ Accepted: 31 January 2021
Doi: https://doi.org/10.54172/mjsc.v36i1.12

Abstract: Groundwater represents one of the main constraints to develop successful sustainable agricultural activity in Libya. Good management and proper planning of this resource requires knowledge of water quality to reduce the problems which may face the users of that resource. This study aims to identify the chemical composition of groundwater in the south of Tripoli area and to assess the quality of groundwater for irrigation purposes. In order to achieve the objectives of this study, 31 samples of groundwater were collected from wells scattered around southern Tripoli during July of 2016. Many chemicals analyze were conducted on these samples to estimate the electrical conductivity(EC), pH and the concentration of some dissolved ions which included sodium (Na^+), potassium (K^+), calcium (Ca^{2+}), magnesium (Mg^{2+}), chloride (Cl^-), bicarbonate (HCO_3^-) and sulfate (SO_4^{2-}). The adjusted percentage of absorbed sodium (SAR^o) was also determined. The five-parameters irrigation water quality index was used. These parameters included EC, Na^+, Cl^-, HCO_3^-, and SAR^o. The inverse distance weighted to the power 2 was used to obtain the maps of the spatial distribution of chemical properties and irrigation water quality index. The results showed that the values of the electrical conductivity were high in the middle of the study area and decreased at its east and west, and the spatial distribution pattern was very similar to the spatial distribution of sodium and chloride ions. The results also indicated that the average relative abundance of dissolved anions as expressed in units of (meq/l) were 65.8, 20.4, and 13.8% for Cl^-, SO_4^{2-}, and HCO_3^-, respectively. The average relative abundance of dissolved cations was 49.3, 28.1, 21.7 and 0.9% for Na^+, Mg^{2+}, Ca^{2+}, and K^+, respectively. The irrigation water quality index values ranged between 41.2 and 76.6. The spatial distribution map of the irrigation water quality index also showed that 62% of the area of the study area was classified as having moderate restrictions and limitations for use for irrigation purposes, and that 37.5% were classified as having high restrictions and limitations.

Keyword: Groundwater, Meireles index, IWQI, IDW, Southern Tripoli.

***Corresponding Author** Ahmed Ibrahim Ekhmaj, ekhmaj@gmail.com , Soil and Water Department, Faculty of Agriculture, University of Tripoli. Tripoli- Libya.

مجلة المختار للعلوم 36 (1): 98-105، 2021

نسبة ظهور حالات الألبومين الدقيق (Microalbuminurea) بين مرضى داء السكري من الرجال المترددين على مستشفى برقن العام بمنطقة الشاطئ /ليبيا

مبروكة محمد الزوي*، أحمد حسين سليمان وصلاح مسعود عمر

قسم المختبرات الطبية، كلية العلوم الهندسية والتقنية، جامعة سبها، براك الشاطئ ليبيا

تاريخ الاستلام: 21 ديسمبر 2020/ تاريخ القبول: 30 يناير 2021

https://doi.org/10.54172/mjsc.v36i1.27:Doi

المستخلص: يعد مرض داء السكري من أكثر الأمراض شيوعاً في جميع أنحاء العالم والذي يصاحبه مضاعفات خطيرة عديدة. اعتلال الكلية السكري هو أحد هذه المضاعفات، وقد يؤدي إلى مرض الكلى المزمن، وينتهي على الصعيد العالمي بالفشل الكلوي في المراحل النهائية. يعتبر الألبومين الدقيق (Microalbuminurea) العلامة الأكثر حساسية للتشخيص المبكر لاعتلال الكلية السكري (Diabetic nephropathy) والذي يوجد في حوالي 30% من هؤلاء المرضى أو أكثر والتشخيص المبكر له قد يساعد في عملية العلاج وتفادي الإصابة بالفشل الكلوي. تهدف هذه الدراسة لتقدير نسبة ظهور الألبومين الدقيق، وعوامل الخطر المحتملة بين مرضى داء السكري المترددين على مستشفى برقن العام بمنطقة الشاطئ جنوب ليبيا، بوصفها علامة لاعتلال الكلية السكري، حيث شملت الدراسة عدد 75 رجل: 50 منهم مصاب بداء السكري و25 من الأصحاء، سُحبت منهم عينات دم لقياس تركيز السكر، والكرياتنين في حالة الصيام، وعينات بول صباحي لتقدير مستوى الألبومين الدقيق والكرياتنين. تبين من خلال النتائج أن 48% من مرضى السكر المترددين على مستشفى برقن لديهم ألبومين دقيق في البول، و8% لديهم حالات Macroalbuminurea. حيث وجدت علاقة ارتباط موجب بين تركيز الألبومين الدقيق، وكل من مدة الإصابة بداء السكري، وعمر المرضى فكانت قيمة r =0.32، 0.39 وقيمة P= 0.034، 0.008 على التوالي، وعلاقة ارتباط موجب مع تركيز الكرياتنين في كل من الدم والبول حيث كانت قيمة r = 0.59، 0.313 وقيمة P= 0.000، 0.033 على التوالي. نستنتج من هذه الدراسة أن حوالي 48% من مرضى السكر المشاركين في هذه الدراسة معرضون لخطر الإصابة بأمراض الكلى نتيجة لارتفاع الألبومين الدقيق لديهم، عليه فإن المتابعة والتشخيص المبكر قد يحد من الإصابة، و8% خطر الإصابة لديهم أشد ويزداد تدريجيًا مع طول مدة الإصابة بداء السكري.

الكلمات المفتاحية: داء السكري، الفشل الكلوي، مضاعفات السكر، الألبومين الدقيق، الكرياتنين في الدم والبول.

المقدمة

داء السكري هو مرض من الأمراض المزمنة الشائعة وغير الانتقالية، فيه يفقد الجسم قدرته على استهلاك السكر وتخزينه مما يؤدي إلى ارتفاع تركيزه في مجرى الدم، لذا يُعد هذا المرض اضطراباً أيضيا متعدد الأسباب، قد تكون هذه الأسباب وراثية، أو بيئية تتصف بفرط الجلوكوز Hyperglycemia المزمن مع اضطراب في أيض الكربوهيدرات، الدهون، والبروتينات نتيجة لخلل في إفراز الأنسولين وفاعليته (Jayasri وآخرون،2008).

تُعرف منظمة الصحة العالمية (WHO) داء السكري من خلال الأعراض المصاحبة له، مثل الجوع، العطش، كثرة التبول، الجفاف، التعب والإجهاد ورجفة الأطراف، بالإضافة إلى تركيز السكر في الدم والذي يكون أعلى من 126 ملجم /ديسيلتر في حالة الصيام، السكر العشوائي

* مبروكة محمد الزوي mab.alzwayi@sebhau.edu.ly ، قسم المختبرات الطبية، كلية العلوم الهندسية والتقنية، جامعة سبها، براك الشاطئ ليبيا

أعلى من أو يساوي 200 ملجم/ديسيلتر، أو أن يكون التركيز بعد ساعتين من حمل الجلوكوز أعلى من 200 ملجم/ديسيلتر (WHO، 2006) .

يُصاحب هذا المرض مضاعفات عديدة حيث إنه من الأسباب الرئيسية للإصابة بالفشل الكلوي، خطر الإصابة بالنوبات القلبية والسكتات الدماغية، ضعف تدفق الدم والاعتلال العصبي في القدمين مما يؤدي إلى زيادة احتمالات الإصابة بتقرح القدم، والعدوى، والذي قد يؤدي إلى ضرورة بتر الأطراف في نهاية المطاف، الإصابة بالعمى ويحدث نتيجة تراكم الضرر الذي يلحق بالأوعية الدموية الصغيرة في الشبكية على المدى البعيد Hofso وآخرون، 2009).

اعتلال الكلية السكري Diabetic nephropathy (DN) يؤدي إلى مرض الكلى المزمن الذي يحتاج فيه المريض إلى الغسيل الكلوي مدى الحياة(Ko وآخرون.1999) ,.أول ما وُصف الألبومين الدقيق(MA) microalbuminuria بواسطة (Keen وآخرون، 1969) على أنه زيادة غير طبيعية في معدل إفراز الألبومين عند مرضى السكر إلى ما بين 30–300 ملجم /24 ساعة، في الثمانينيات أوضحت دراسات عديدة على مرضى السكر أن الألبومين الدقيق يعد علامة خطر قوية على الإصابة، أو تطور اعتلال الكلى السكري (Parving وآخرون، 1982؛ Mogensen؛ 1984)، يعاني حوالي 50% من مرضى السكري المصابين أكثر من 20 عامًا من هذه المضاعفات، حيث إن زيادة مستوى الجلوكوز لديهم يؤدي بطريقة غير مباشرة، ومن خلال مسارات أيضية مختلفة إلى تلف الطبقة البطانية (Satchell و Tooke، 2008) وهذا التلف ينعكس بواسطة الألبومين الدقيق (Sachdev وآخرون، 2008؛ Waghmareو Goswami ، 2016) معدل انتشار الألبومين الدقيق في عموم الناس يشكل ما بين 14–16% بمعدلات أكثر في الناس الأكثر عرضة للإصابة بداء السكري، حوالي ثلث مرضى داء السكري أو أكثر لديهم ارتفاع في الألبومين الدقيق (Tobe وآخرون، 2002).

أوضحت الإحصائيات الحديثة زيادة في انتشار داء السكري في جميع أنحاء العالم خصوصاً في الدول النامية (King وآخرون، 1998) وزيادة انتشاره في دول الشرق الأوسط جعلها واحدة من النقاط الساخنة في هذا المرض ونظرًا للنمو الاجتماعي، والاقتصادي السريع، وتغيرات نمط الحياة، وزيادة انتشار السمنة، من المتوقع أن يتضاعف عدد المصابين بالسكري بحلول عام 2045 في هذه المنطقة (Al Busaidi وآخرون، 2019).

تعد زيادة معدل الألبومين الدقيق في البول العلامة الأكثر حساسية للاعتلال الكلوي السكري (Al Busaidi وآخرون، 2019). والذي قد يبدأ في الارتفاع قبل تشخيص داء السكري، السبب الأساسي في ظهور الزلال في البول و بالتالي الخلل في الكلى هو سوء التحكم في معدل السكر في الدم لهؤلاء المرضى (Lutale وآخرون، 2007).

أجريت دراسات عديدة في الدول النامية حول نسبة ظهور الألبومين الدقيق في البول عند مرضى السكري من النوع الثاني، وفي دراسة أجريت في الباكستان وجدت النسبة تصل إلى حوالي 31.56% (Ahmad وآخرون، 2017). في حين في نيبال بالهند وجدت النسبة أقل قليلاً حيث كانت 20.3% (Thakur وآخرون، 2019).

على الرغم من أن بعض الدراسات الأخرى أظهرت انتشارا يصل إلى 55.2 % (Ramidha وآخرون، 2019). في نيجيريا، أفادت دراسات عديدة وجود اختلاف في انتشار الألبومين الدقيق في مرضى السكر النوع 2 على نطاق واسع تراوحت النسب بين 16.1 – 41.2٪ (Agaba وآخرون، 2004؛ Blessing وآخرون، 2011؛ Udenze وآخرون، 2013). وبالتالي فإن متابعة مرض داء السكري ضرورية لتفادي مثل تلك المضاعفات ونظراً

ISSN: online 2617-2186 print 2617-2178

لندرة أو انعدام الدراسات المنشورة في ليبيا خصوصا في الجنوب حول هذا الموضوع أجريت هذه الدراسة لمعرفة نسبة ظهور الألبومين الدقيق بين مرضى داء السكري النوع الثاني المترددين على مستشفى برقن العام الشاطئ- ليبيا.

المواد وطرق البحث

أُجريت هذه الدراسة في مستشفى برقن العام بمنطقة الشاطئ جنوب ليبيا، شملت 75 رجلا، 50 منهم مرضى مصابين بداء السكري، و25 من الرجال الأصحاء تم استخدامهم عينات ضابطة وذلك خلال الفترة من 12-1-2019 إلى 28-2-2019، جُمعت منهم عينات دم في حالة الصيام بعد استكمال الاستبيان المخصص للدراسة والذي اشتمل على مجموعة من البيانات منها العمر، الطول، الوزن، نوع العلاج المتناول وفترة الإصابة بالمرض (داء السكري).

قُسمت العينات بين أنابيب جمع عينات الدم تحتوي على مانع التجلط فلوريد أوكسالات (Flurid Oxalate) وأنابيب خالية من مانع التجلط، فُصلت البلازما عن خلايا الدم لقياس تركيز السكر، وتُركت الأنابيب الخالية من مانع التجلط حتى تجلطت ثم فُصل المصل منها أيضاً باستخدام جهاز الطرد المركزي عند سرعة 3000 دورة/دقيقة لمدة 10 دقائق، وأُجري عليها اختبار قياس تركيز الكرياتنين.

كما جُمعت عينات بول صباحية من المتبرعين في أنابيب معقمة خاصة بجمع عينات البول، أُخذت كمية منها لقياس الألبومين الدقيق وكمية أخرى تم تخفيفها بنسبة 20/1 لقياس تركيز الكرياتنين في البول.

أُجري قياس تركيز السكر بواسطة المحاليل الجاهزة " المحضرة من شركة Dalma والتي تعتمد على الطريقة الإنزيمية. وقياس تركيز الكرياتين في الدم والبول باستخدام المحاليل المحضرة من شركة Biomagrab التي تعتمد على الطريقة اللونية باستخدام جهاز Photometer4040. واستخدم جهاز Ichroma لتقدير الألبومين الدقيق في البول.

التحليل الاحصائي: حُللت البيانات المتحصل عليها إحصائياً باستخدام برنامج الـ Minitab 16، لإيجاد المتوسط الحسابي، والانحراف المعياري للمتغيرات، وحساب ما إذا كان هناك فروق معنوية بين المرضى والأصحاء باستخدام اختبار 2 sample t-test، كما تم اختبار العلاقة بين المتغيرات باستخدام اختبار Person correlationعند مستوى معنوية 0.05.

النتائج

أظهرت نتائج هذه الدراسة عدم وجود فروق معنوية بين المجموعة الضابطة، والمرضى من حيث القياسات الأنثروميترية كما هو مبين في الجدول رقم (1).

جدول (1): يوضح المتوسط الحسابي والانحراف المعياري للصفات العامة لمجموعتي الدراسة

المتغير	العينات الضابطة	العينات المرضية	P-value
	المتوسط الحسابي ± الأنحراف المعياري		
العمر سنة	7.3 ± 42.9	7.0 ± 46.3	0.07
الوزن كجم	11.1 ± 82.1	7.9 ± 84.4	0.36
الطول سم	7.3 ± 175.6	4.7 ± 176.6	0.54
مؤشر كتلة الجسم كجم/م^2	3.4 ± 26.7	27.1 ± 2.8	0.55

في حين وجد فرق معنوي واضح بين متوسط تركيز الألبومين الدقيق للمرضى 37.0 ± 23.4 ملجم/لتر والأصحاء 9.5 ± 5.1 ملجم/لتر، حيث كانت قيمة P المعنوي أقل من 0.0001 .كما تبين من خلال التحليل الإحصائي للنتائج وجود فروق معنوية بين المجموعتين في كل من: تركيز الكرياتين في المصل و البول وتركيز السكر الصيامي في الدم وكانت النتائج في المرضى والأصحاء على التوالي 0.95 ± 0.23 و 0.81 ± 0.12

ISSN: online 2617-2186 print 2617-2178

ملجم/ديسيلتر، 49.5 ± 24.3 و 84.9 ± 35.2 ملجم /لتر و 201.9 ± 77.6 و 83.1 ±13.7ملجم/ديسيلتر حيث قيمة P المعنوية 0.002 وأقل لجميع المتغيرات .قُسمت مجموعة المرضى إلى ثلاثة مجاميع على حسب التركيز المتحصل عليه للألبومين الدقيق في البول وهي: أقل من 30، ما بين 30–299، وأكثر من 300 ملجم/لتر فاحتوت المجموعة الأولى على 22 مريضا بنسبة 44%، والمجموعة الثانية على 24 مريضا بنسبة 48% في حين احتوت المجموعة الثالثة على 4 مرضى بنسبة 8%.

أظهر التحليل الإحصائي باستخدام اختبار t وجود فرق معنوي بين المجموعتين الأولى، والثانية في كل من الميكرو ألبومين، والعمر، وتركيز الكرياتين في الدم حيث كانت قيمة P المعنوية أقل من 0.05، في حين لم تُظهر بقية المتغيرات أي فروق معنوية كما هو مبين بالجدول رقم (2). التحليل الإحصائي لم يشمل المجموعة الثالثة وذلك لقلة العدد الموجود بها

جدول رقم (2): يبين تقسيم مجموعة المرضى على حسب تركيز الألبومين الدقيق في البول والمتوسط الحسابي، والانحراف المعياري للمتغيرات في كل مجموعة.

لمتغير	Normo-albuminurea أقل من 30	Micro-albuminurea 299 –30	P-value
العدد	22	24	
الألبومين الدقيق ملجم/لتر	13.9 ±29.	33.61±58.24	0.00*
العمر (سنة)	10.4± 48.1	± 54.710.1	0.034*
مؤشر كتلة الجسم (كجم/م^2)	26. 5 ± 2.8	827 ± 2.6	0.11
الكرياتين في الدم(ملجم/ديسيلتر)	90.17±0.	1.02 ± 0.26	0.01*
الكرياتين في البول(ملجم/ديسيلتر)	21.3± 54.6	43.9 26.5±	0.14
السكر في الدم (ملجم/ديسيلتر)	83.4 ± 205.3	198.8 ±73.5	0.78

* وجود فرق معنوي بين المجموعتين

عند دراسة العلاقة بين تركيز الألبومين الدقيق وكل من مدة الإصابة بداء السكري، وعمر المرضى وجدت علاقة ارتباط موجب بينهما حيث كانت قيمة r=0.32، 0.39 وقيمة P= 0.034، 0.008 على التوالي، كما وجدت علاقة ارتباط موجب بينه وبين كل من تركيز الكرياتين في الدم والبول حيث كانت قيمة r = 0.59، 0.313 وقيمة P= 0.000، 0.033 على التوالي كما هو مبين بالشكل رقم (1)، في حين لم توجد علاقة ارتباط مع بقية المتغيرات.

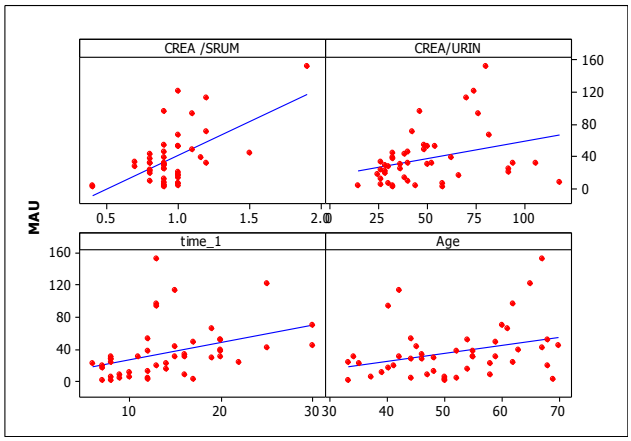

شكل رقم (1): يبين العلاقة بين الألبومين الدقيق وكل من العمر، مدة الإصابة بداء السكري وتركيز الكرياتين في الدم والبول

المناقشة

نظرًا لأن ارتفاع السكر في الدم على المدى الطويل في مرضى داء السكري يمكن أن يؤدي إلى اختلال وظيفي دائم في الأعضاء بما في ذلك الكلى، لذلك فإن المراقبة المنتظمة ضرورية لمستويات السكر في الدم، نسبة السكر التراكمي والعلامات الحيوية الخاصة بالأعضاء. يمكن مراقبة تدهور وظائف الكلى الناتجة عن ارتفاع مستويات الجلوكوز غير المنضبط في الدم تدريجياً باستخدام مستويات الكرياتينين في البلازما. في الواقع تكون تركيزات الكرياتين، واليوريا في البلازما أعلى بشكل ملحوظ لدى مريض السكري مقارنة بالأشخاص غير المصابين بالسكري (Agaba وآخرون، 2004)، والذي أوضحته هذه الدراسة رغم أن تركيز الكرياتين كان لا يزال في الحدود الطبيعية إلا أنه اختلف بفرق معنوي

ISSN: online 2617-2186 print 2617-2178

عن الأصحاء وكان تركيزه في البول للمرضى أقل منه في الأصحاء والذي قد يعكس عدم قدرة الكلية على التخلص منه نتيجة لتلف أو ضعف خلاياها.

كما أن تركيز السكر في الدم للمرضى أعلى منه في الأشخاص الأصحاء، بالإضافة إلى الارتفاع في تركيز الألبومين الدقيق الذي وجد مرتفعا بصورة ملحوظة في مرضى السكر عن الأصحاء الأمر الذي أثبتته دراسات عديدة (Karar وآخرون، 2015؛ Khadka وآخرون، 2018؛ Amin وآخرون، 2019)، من خلال هذه الدراسة تبين أن حوالي 48% من المرضى المسجلين فيها لديهم ميكرو ألبومين، والذي جاء متفقا مع الدراسة التي أجريت في السعودية على 400 مريض من مرضى السكر، والتي أوضحت أن حوالي نصف المرضى المسجلين كان لديهم ميكرو ألبومين في البول (Khadka وآخرون، 2018) ، هذه النسبة مطابقة للنسب التي سُجلت في عدد من الدول العربية لكنها كبيرة مقارنة بالنسب المسجلة في عدد من الدول الأوروبية (Abdulrhman، 2017) قريبة من الدراسة التي أجريت في الهند والتي سجلت نسبة 41% (Ambayiram وآخرون، 2016)، وأعلى من النسبة التي سُجلت في جوبا حيث سُجلت بحوالي 35 % (Maharjan وآخرون، 2010)، أما بقية الحالات في هذه الدراسة فتوزعت بين طبيعية والتي سجلت نسبة 44% وأربع حالات متأخرة Macroalbuminurea بنسبة 8% وهذه النسبة متفقة مع النسبة التي وجدت في السعودية حيث سجلت 8.1% في حين كانت أقل من النسبة التي سُجلت في مصر والكويت حيث كانت 12.8% و 16.2 % (Al-Adsani ، 2012؛ Farahat وآخرون، 2014). هذا الاختلاف في القيم قد يعود إلى عدة أسباب منها عدد العينات، عملية الإعداد للتجربة، العوامل الاجتماعية وتعريف الألبومين في البول (Khadka وآخرون2018) بالإضافة إلى ذلك؛ سجلت هذه الدراسة علاقة ارتباط موجب بين الميكرو ألبومين وكل من العمر ومدة الإصابة بداء السكري، وهذا متفق مع دراسات عديدة (Sigdel وآخرون، 2008، Ambayiram وآخرون، 2016؛ Khadka وآخرون، 2018). وقد يعود تفسير ذلك إلى طول فترة الإصابة والذي قد يعود إلى عدم التحكم في السكر بصورة جيدة أو قد يعود إلى التلف الذي يصيب الكبيبة مع التقدم في العمر، في حين لم تُظهر دراسات أخرى هذه العلاقة (Zakkerkish وآخرون، 2013).

كما كان من ضمن نتائج هذه الدراسة وجود علاقة ارتباط موجب بين الميكرو ألبومين وكل من تركيز الكرياتين في البول والدم والذي بينته دراسات عديدة (Blessing وآخرون، 2011؛ Ghosh وآخرون، 2012؛ Karar وآخرون، 2015؛ Khadka وآخرون، 2018)، في حين لم توجد علاقة ارتباط مع تركيز السكر في الدم في دراستنا هذه، والذي جاء مخالفا لبعض الدراسات الأخرى Karar وآخرون، 2015؛Khadka وآخرون، 2018)، من محدوديات هذه الدراسة عدم قياس السكر التراكمي والذي قد يكون مؤشرا أكثر حساسية للتحكم في السكر في الدم، كما أنه لم يتم قياس الضغط وظروف التدخين وتأثيرها.مع ذلك فإن الدراسة أعطت مؤشرا لضرورة متابعة مرضى السكري بصورة دورية للتقليل من خطر الإصابة بأمراض الكلى.

الاستنتاج

نستنتج من هذه الدراسة أن حوالي 48% من مرضى السكر معرضون لخطر الإصابة بأمراض الكلى، عليه فإن المتابعة والتشخيص المبكر قد يحد من الإصابة بالمضاعفات الكلوية لداء السكري.

الشكر والتقدير

نشكر جميع العاملين بمستشفى برقن العام ابتداءً من مديره، ورؤساء الأقسام إلى العاملين به، كما نشكر جزيل الشكر المتبرعين في هذه الدراسة على وقتهم، فلكم منّا جزيل الشكر والعرفان وفائق الاحترام لكل من ساهم في إنجاز هذا العمل.

المراجع

Agaba, E., Agaba, P., & Puepet, F. (2004). Prevalence of microalbuminuria in newly diagnosed type 2 diabetic pa-

ISSN: online 2617-2186 print 2617-2178

Tanzania. *African Journal of Diabetes Medicine [Internet], 20*(2).

Hofsø, D., Jenssen, T., Bollerslev, J., Røislien, J., Hager, H., & Hjelmesæth, J. (2009). Anthropometric characteristics and type 2 diabetes in extremely obese Caucasian subjects: a cross-sectional study. *Diabetes Research and Clinical Practice, 86*(1), e9-e11.

Idonije, B. O., Festus, O., & Oluba, O. M. (2011). Plasma glucose, creatinine and urea levels in type 2 diabetic patients attending a Nigerian teaching hospital. *Research journal of medical sciences, 5*(1), 1-3.

Jarrett, R., Keen, H., Boyns, D., Chlouverakis, C., & Fuller, J. (1969). The concomitants of raised blood sugar: studies in newly-detected hyperglycaemics. I. A comparative assessment of neurological functions in blood sugar groups. *Guy's Hospital reports, 118*(2), 237-246.

Jayasri, M., Gunasekaran, S., Radha, A., & Mathew, T. (2008). Anti-diabetic effect of Costus pictus leaves in normal and streptozotocin-induced diabetic rats. *Int J Diabetes Metab, 16*(3), 117-122.

Karar, T., Alniwaider, R. A. R., Fattah, M. A., Al Tamimi, W., Alanazi, A., & Qureshi, S. (2015). Assessment of microalbuminuria and albumin creatinine ratio in patients with type 2 diabetes mellitus. *Journal of natural science, biology, and medicine, 6*(Suppl 1), S89.

Khadka, B., Tiwari, M. L., Timalsina, B., Risal, P., Gupta, S., & Acharya, D. (2018). Prevalence and factors associated with microalbuminuria among type 2 diabetic patients: A hospital based study. *Age (years), 50*(107), 26.28.

tients in Jos Nigeria. *African journal of medicine and medical sciences, 33*(1), 19-22.

Al Busaidi, N., Shanmugam, P., & Manoharan, D. (2019). Diabetes in the Middle East: government health care policies and strategies that address the growing diabetes prevalence in the Middle East. *Current diabetes reports, 19*(2), 8.

Al-Adsani, A. (2012). Risk factors associated with albuminuria in Kuwaiti adults with type 2 diabetes. *Saudi Journal of Kidney Diseases and Transplantation, 23*(4), 860.

Aldukhayel, A. (2017). Prevalence of diabetic nephropathy among Type 2 diabetic patients in some of the Arab countries. *International journal of health sciences, 11*(1), 1.

Ambayiram, A. V., Kalyani, P., Felix, A., & Govindarajan, P. (2016). Prevalence of microalbuminuria among type II diabetes mellitus patients in urban Chidambaram. *Saudi J Med, 1*(3), 57-62.

Amin, R. F., El Bendary, A. S., Ezzat, S. E., & Mohamed, W. S. (2019). Serum Ferritin level, microalbuminuria and non-alcoholic fatty liver disease in type 2 diabetic patients. *Diabetes & Metabolic Syndrome: Clinical Research & Reviews, 13*(3), 2226-2229.

Farahat, T. M., Elsaeed, G. K., Gazareen, S. S., & Elsayed, T. I. (2014). Prevalence of proteinuria among type 2 diabetic patients in Menoufia governorate, Egypt. *Menoufia Medical Journal, 27*(2), 363.

Ghosh, S., Lyaruu, I., & Yeates, K. (2012). Prevalence and factors associated with microalbuminuria in type 2 diabetic patients at a diabetes clinic in northern

ISSN: online 2617-2186 print 2617-2178

Sachdev, Y.. (2008). Diabetic Nephropathy. In Y. Sachdev (Ed.), Clinical Endocrinology and diabetes mellitus. *JAYPEE brothers* (1st ed., pp. 1000–1007)

Sigdel, M., Rajbhandari, N., Basnet, S., Nagila, A., Basnet, P., & Tamrakar, B. (2008). Microalbuminuria among type-2 diabetes mellitus patients in Pokhara, Nepal. *Nepal Med Coll J, 10*(4), 242-245.

Thakur, S. K., Dhakal, S. P., Parajuli, S., Sah, A. K., Nepal, S. P., & Paudel, B. D. (2019). Microalbuminuria and its risk factors in type 2 diabetic patients. *Journal of Nepal Health Research Council, 17*(1), 61-65.

Tobe, S. W., McFarlane, P. A., & Naimark, D. M. (2002). Microalbuminuria in diabetes mellitus. *Cmaj, 167*(5), 499-503.

Udenze, I., Azinge, E., Adesina, P., Egbuagha, E., Onyenekwu, C., Ayodele, O., & Adizua, U. The Prevalence of Metabolic Syndrome in Persons with Type 2 Diabetes at the Lagos UniversityTeaching Hospital, Lagos, Nigeria.

Waghmare, P., & Goswami, K. (2016). Microalbuminuria: A Mere Marker or An Ominous Sign? *The Journal of the Association of Physicians of India, 64*(3), 61-65.

Zakerkish, M., Shahbazian, H. B., Shahbazian, H., Latifi, S. M., & Aleali, A. M. (2013). Albuminuria and its correlates in type 2 diabetic patients. *Iranian journal of kidney diseases, 7*(4), 268.

King, H., Aubert, R. E., & Herman, W. H. (1998). Global burden of diabetes, 1995–2025: prevalence, numerical estimates, and projections. *Diabetes care, 21*(9), 1414-1431.

Lutale, J. J. K., Thordarson, H., Abbas, Z. G., & Vetvik, K. (2007). Microalbuminuria among type 1 and type 2 diabetic patients of African origin in Dar Es Salaam, Tanzania. *BMC nephrology, 8*(1), 1-8.

Maharjan, B., Bhandary, S., Risal, P., Sedhain, A., & Gautam, M. (2010). Microalbuminuria and macroalbuminuria in type 2 diabetes. *Journal of Nepal Health Research Council*.

Mogensen, C. (1984). Microalbuminuria predicts clinical proteinuria and early mortality in maturity-onset diabetes. *New England Journal of Medicine, 310*(6), 356-360.

Organization, W. H. (2006). Definition and diagnosis of diabetes mellitus and intermediate hyperglycaemia: report of a WHO/IDF consultation.

Parving, H.-H., Oxenbøll, B., Svendsen, P. A., Christiansen, J. S., & Andersen, A. (1982). Early detection of patients at risk of developing diabetic nephropathy. A longitudinal study of urinary albumin excretion. *European Journal of Endocrinology, 100*(4), 550-555.

Ramidha, V., Sebastin, N., & Bhavani, N. (2019). Micro albuminuria in type 2 DM-prevalence and its association with microvascular complications. *Indian Journal of Clinical Anatomy and Physiology, 6*(1), 93-97.

Satchell, S., & Tooke, J. (2008). What is the mechanism of microalbuminuria in diabetes: a role for the glomerular endothelium? *Diabetologia, 51*(5), 714-725.

ISSN: online 2617-2186 print 2617-2178

Al-Mukhtar Journal of Sciences 36 (1): 98-105, 2021

Prevalence of Microalbuminuria Among Diabetic Male Patients Attending Bergan General Hospital / South of Libya

Mabroukah Mohamad Al-Zwayi *, Ahmed Hussein Suleiman and Salah Masoud Omar

Department of Medical Laboratories, Faculty of Engineering and Technical Sciences, Sebha University, Brak A

Received: 21 December 2020/ Accepted: 30 January 2021
Doi: https://doi.org/10.54172/mjsc.v36i1.27

Abstract: Diabetes mellitus has become increasingly common worldwide, with many serious complications. Diabetic nephropathy is one such complication that affects the kidney and leads to end-stage renal failure worldwide. Microalbuminuria represents an abnormal elevation in urine albumin levels, which is an early marker of diabetic nephropathy. It is likely to be found in one-third or more of diabetic patients. Early recognition of microalbuminuria in diabetic nephropathy permits successful therapeutic intervention and significant postponement of terminal renal failure. This study aimed to estimate the prevalence of microalbuminuria and the potential risk factors among patients with type 2 diabetes mellitus who attended Bergin General Hospital-AL-Shati, Southern Libya, as a sign of diabetic nephropathy. 75 men were recruited for this study: 50 of them had type 2 diabetes, and 25 men were healthy and used as a control. Morning fasting blood samples were collected from all of them to estimate the concentration of plasma glucose and creatinine, and first morning urine samples were collected for microalbinurea and creatinin estimation. The results show that 48% of the diabetic patients attending Bergin Hospital had Microalbuminuria, and 8% had Microalbuminuria. A positive correlation was found between the concentration of microalbumin and both duration of diabetes and the age of diabetic patients, r value was 0.32, 0.39, and the P-value = 0.034, 0.008, respectively. In addition, a positive correlation was found with the concentration of creatinine in both blood and urine where the value of r = 0.59, 0.313, and P-value = 0.000 and 0.033 respectively. In conclusion, about 48 % of diabetics in this study are at risk of developing kidney disease due to their high microalbumin level. Early diagnosis and monitoring of this condition could prevent nephropathy in this group of patients. Also, for 8 %, the risk is higher and gradually increases with the length of time they have diabetes.

Key words: Diabetes, Kidney Failure, Diabetes Complications, Microalbumin, Creatinine in Blood and Urine.

***Corresponding Author:** Mabroukah Mohamad Al-Zwayi *mab.alzwayi@sebhau.edu.ly* , Department of Medical Laboratories, Faculty of Engineering and Technical Sciences, Sebha University, Brak A.